ISSN 1023-9855

Thoracic Medicine

Volume 40 • Number 2 • June 2025

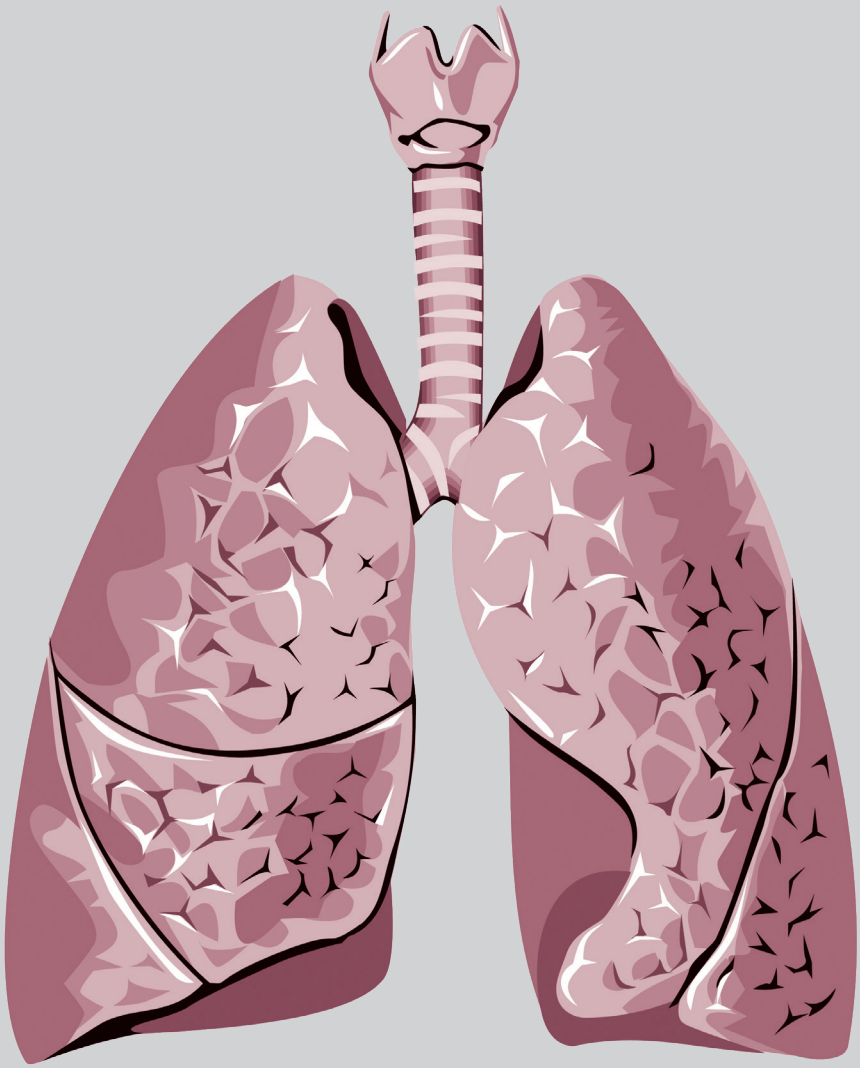

The Official Journal of

Taiwan Society of Pulmonary and Critical Care Medicine

Taiwan Society of Sleep Medicine

Taiwan Society for Respiratory Therapy

Taiwan Society of Tuberculosis and Lung Diseases

Thoracic Medicine

The Official Journal of
Taiwan Society of Pulmonary and Critical Care Medicine
Taiwan Society for Respiratory Therapy
Taiwan Society of Sleep Medicine
Taiwan Society of Tuberculosis and Lung Diseases

Thoracic Medicine

The Official Journal of
Taiwan Society of Pulmonary and Critical Care Medicine
Taiwan Society for Respiratory Therapy
Taiwan Society of Sleep Medicine
Taiwan Society of Tuberculosis and Lung Diseases

Volume 40
Number 2
June 2025

CONTENTS

Orginial Articles

Case Reports

Role of Bronchoscopic Lung Cryobiopsy in Diagnosing Pulmonary Alveolar Proteinosis

Yu-Chang Fu[1], Chih-Yen Tu[1], Wen-Chien Cheng[1], Biing-Ru Wu[1], Yu-Hua Su[1], Chih-Yu Chen[1], Wei-Chun Chen[1], Wei-chih Liao[1], Chia-Hung Chen[1]

Background: The diagnosis of pulmonary alveolar proteinosis (PAP) is typically secured through bronchoalveolar lavage, transbronchial lung biopsy (TBLB), or rarely, surgical lung biopsy (SLB). Bronchoscopic lung cryobiopsy (BLC) has emerged as a reliable method for diagnosing diffuse parenchymal lung diseases (DPLD), although its utility in diagnosing PAP is not extensively documented. To our knowledge, existing literature consists mainly of case reports or inclusion in DPLD case series. Therefore, this study aimed to compare TBLB and BLC in the diagnosis of PAP.

Methods: We enrolled patients with PAP who underwent radial probe endobronchial ultrasound without fluoroscopy to locate target lesions, followed by sampling with conventional TBLB and BLC from January 2015 to March 2024.

Results: Seven patients were enrolled in our study. BLC was performed at the right middle lobe in 3 patients and the lower lobe in the remaining patients. BLC yielded larger tissue fragments than conventional forceps biopsy. Moderate bleeding occurred in 5 patients, and was managed with epinephrine and tranexamic acid. Five patients developed pneumothorax requiring chest tube insertion. Most patients underwent whole lung lavage, showing clinical and radiological improvement.

Conclusion: With a safety profile comparable to SLB and a more favorable diagnostic yield than TBLB, BLC could be considered more often in the diagnosis of PAP. ***(Thorac Med 2025; 40: 99-106)***

Key words: Pulmonary alveolar proteinosis, bronchoscopic lung cryobiopsy, diffuse parenchymal lung disease

[1]Division of Pulmonary and Critical Care, Department of Internal Medicine, China Medical University Hospital, Taichung, Taiwan.
Address reprint requests to: Dr. Chia-Hung Chen, Division of Pulmonary and Critical Care, Department of Internal Medicine, China Medical University Hospital, Taichung, Taiwan. No. 2, Yude Rd, North District, Taichung City, 404

Introduction

Pulmonary alveolar proteinosis (PAP) is a rare disease characterised by accumulation of periodic acid-Schiff (PAS)-positive proteinaceous material in the distal air spaces [1-2]. The gold standard for tissue diagnosis is surgical lung biopsy (SLB), which can be performed via an open method or video-assisted thoracoscopic surgery (VATS). In cases of PAP, bronchoscopic examination usually appears unremarkable. Bronchoalveolar lavage (BAL) fluid typically has a milky, turbid appearance with thick sediment. Cytological analysis of the BAL fluid reveals large foamy macrophages that stain positive with PAS, and oil-red-O with dirty-appearing sediment [2]. Although BAL is safer and easier to perform than SLB, it may provide less definitive diagnostic information because of the non-specific cytological findings, compared to the detailed histological analysis provided by SLB [2-3]. However, compared to SLB, which has a higher associated mortality [4], bronchoscopic lung cryobiopsy (BLC) using a flexible cryoprobe in diagnosing diffuse lung diseases is gaining popularity with its advantages in specimen size, safety, and quality, resulting in a higher diagnostic yield compared to transbronchial lung biopsy (TBLB) [5-7]. Very few data are available regarding the utility of cryobiopsy in diagnosing PAP, so our study aimed to investigate the feasibility and safety of BLC compared to TBLB.

Methods

The procedures were carried out at a high-volume tertiary care center for interventional pulmonology (IP) by doctors with more than 10 years of experience in the field. We enrolled patients with PAP who underwent radial probe endobronchial ultrasound (R-EBUS) without fluoroscopy to locate target lesions, followed by sampling with conventional TBLB and BLC from January 2015 to March 2024.

Patients primarily presented to the pulmonology outpatient clinic with cough, with or without dyspnea. Following a thorough history-taking and clinical examination, all patients underwent chest X-ray followed by high-resolution computed tomography (HRCT) of the thorax. When the CT findings indicated a crazy-paving pattern, bronchoscopy was scheduled. Prior to each bronchoscopy, potential sites for biopsy were identified topographically, after carefully screening 1-mm CT cuts of the lung parenchyma in both axial and coronal planes. Bronchoscopy was performed (Olympus BF1T260) along with R-EBUS (UM-S20-20R or UM-S20-17S, Olympus) under conscious sedation without the use of an artificial airway or fluoroscopy. The biopsy site was chosen based on either the blizzard sign or a type I homogenous pattern found within the lesion by radial probe EBUS. All patients underwent BAL, brush cytology, forceps biopsy and flexible cryobiopsy, either 2.4 mm (the first 3 patients) or 1.9 mm in diameter (the last 4 patients) (Erbe Elektromedizin GmbH). Cryobiopsy was performed with a freeze time of 3-6 seconds, and the tissue was immediately fixed with formalin.

Bronchoscopic instillation of epinephrine (1:10000) or tranexamic acid was performed for the control of bleeding, and hemostasis was successfully achieved in all patients. Mild bleeding indicated the use of suction alone. Moderate bleeding involved the use of any additional intervention such as instillation of ice-cold saline, vasoconstrictive drugs, or endobronchial blocker, and severe bleeding required

further interventions, such as surgery, administering blood products, or admitting the patient to a critical care unit [4, 8]. Rapid on-site evaluation (ROSE) was performed for all except 2 of the patients. After the procedure was completed, patients were monitored closely for 2 hours, followed by a chest radiograph. If there was no pneumothorax, the patients were discharged on the same day; otherwise, they were admitted for management.

Results

Seven patients were enrolled in our study. A summary of patient data is provided in Table 1. All patients except 1 presented with symptoms. The exception was a 44-year-old male laborer who came for a regular health examination, and chest X-ray showed areas of increased density incidentally (Patient 4). Subsequent HRCT of the thorax revealed patchy areas of ground-glass suggestive of a crazy-paving pattern compatible with PAP. The right middle lobe was chosen for cryobiopsy in 3 patients (Patients 3, 5, & 7 – RB5, RB4, and RB4, respectively), based on the HRCT finding [Fig. 1]. The lower lobe was chosen in the remaining patients (RB7, RB8, LB9 and RB7 for patients 1, 2, 4, & 7, respectively). The size of the tissue fragments obtained was larger in the cryobiopsy than in the conventional forceps biopsy.

All patients underwent BAL and brush cytology, which revealed negative findings for PAP, malignancy and infection. ROSE was performed for all patients except 2 (patients 2 & 6), and no malignancies or granuloma were identified. BLC was responsible for diagnosing 4 patients (patients 1, 2, 4 & 6), while the remaining cases were diagnosed by both BLC and TBLB (patients 3, 5 & 7).

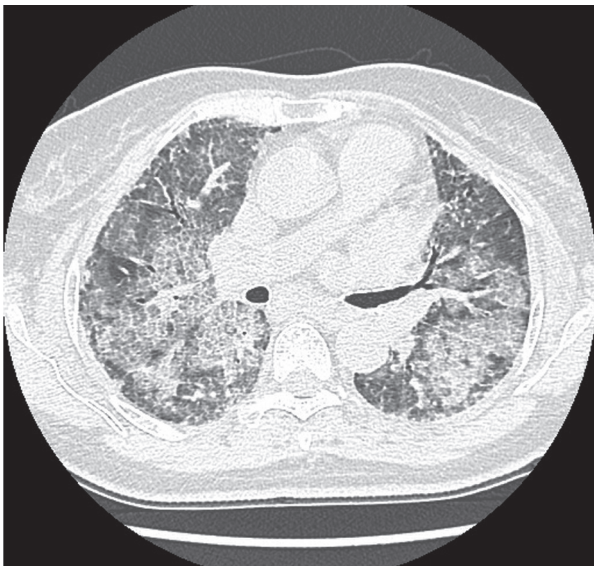

Fig. 1. High-resolution chest tomography of patient 3 showing bilateral diffuse ground glass opacities with thickened interlobular septa, characteristic of a crazy-paving pattern.

Five patients had moderate bleeding during the procedure, which was managed by 1:10,000 epinephrine and tranexamic acid. Five patients developed pneumothorax following the biopsy, warranting chest tube insertion. One patient with stable disease did not undergo whole lung lavage (WLL) due to stable clinical status; the remaining 6 patients underwent WLL and showed clinico-radiological improvement following the procedure [Fig. 2].

Discussion

In 1958, Samuel Rosen, *et al*. first described 27 cases of a lung disease characterised by PAS-positive proteinaceous fluid filling the alveoli [1]. The presentation of the disease can be an incidental finding on X-rays, or symptoms including exertional dyspnea, cough, fatigue and weight loss, and even respiratory failure [2].

In cases of PAP, there is a defect in either the production (congenital PAP) or clearance

Table 1. Characteristics and Bbiopsy Results of the 7 Patients

Patient	**1**	**2**	**3**	**4**	**5**	**6**	**7**
Age, years	51	36	69	44	47	51	48
Gender	Male	Male	Female	Male	Male	Male	Male
Symptoms	cough with sputum for several months	chronic dry cough for 1 year	chronic dry cough for 6 months	incidental finding at health examination	cough for 3 years	cough with some sputum for several months	cough for 3 years
Comorbid condition	NIL	NIL	type 2 DM, HTN and bronchiectasis	NIL	HTN and dyslipid-emia	Hyperuricemia	HTN and dyslipid-emia
Smoking status	Former	Current	Never	Never	Never	Former	Former
Packs per day x year	20	20	0	0	0	20	10
Radial EBUS pattern	Type 1 homogenous pattern; within lesion	Type 1 homogenous pattern; within lesion	blizzard sign	blizzard sign	Type 1 homogenous pattern; within lesion	Type 1 homogenous pattern; within lesion	Type 1 homogenous pattern; within lesion
Site of forceps biopsy	RB10	LB10	RB5	LB9	RB10	RB5	RB10
Number of biopsies	3	4	5	2	2	2	2
Forceps biopsy specimen size, cm	0.1 x 0.1 x 0.1	0.4 x 0.3 x 0.1	0.1 x 0.1 x 0.1	0.2 x 0.2 x 0.1	0.5 x 0.3 x 0.1	0.1x0.1x0.1	0.5x0.3x0.1
Site of cryobiopsy	RB7	RB8	RB5	LB9	RB4	RB7	RB4
Number of biopsies	3	2	3	3	2	3	2
Cryobiopsy specimen size, cm	0.3 x 0.3 x 0.1	0.6 x 0.5 x 0.2	0.1 x 0.1 x 0.1	0.4 x 0.3 x 0.2	0.6 x 0.5 x 0.2	0.3x0.3x0.1	0.6x0.5x0.2
Mode of diagnosis	BLC	BLC	BLC and forceps biopsy	BLC	BLC and forceps biopsy	BLC and forceps biopsy	BLC and forceps biopsy
Complications	moderate bleeding; right pneumothorax	NIL	right pneumothorax	moderate bleeding	moderate bleeding; right pneumothorax	moderate bleeding; right pneumothorax	moderate bleeding; right pneumothorax
Management	1:10000 epinephrine; intercostal drain insertion	N/A	intercostal drain insertion	tranexamic acid	1:10000 epinephrine; intercostal drain insertion	1:10000 epinephrine; intercostal drain insertion	1:10000 epinephrine; intercostal drain insertion
Post-WLL image	improved	improved	improved	N/A	improved	improved	improved

DM=diabetes mellitus, HTN=hypertension, EBUS=endobronchial ultrasound, WLL=whole lung lavage

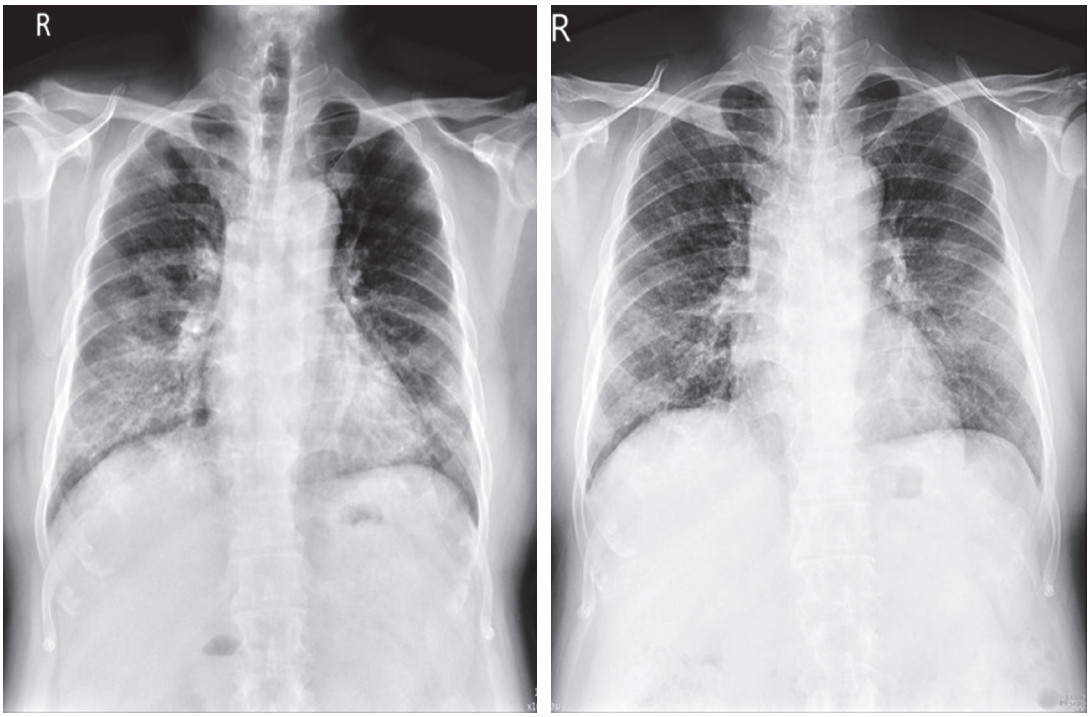

Fig. 2. Chest X-ray of patient 5, showing a diffuse interstitial pattern predominantly in the lower zones (left) and resolution of the same, 4 weeks after whole lung lavage.

(autoimmune PAP) of surfactant. Secondary PAP is linked to infections, various dust exposures, or hematologic/immunologic diseases. Autoimmune PAP is by far the most common type and WLL is the most widely accepted therapy [2]. Seymour, *et al*. conducted a comprehensive study that found that patients with PAP who underwent WLL had a higher 5-year survival rate than untreated patients (94±2% vs. 85±5%; n=146 and 85; *P*=0.04) [9]. Newer therapies, such as recombinant GM-CSF, have shown a significant reduction in the need for subsequent WLL therapy (time to first-rescue WLL: 30 vs. 18 months, n=9 per group, *P*=0.0078), and can be considered when WLL fails [10-11].

There is limited literature on the diagnosis of PAP through BLC. Poletti, *et al*. presented case series involving 176 patients with diffuse parenchymal lung diseases (DPLD) who underwent BLC, and 1 of the 176 patients was diagnosed as having PAP [12]. Ussavarungsi, *et al*. conducted a retrospective analysis of 74 patients with DPLD who received BLC, and only 1 of them was diagnosed with PAP [13]. Gando, *et al*., Shen, *et al*., Marwah, *et al*., and Wu, *et al*. also reported individual cases of PAP diagnosed via BLC, respectively [14-17].

In our study, BAL did not establish the diagnosis of PAP, which contrasts with the findings of Trapnell, *et al*., in which 75% of the diagnoses were made by lavage, possibly due to the inadequate amount of fluid specimens (approximately 5-10 ml) [18].

Though it had a slightly lower pooled sensitivity than SLB in diagnosing DPLD in a meta-analysis (87% of BLC versus 91% of SLB), BLC is preferred due to its better safety profile

and cost-effectiveness [19]. Han, *et al*., in their real-world prospective study on the application of BLC and uniportal and tubeless VATS in the multidisciplinary diagnosis of interstitial lung disease, concluded that BLC is the preferred diagnostic method over VATS when the initial diagnosis suggests PAP, which is related to the radiological features of a homogeneous pattern with broncho-centric or peri-lymphatic distribution with a comparable diagnostic yield and a less invasive nature [20]. The larger tissue size and the ability to preserve lung architecture are the positive aspects of cryobiopsy relative to TBLB [5, 6, 7].

BLC has the mechanical advantage of obtaining tissue from the lateral aspects of the probe during freezing, apart from the tip, which differentiates it from conventional TBLB. Consequently, the tissue samples obtained with BLC are larger than those obtained with forceps biopsy, as observed in our series, while retaining the lung architecture [12, 21].

BLC was exclusively responsible for diagnosing 4 of our patients (patients 1, 2, 4 & 6), while the remaining cases were diagnosed by both BLC and TBLB (patients 3, 5 & 7). Thus, it seems that BLC is a reliable diagnostic tool for PAP. ROSE demonstrates its significant importance and value in the diagnostic yield for peripheral lung lesions with its rapid stain and real-time assessment for direct slides [22-25]. The availability of ROSE in our setup (except for patients 2 and 6) helped in ensuring sample adequacy and in ruling out malignancy and granuloma.

Bleeding and pneumothorax were the complications encountered in our patients (bleeding – patients 1, 4, 5, 6 & 7; right-side pneumothorax – patients 1, 3, 5, 6 & 7). For patients 3, 5 and 7, the middle lobe was chosen based on CT findings, and pneumothorax in this lobe is a common complication of TBLB [26]. Moderate bleeding warranted instillation of 1:10,000 epinephrine in 3 (patients 1, 5, and 7), while bronchoscopic instillation of tranexamic acid was used for the fourth patient. Hemostasis was achieved in all cases. Patients with pneumothorax were managed with pig-tail insertion within a few days.

A meta-analysis revealed that the pooled incidence of pneumothorax is 5.6%, with the maximum being 22.4% [4]; our study, on the other hand, found an incidence of 71.4% (5/7). Furthermore, the pooled incidence of significant bleeding was 6.9% (with a patient number greater than 70), compared to our study's incidence of 71.4% (5/7) [4]. As we know, biopsy using BLC for interstitial lung disease carries a higher risk of bleeding and pneumothorax compared to using TBLB, due to the larger sample size [27]. We thought that the high incidence of bleeding and pneumothorax could be related to compensatory emphysema and subpleural bullae, due to excessive deposition of protein-like substances in the alveoli and interstitial fibrosis in PAP patients [17]. In a low-volume center with limited resources, extra caution is necessary when performing these procedures. Our study revealed that BLC has a more favorable diagnostic yield than TBLB, with manageable complications.

Conclusion

BLC is a recommended procedure for diagnosing PAP. It has the feasibility to diagnose PAP with a favorable diagnostic yield. However, caution is warranted while performing flexible cryobiopsy in low-volume centers under conscious sedation and without the use of

fluoroscopy. In a resource-limited setting with a limited armamentarium, BLC could be considered to obtain relatively reliable specimens in diagnosing PAP, compared to conventional TBLB, and it offers a less invasive profile than surgical procedures.

References

1. Rosen SH, Castleman B, Liebow AA, *et al*. Pulmonary alveolar proteinosis. N Engl J Med 1958; 258: 1123-42.
2. Suzuki T, Trapnell BC. Pulmonary alveolar proteinosis syndrome. Clin Chest Med 2016; 37: 431-40.
3. Burkhalter A, Silverman JF, Hopkins MB 3rd, *et al*. Bronchoalveolar lavage cytology in pulmonary alveolar proteinosis. Am J Clin Pathol 1996 Oct; 106(4): 504-10.
4. Rodrigues I, Gomes RE, Coutinho LM, *et al*. Diagnostic yield and safety of transbronchial lung cryobiopsy and surgical lung biopsy in interstitial lung diseases: a systematic review and meta-analysis. Eur Respir Rev 2022 Oct 5; 31(166): 210280.
5. Lentz RJ, Taylor TM, Kropski JA, *et al*. Utility of flexible bronchoscopic cryobiopsy for diagnosis of diffuse parenchymal lung diseases. J Bronchology Interv Pulmonol 2018 Apr; 25(2): 88-96.
6. Shafin Babu PS Sr., Marwah V, Katoch C, *et al*. Diagnostic yield and safety of bronchoscopic lung cryobiopsy in evaluation of lung mass. Cureus 2021 Nov 27; 13(11): e19940.
7. Tang Y, Tian S, Chen H, *et al*. Transbronchial lung cryobiopsy for peripheral pulmonary lesions. A narrative review. Pulmonology 2023 Oct 30: S2531-0437(23)00163-0.
8. Hetzel J, Eberhardt R, Petermann C, *et al*. Bleeding risk of transbronchial cryobiopsy compared to transbronchial forceps biopsy in interstitial lung disease - a prospective, randomized, multicentre cross-over trial. Respir Res 2019 Jul 5; 20(1): 140.
9. Seymour JF, Presneill JJ. Pulmonary alveolar proteinosis: progress in the first 44 years. Am J Respir Crit Care Med 2002 Jul 15; 166(2): 215-35.
10. Campo I, Carey BC, Paracchini E, *et al*. Inhaled recombinant GM-CSF reduces the need for whole lung lavage and improves gas exchange in autoimmune pulmonary alveolar proteinosis patients. Eur Respir J 2024 Jan 4; 63(1): 2301233.
11. Tanner LM, Kurko J, Tringham M, *et al*. Inhaled sargramostim induced resolution of pulmonary alveolar proteinosis in lysinuric protein intolerance. JIMD Rep 2017; 34: 97-104.
12. Poletti V, Casoni GL, Gurioli C, *et al*. Lung cryobiopsies: a paradigm shift in diagnostic bronchoscopy? Respirology 2014; 19: 645-54.
13. Ussavarungsi K, Kern RM, Roden AC, *et al*. 2017. Transbronchial cryobiopsy in diffuse parenchymal lung disease: retrospective analysis of 74 cases. Chest 2017 Feb; 151(2): 400-408.
14. Gando S, Dure R, Violi D, *et al*. Bilateral lung disease, extensive and diffuse. Diagnosis of pulmonary alveolar proteinosis by bronchoscopic cryobiopsy. Respir Med Case Rep 2017; 22: 260-262.
15. Shen MF, Ju TR, Lee CC, *et al*. Novel application of cryobiopsy in the diagnosis of pulmonary alveolar proteinosis. Respirol Case Rep 2018; 6: e00336.
16. Marwah V, Katoch CDS, Sengupta P, *et al*. Bronchoscopic lung cryobiopsy for the diagnosis of pulmonary alveolar proteinosis in a hypoxemic patient. Lung India 2020 Jul-Aug; 37(4): 336-339.
17. Wu HM, Wen YL, He XY, *et al*. Selective bronchial occlusion for the prevention of pneumothorax after transbronchial lung cryobiopsy in a pulmonary alveolar proteinosis patient: a case report. Front Med (Lausanne) 2023 Nov 27; 10: 1265373.
18. Trapnell BC, Whitsett JA, Nakata K. Pulmonary alveolar proteinosis. N Engl J Med 2003; 349: 2527-39.
19. Iftikhar IH, Alghothani L, Sardi A, *et al*. Transbronchial lung cryobiopsy and video-assisted thoracoscopic lung biopsy in the diagnosis of diffuse parenchymal lung disease. A meta-analysis of diagnostic test accuracy. Ann Am Thorac Soc 2017; 14: 1197-1211.
20. Han Q, Chen X, Xu X, *et al*. The application of transbronchial lung cryobiopsy and uniportal and tubeless video-assisted thoracic surgery in the multidisciplinary diagnosis of interstitial lung disease - a real-world prospective study. Front Mol Biosci 2021; 8: 681669.
21. Pajares V, Puzo C, Castillo D, *et al*. Diagnostic yield of transbronchial cryobiopsy in interstitial lung disease: a randomized trial. Respirology 2014; 19: 900-6.
22. Leoncini F, Levi G, Novali M, *et al*., Impact of ROSE on

the diagnostic yield of fluoroscopy-guided bronchoscopy in diagnosing peripheral pulmonary lesions, Eur Respir J 2020 Sep; 56(64): 2842.

23. Xu CH, Wang JW, Wang W, *et al*. The diagnosis value of endobronchial ultrasound transbronchial lung biopsy combined with rapid on-site evaluation in peripheral lung cancer, Clin Res J 2020; 14(5): 447-452.
24. Xu C, Liu W, Wang W, *et al*. Diagnostic value of endobronchial ultrasound combined with rapid on-site evaluation of transbronchial lung biopsy for peripheral pulmonary lesions, Diagn Cytopathol 2021; 49: 706-710.
25. Qi JC, Liao L, Zhao Z, *et al*. Impact of rapid on-site evaluation combined with endobronchial ultrasound and virtual bronchoscopic navigation in diagnosing peripheral lung lesions, BMC Pulm Med 2022; 22(1): 117.
26. Andersen HA. Transbronchoscopic lung biopsy for diffuse pulmonary diseases. Results in 939 patients. Chest 1978; 73(5): 734-6.
27. Ramaswamy A, Homer R, Killam J, *et al*. Comparison of transbronchial and cryobiopsies in evaluation of diffuse parenchymal lung disease. J Bronchology Interv Pulmonol 2016 Jan; 23(1): 14-21.

Clinical Characteristics and Mortality Rates of COVID-19 Patients with Malignancies

Hsin-I Cheng[1], Shu-Min Lin[1,2,3,4], Po-Jui Chang[1,4], Horng-Chyuan Lin[1,4], Ko-Wei Chang[1,4]

Objectives: Early reports have indicated that patients with cancer may be associated with a higher possibility of being infected by coronavirus disease 2019 (COVID-19). However, the mortality rate of patients with cancer infected by COVID-19 in Taiwan has not been well described.

Methods: This retrospective observational study was conducted at the Linkou Branch of Chang Gung Memorial Hospital, Taiwan, from May 2022 to September 2022. All patients who had confirmed SARS-CoV-2 infection and were admitted to the ward were enrolled. Demographic data, laboratory results, and treatment information were collected and analyzed. In addition, clinical outcomes for patients with and without cancer were analyzed.

Results: In total, 620 patients with COVID-19 were included in this study, and 132 of them had cancer. After matching, 132 patients were categorized into the cancer group, and 128 without cancer were placed in the no-cancer group. The no-cancer group had a higher prevalence of underlying heart failure, elevated leukocyte counts, and increased levels of blood urea nitrogen (BUN) and creatinine. The cancer group had higher C-reactive protein (CRP) levels and significantly greater in-hospital mortality rates (21.2% vs. 3.1%, $P < 0.001$). Independent risk factors for in-hospital mortality included having a malignancy as an underlying condition and advanced age.

Conclusion: Our research found that COVID-19 patients with cancer had notably higher death rates, and that cancer was an independent risk factor for in-hospital mortality. Those who were adequately vaccinated demonstrated a much lower likelihood of disease progression. We suggest encouraging vaccination and providing rigorous monitoring throughout the treatment period. ***(Thorac Med 2025; 40: 107-116)***

Key words: COVID-19, cancer, mortality

[1]Department of Thoracic Medicine, Chang Gung Memorial Hospital, Linkou, Taiwan. [2]Department of Respiratory Therapy, Chang Gung Memorial Hospital, Linkou, Taiwan. [3]School of Medicine, National Tsing Hua University, Hsin-Chu, Taiwan. [4]School of Medicine, Chang Gung University, Taoyuan, Taiwan.
Address reprint requests to: Dr. Ko-Wei Chang, Department of Thoracic Medicine, Chang Gung Memorial Hospital, 199 Tun-Hwa N. Rd., Taipei, Taiwan.

Introduction

The World Health Organization declared the coronavirus disease 2019 (COVID-19) outbreak a pandemic on March 11, 2020. COVID-19 is caused by the severe acute respiratory syndrome coronavirus 2 (SARS-CoV-2) virus. By the close of 2023, there have been 774 million confirmed cases globally, with over 7 million fatalities attributed to the pandemic [1]. Since SARS-CoV-2 first emerged, 5 significant variants have been identified: Alpha, Beta, Gamma, Delta, and Omicron. The Omicron variant was responsible for 2 major waves of community spread between January and December 2022 [2]. Taiwan's healthcare system has been significantly impacted by the pandemic; as of March 2023, Taiwan reported 10 million confirmed cases and 19,000 deaths related to COVID-19.

In Taiwan, cancer has persistently remained the leading cause of death, claiming over 53,000 lives in 2023 [3]. In addition, COVID-19 accounted for approximately 9,000 deaths that year, making it the sixth most common cause of death in the nation [3]. The CDC has provided guidelines for individuals at heightened risk of severe COVID-19 complications, including those with cancer, cardiovascular disease, diabetes, and various other chronic illnesses [4]. However, there is a lack of comprehensive data on the risk of mortality associated with many comorbid conditions. A retrospective cohort study conducted in the United States examined the outcomes of patients who had both cancer and COVID-19 [5]. The findings indicated that cancer did not independently affect the mortality rate of COVID-19. Presently, there is limited research on how mortality risk from COVID-19 compares between cancer patients and those without cancer.

This study investigated the characteristics of patients with cancer who were hospitalized due to COVID-19 during the periods when the Omicron variant was prevalent in Taiwan. It also explored possible factors that could predict mortality in these patients.

Materials and Methods

Study Design and Patient Selection

This retrospective observational study was carried out at the Linkou Branch of Chang Gung Memorial Hospital in Taoyuan, Taiwan, the nation's largest medical facility with 3,700 beds. The research spanned from May 2022 to September 2022, coinciding with the Omicron variant outbreaks in Taiwan. Participants included patients who had PCR-confirmed SARS-CoV-2 infections according to guidelines set by the Taiwan Centers for Disease Control. All participants were admitted to quarantine wards designated for COVID-19 cases. Exclusion criteria were patients under 18 years of age or those with a concurrent human immunodeficiency virus infection. The study received ethical approval from the Institutional Review Board of the Chang Gung Memorial Foundation (IRB No. 202400546B0), and informed consent was waived due to its retrospective nature. Data were extracted from electronic medical records and included laboratory results obtained within 24 hours of admission, which served as baseline data (day 0).

COVID-19 Management Protocol

The strategies used to manage COVID-19 followed the Interim Guidelines for Clinical Management of SARS-CoV-2 Infection [6]. These methods included regular checks of vital signs and oxygen levels (with continuous

monitoring for severe cases), enhanced supportive care, ensuring proper caloric intake, and maintaining homeostasis (such as adequate hydration, electrolyte balance, and acid-base equilibrium). For patients with low blood oxygen levels, supplemental oxygen was given immediately. The goal was to achieve a pulse oxygen saturation of 90%. If standard oxygen therapy was ineffective, high-flow nasal cannula or noninvasive ventilation was employed. Should noninvasive ventilation prove insufficient, invasive mechanical ventilation (MV) was initiated. Antiviral and anti-inflammatory treatments were provided according to established guidelines. Remdesivir was used for patients with an SpO2 of 94% on room air or supplied oxygen. Low-dose dexamethasone (6 mg daily for up to 10 days) was administered to those with an SpO2 of 94% on room air or supplied oxygen, those experiencing respiratory failure, and those on extracorporeal membrane oxygenation. Antibiotics were prescribed based on the patient's condition. All medical costs were covered by Taiwan's National Health Insurance program. Antiviral and anti-inflammatory medications were supplied by the Taiwanese Centers for Disease Control and administered according to standard guidelines, ensuring that medical interventions across hospitals remained consistent and uniform in adherence to these guidelines.

Data Collection and Measurement

We gathered information from electronic medical records using a case report form, capturing demographic details such as age, gender, pre-existing conditions, and laboratory results. We also documented treatment specifics like the administration of remdesivir, dexamethasone, nirmatrelvir-ritonavir (Paxlovid), molnupiravir, and antibiotics. This research examined each patient's clinical progression and outcomes, including the use of MV; incidence of acute kidney injury; length of hospital stay; and in-hospital mortality rates. Adequately vaccinated adults were identified as non-immunocompromised individuals who had received the second dose of a 2-dose COVID-19 vaccine series at least 14 days prior to testing positive for SARS-CoV-2 related to their hospitalization. Acute kidney injury was classified based on the Kidney Disease Improving Global Outcomes criteria [7]. Two independent physicians reviewed the reasons for admission. For cases admitted due to a positive SARS-CoV-2 RT-PCR test result, COVID-19 was confirmed as the reason for admission if the admitting provider verified the infection or if no other clear alternative cause unrelated to SARS-CoV-2 could be identified by reviewers. Alternative causes included trauma, surgeries, uncomplicated labor, psychiatric care, or unrelated medical diagnoses like cellulitis or gastrointestinal bleeding. Exacerbations of chronic conditions such as congestive heart failure or asthma were considered linked to COVID-19. Any positive RT-PCR test result occurring 7 days after an initial negative test upon admission was deemed indicative of nosocomial SARS-CoV-2 infection and thus not attributed to COVID-19 as the cause for admission.

Statistical Analysis

The study results are presented as means with standard deviations or as numbers with percentages where appropriate. The independent Student’s t test was used to compare continuous variables with a normal distribution. Pearson’s chi-square test or Fisher’s exact test was used to compare categorical variables. In addition, we matched patients with and without

cancers based on severity, vaccination condition, and COVID-19-related admission using propensity scores with a match tolerance cutoff of 0.02. Variables with a p value of less than 0.1 were included in univariate and multivariate logistic regression analyses conducted to identify the factors independently predicting in-hospital mortality. Odds ratios (ORs) and 95% confidence intervals (CIs) were calculated using a logistic regression model. A significance level was set at $p < 0.05$. Kaplan-Meier survival curves were plotted, and the log-rank test was used to compare mortality rates between patients with and without malignancy. All tests were 2-tailed with significance considered at $p < 0.05$. Statistical analyses were performed using IBM SPSS Statistics for Windows Macintosh version 27.0 (IBM, Armonk, NY, USA), and all curves were generated using GraphPad Prism for Windows version 9.0 (GraphPad Software, Boston, MA, USA).

Results

During the study period, 620 patients with COVID-19 met the inclusion criteria (Fig. 1). After matching, 132 and 128 patients with COVID-19 infection were classified into the cancer and no-cancer groups, respectively.

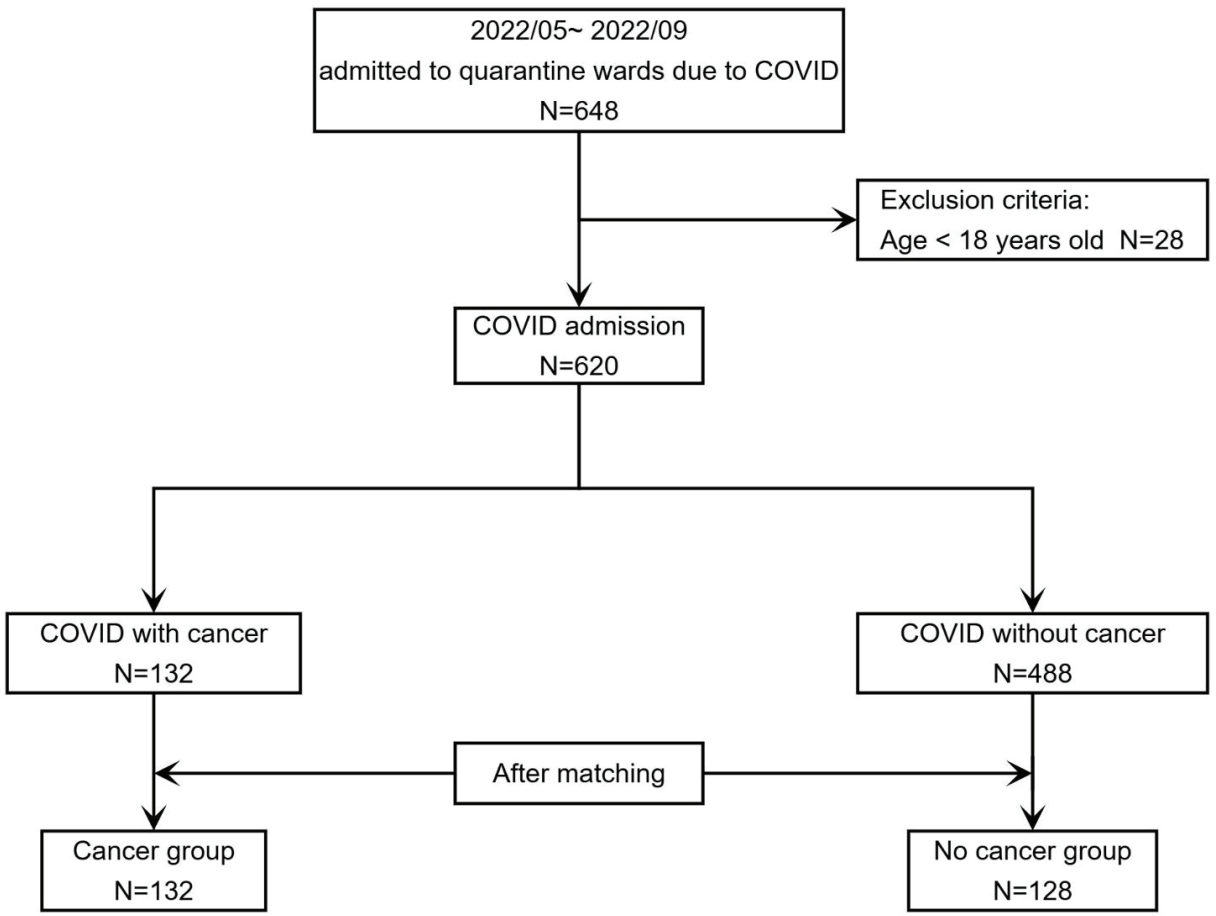

Fig. 1. Study Flowchart.

Baseline Characteristics and Treatments

The average age of the patients was 65.4±16.8 years, and about two-thirds were males (155/260). The cancer group of patients were notably older (67.9±12.7 years in the cancer group and 62.9±19.9 years in the no-cancer group, $P = 0.018$) and had a significantly lower BMI (22.7±4.8 kg/m2 in the cancer group and 24.0±4.5 kg/m2 in the no-cancer group, $P = 0.02$). Hypertension was the most prevalent comorbidity, affecting 46.2% of patients (120/260). There were no significant differences in the prevalence of most chronic comorbidities between the cancer and no-cancer groups, except for heart failure, which was more common in the no-cancer group (14.1%) compared to the cancer group (6.1%), with a *P*-value of 0.032. Both groups showed no significant differences in receiving antiviral treatments such as nirmatrelvir-ritonavir, molnupiravir, and remdesivir or dexamethasone therapy. However, a significantly higher proportion of patients in the cancer group had received antimicrobial agents (80.3% in the cancer group and 68.8% in the no-cancer group, $P = 0.032$) (Table 1).

Laboratory Findings and Clinical Outcomes

Patients in the cancer group had notably higher levels of C-reactive protein (CRP) (71.4 mg/dL compared to 52.1 mg/dL, $P = 0.041$) and had significantly lower leukocyte counts (8300/μL versus 9800/μL, P = 0.024), blood

Table 1. Baseline Characteristics and Treatments of Patients with COVID-19 and Cancer

	Total cohort N=260	Cancer n=132	No cancer n=128	*P* value
Age, yr	65.4±16.8	67.9±12.7	62.9±19.9	0.018
Male gender	155 (59.6)	84 (63.6)	71 (55.5)	0.180
BMI, kg/m^2	23.3±4.7	22.7±4.8	24.0±4.5	0.020
Adequately vaccinated	129 (49.6)	71 (53.8)	58 (45.3)	0.172
Active smoker	36 (13.8)	14 (10.6)	22 (17.2)	0.125
Comorbidities				
Hypertension	120 (46.2)	56 (42.4)	64 (50.0)	0.221
CAD	32 (12.3)	17 (12.9)	15 (11.7)	0.776
Heart failure	26 (10.0)	8 (6.1)	18 (14.1)	0.032
Af	29 (11.2)	13 (9.8)	16 (12.5)	0.497
CKD	33 (12.7)	13 (9.8)	20 (15.6)	0.162
DM	100 (38.5)	50 (37.9)	50 (39.1)	0.845
Treatment				
Antimicrobial agents	194 (74.6)	106 (80.3)	88 (68.8)	0.032
Nirmatrelvir-Ritonavir	26 (10.0)	14 (10.6)	12 (9.4)	0.741
Molnupiravir	43 (16.5)	19 (14.4)	24 (18.8)	0.345
Remdesivir	94 (36.2)	53 (40.2)	41 (32.0)	0.173
Dexamethasone	81 (31.2)	47 (35.6)	34 (26.6)	0.115

Data are expressed as *n* (%) and median [IQR]

Acronyms:

COVID-19: coronavirus disease 2019
BMI: body mass index
CAD: coronary arterial disease
Af: atrial fibrillation
CVA: cerebrovascular accident
DM: diabetes mellitus
CKD: chronic kidney disease
COPD: chronic obstructive pulmonary disease

Table 2. Laboratory Findings and Outcomes of Patients with COVID-19 with and without Cancer

	Total cohort N=260	Cancer n=132	No cancer n=128	*P* value
Laboratory findings				
WBC, 1000/μL	9.0±5.4	8.3±5.3	9.8±5.5	0.024
Lymphocyte count, 1000/μL	1.2±1.3	1.1±0.9	1.4±1.7	0.057
Platelets, 1000/μL	221±122	231±116	210±127	0.178
Prothrombin time, seconds	14.7±7.5	15.6±10.0	13.6±2.6	0.078
aPTT, seconds	30.9±9.0	30.8±7.6	30.9±10.4	0.917
BUN, mg/dL	30.6±27.9	26.9±23.7	34.9±31.7	0.032
Creatinine, mg/dL	1.80±2.29	1.42±2.00	2.15±2.53	0.013
AST, U/L	50.9±117.5	64.4±157.8	35.4±27.6	0.102
ALT, U/L	45.5±126.0	56.1±169.9	34.1±40.3	0.167
Total bilirubin, mg/dL	1.4±2.3	1.2±2.4	0.8±1.5	0.248
CRP, mg/L	62.0±67.9	71.4±67.2	52.1±67.6	0.041
Ct value	22.0±8.00	22.16±8.05	21.75±7.98	0.685
Outcomes				
Respiratory failure	37 (14.2)	23 (17.4)	14 (10.9)	0.134
Acute kidney injury	49 (18.8)	28 (21.2)	21 (16.4)	0.322
Mortality	32 (12.3)	28 (21.2)	4 (3.1)	<0.001
Hospitalized (days)	21.0±30.2	18.7±18.5	23.0±38.2	0.266

Data are expressed as *n* (%) and median [IQR]
Acronyms:
WBC: white blood cells
aPTT: activated partial prothrombin time
AST: aspartate transaminase
CRP: C-reactive protein
PT: prothrombin time
BUN: blood urea nitrogen
ALT: alanine transaminase

urea nitrogen (BUN) levels (26.9 mg/dL versus 34.9 mg/dL, $P = 0.032$), and creatinine levels (1.42 mg/dL versus 2.15 mg/dL, $P = 0.013$), as shown in Table 2. The findings indicated an overall mortality rate of 12.3% (Table 2). Mortality was significantly elevated in the cancer group compared to the no-cancer group (21.2% vs. 3.1%, $P < 0.001$). However, no significant differences were observed between the 2 groups regarding respiratory failure during hospitalization, acute kidney injury, and length of hospital stay. The Kaplan–Meier survival curve (Fig. 2) was used to compare mortality rates between the cancer group and the no-cancer group, and revealed significantly higher mortality in the cancer group than in the no-cancer group (HR = 7.49, reference: no cancer group; 95% CI = 3.747–14.99, log-rank test $p < 0.001$).

Univariate and Multivariate Logistic Regression

For the cancer patients, factors such as age, body mass index (BMI), underlying heart failure, usage of antimicrobial agents, adequate vaccination, leukocyte count, prothrombin time

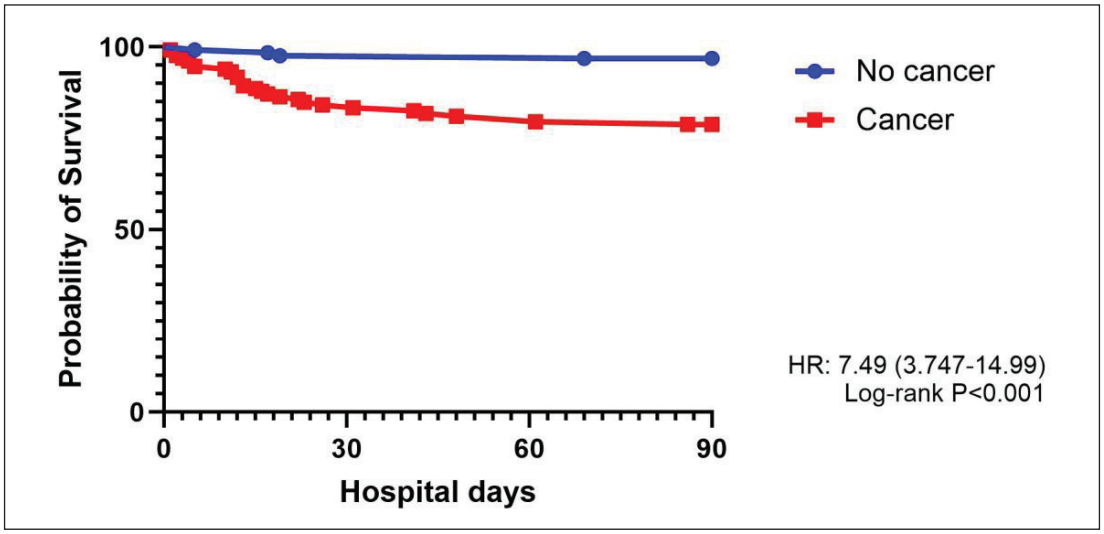

Fig. 2. Survival Curves of Patients with COVID-19 with and without Malignancy.

(PT), creatine, and CRP level were selected in the univariate analysis (Table 3). In multivariate binary logistic regression (Table 3), underlying malignancy (adjusted OR = 8.05, 95% CI = 2.71–23.90, $p < 0.001$) and age (adjusted OR = 1.03, 95% CI = 1.00–1.07, $p = 0.032$) were identified as independent predictors of in-hospital mortality.

Table 3. Risk Factors Associated with In-hospital Mortality

	Univariate analysis		Multivariate analysis	
	Odds ratio (95% C.I.)	***P* value**	**Odds ratio (95% C.I.)**	***P* value**
Age, per 1 year increment	1.05 (1.00-1.09)	0.059	1.03 (1.00-1.07)	0.032
BMI, per 1 kg/m2 increment	0.94 (0.84-1.07)	0.348		
WBC, per 1000/μL increment	1.03 (0.94-1.14)	0.527		
PT, per 1 second increment	1.01 (0.96-1.08)	0.627		
Creatine, per 1 mg/dL increment	1.05 (0.84-1.31)	0.683		
CRP, per 1 mg/L increment	1 (1.00-1.01)	0.233		
Heart failure				
No	1 (reference)			
Yes	3.33 (0.52-21.17)	0.203		
Antimicrobial agents				
No	1 (reference)			
Yes	5.29 (0.32-87.12)	0.244		
Cancers				
No	1 (reference)			
Yes	8.56 (1.91-38.33)	0.005	8.05 (2.71-23.90)	<0.001

Acronyms:
BMI: body mass index
WBC: white blood cell
PT: prothrombin time
CRP: C-reactive protein

Table 4. Prognosis of Patients with and without Adequate Vaccination

	Adequate vaccination N=71	Inadequate vaccination N=61	*P* value
Prognosis			
Disease progression	7 (9.9)	14 (23.0)	0.040
Acute kidney injury	10 (14.1)	18 (29.5)	0.031
Respiratory failure	9 (12.7)	14 (23.0)	0.121
Mortality	11 (15.5)	17 (27.9)	0.083
Hospitalized (days)	14.5±11.0	23.9±23.9	0.009

Adequately Vaccinated Versus Inadequately Vaccinated Patients

We conducted an analysis of COVID-19 patients diagnosed with cancer, comparing those who were adequately vaccinated to those who were inadequately vaccinated (Table 4). Our findings revealed that patients with cancer who were inadequately vaccinated showed a significantly greater rate of disease progression (23.0% vs. 9.9%, $P = 0.04$), acute kidney injury (29.5% vs. 14.1%, $P = 0.031$) and extended hospital stays (23.9±23.9 days in the inadequately vaccinated group and 14.5±11.0 days in the adequately vaccinated group, $P = 0.009$). Furthermore, the inadequately vaccinated group also had an increased risk of in-hospital mortality and a higher incidence of respiratory failure.

Discussion

This study revealed a significantly higher mortality rate in COVID-19 patients with cancers than in those without cancers. In multivariate analysis, having cancer was an independent risk factor for an increased mortality rate. We also found that cancer patients who received adequate vaccination had a lower rate of mortality and progressive disease.

A retrospective multi-center study of 105 cancer patients with COVID-19 found that those with metastatic solid tumors had a significant risk of severe symptoms, measured at 34.29% [8]. Furthermore, the COVID-19 and Cancer Consortium (CCC19) cohort study, which included 1,018 patients, reported that cancer patients with COVID-19 experienced higher mortality rates and more severe illness compared to the general population [9]. Similarly, a national cohort study in China revealed that cancer patients were not only more likely to contract SARS-CoV-2, but also had a higher mortality rate than non-cancer individuals [10]. It is important to note that all of these studies were conducted in 2020, before vaccines and effective treatments were available. At the same time, the virus has evolved from the wild-type to the current Omicron variant. In our study, we focused on Omicron variant patients, and also found that patients with cancer had a higher mortality rate.

The European Cohorts of Patients and Schools to Advance Response to Epidemics (EuCARE) cohort study, encompassing 38,585 patients and ranging from wild-type to Omicron variants, found that individuals infected with the Omicron variant tended to have higher rates

of comorbidities such as cancer, cardiac or cerebrovascular diseases, and other chronic conditions [11]. Additionally, the study indicated that the mortality rate for patients with Omicron infections is lower.

According to a report in the British Medical Journal, while Omicron has led to more infections in South Africa compared to the Delta variant, it has resulted in fewer hospital admissions [12]. A cohort study in France, involving 600 patients, found that cancer patients exhibited a significantly higher mortality rate following COVID-19 infection [13]. Despite this, multivariate logistic regression indicated that cancer was not an independent risk factor for mortality. However, our research found that cancer served as an independent risk factor for mortality in Taiwan during the Omicron period.

Currently, numerous vaccines have been shown to be effective. The safety of various COVID-19 vaccines has been thoroughly evaluated. According to a single-center cohort study, cancer patients who received COVID-19 vaccines experienced only mild side effects [14]. Furthermore, a multicenter cohort study in China found no significant differences in adverse events reported by breast cancer patients compared to others [15]. In addition, 2 extensive meta-analyses and systematic reviews indicated that the adverse effect profiles of the vaccines are similar for both cancer patients and healthy individuals [16-17]. The only contraindication was that individuals who underwent hematopoietic stem cell transplantation or chimeric antigen receptor T-cell therapy should delay COVID-19 vaccination until at least 3 months after the completion of treatment [18]. Patients with malignancies exhibited notably lower seroconversion rates following COVID-19 vaccination [17, 19-22]. Consequently, it was advised that they should get a booster dose. Our research indicated that patients who were fully vaccinated experienced notably less disease progression and had shorter hospital stays.

Our study has several limitations. One major limitation of this study is its retrospective nature, which may have introduced selection bias. In addition, because of the small sample size, the results should be interpreted with caution. In Taiwan, all patients with confirmed cases received treatment in accordance with guidelines from the Taiwanese Centers for Disease Control. This enabled longitudinal follow-up and ensured consistent treatment regimens across hospitals. In the Omicron era, a portion of patients were not admitted to isolation wards due to pneumonia, which may lead to bias. Also, the mortality rate may be affected by the conditions upon admission. We used propensity score matching to minimize the bias.

Conclusion

Our research found that COVID-19 patients with cancer had notably higher death rates, and that cancer was an independent risk factor for in-hospital mortality. Those who were adequately vaccinated had a much lower likelihood of disease progression. We suggest encouraging vaccination and rigorous monitoring throughout the treatment period.

References

1. World Health Organization. COVID-19 epidemiological update – 19 January 2024. Available from: https://www.who.int/publications/m/item/covid-19-epidemiological-update---19-january-2024.
2. Chen WC, Huang AS. COVID-19 public health surveillance and response in Taiwan: from containment to mitigation. J Formos Med Assoc 2024; 123 Suppl 1:

S17-s26.
3. Taiwan Ministry of Health and Welfare. Top 10 causes of death in 2023. 2024. Available from: https://www.mohw.gov.tw/cp-6650-79055-1.html.
4. US Centers for Disease Control and Prevention. People with certain medical conditions and COVID-19 risk factors. 2024. Available from: https://www.cdc.gov/covid/risk-factors/index.html.
5. Aboueshia M, Hussain MH, Attia AS, *et al*. Cancer and COVID-19: analysis of patient outcomes. Future Oncol 2021; 17(26): 3499-3510.
6. Taiwan Centers for Disease Control, Ministry of Health and Welfare, Taiwan, Interim guidelines for clinical management of SARS-CoV-2 infection. 11th ed. 2021.
7. Khwaja A. KDIGO clinical practice guidelines for acute kidney injury. Nephron Clin Pract 2012; 120(4): c179-84.
8. Dai M, Liu D, Liu M, *et al*. Patients with cancer appear more vulnerable to SARS-CoV-2: a multicenter study during the COVID-19 outbreak. Cancer Discov 2020; 10(6): 783-791.
9. Kuderer NM, Choueiri TK, Shah DP, *et al*. Clinical impact of COVID-19 on patients with cancer (CCC19): a cohort study. Lancet 2020; 395(10241): 1907-1918.
10. Liang W, Guan W, Chen R, *et al*. Cancer patients in SARS-CoV-2 infection: a nationwide analysis in China. Lancet Oncol 2020; 21(3): 335-337.
11. Hedberg P, Parczewski M, Serwin K, *et al*. In-hospital mortality during the wild-type, alpha, delta, and omicron SARS-CoV-2 waves: a multinational cohort study in the EuCARE project. Lancet Reg Health Eur 2024; 38: 100855.
12. Dyer O. Covid-19: Omicron is causing more infections but fewer hospital admissions than delta, South African data show. BMJ 2021; 375: n3104.
13. Martinot M, Eyriey M, Gravier S, *et al*. Predictors of mortality, ICU hospitalization, and extrapulmonary complications in COVID-19 patients. Infect Dis Now 2021; 51(6):518-525.
14. So ACP, McGrath H, Ting J, *et al*. COVID-19 vaccine safety in cancer patients: a single centre experience. Cancers (Basel) 2021; 13(14).
15. Zhang S, Li J, Xu R, *et al*. Safety of COVID-19 vaccination in patients with breast cancer: cross-sectional study in China. JMIR Public Health Surveill 2023; 9: e46009.
16. Seneviratne SL, Yasawardene J, Wijerathne W, *et al*. COVID-19 vaccination in cancer patients: a narrative review. J Int Med Res 2022; 50(3): 3000605221086155.
17. Sun H, Bu F, Li L, *et al*. COVID-19 vaccine response and safety in patients with cancer: an overview of systematic reviews. Front Public Health 2022; 10: 1072137.
18. Mandal A, Singh P, Samaddar A, *et al*. Vaccination of cancer patients against COVID-19: towards the end of a dilemma. Med Oncol 2021; 38(8): 92.
19. Lee ARYB, Wong SY, Chai LYA, *et al*. Efficacy of covid-19 vaccines in immunocompromised patients: systematic review and meta-analysis. BMJ 2022; 376: e068632.
20. Chang MH, Liao KM. The association between COVID-19 vaccination and confirmed patients with hospitalization in Omicron era: a retrospective study. Medicine (Baltimore) 2023; 102(52): e36777.
21. Fendler A, de Vries EGE, GeurtsvanKessel CH, *et al*. COVID-19 vaccines in patients with cancer: immunogenicity, efficacy and safety. Nat Rev Clin Oncol 2022; 19(6): 385-401.
22. Yasin AI, Aydin SG, Sumbul, B, *et al*. Efficacy and safety profile of COVID-19 vaccine in cancer patients: a prospective, multicenter cohort study. Future Oncol 2022; 18(10): 1235-1244.

An Asthma Patient with Eosinophilic Granulomatosis with Polyangiitis Presenting as Multi-Organ Involvement-Case Report and Literature Review

Liang-Shiung Guo[1], Shih-Ming Tsao[2,3], Frank Cheau-Feng Lin[1,3]

Eosinophilic granulomatosis with polyangiitis (EGPA), known as Churg-Strauss syndrome, is a rare autoimmune, small-vessel, eosinophilic vasculitis that is often challenging to recognize early. We reported a middle-aged female with chronic asthma, who underwent lobectomy due to recurrent collapse of the right middle lobe. The subsequent pathology report confirmed a diagnosis of EGPA. The review of her medical history for the past decade showed involvement of multiple organs with nonspecific symptoms related to EGPA. She is currently in stable condition being treated with a combination agent consisting of inhaled corticosteroids and a long-acting beta agonist, as well as an interleukin-5 antagonist. This report provides data to assist clinicians in recognizing the progression of seronegative EGPA, thereby facilitating earlier diagnosis and further treatment. ***(Thorac Med 2025; 40: 117-124)***

Key words: eosinophilic granulomatosis with polyangiitis (Churg-Strauss Syndrome), anti-neutrophil cytoplasmic antibody (ANCA), antinuclear antibody, right middle lobe syndrome, asthma, mepolizumab

Introduction

Eosinophilic granulomatosis with polyangiitis (EGPA) is a systemic inflammatory disease mediated by eosinophils. It gradually reveals eosinophil-mediated tissue infiltration, leading to multi-organ damage. The diagnostic criteria of EGPA include symptoms related to the respiratory, neurological, and gastrointestinal systems, as well as laboratory detection of eosinophils in blood and pathological specimens [1]. Laboratory data for C-anti-neutrophil cytoplasmic antibody (C-ANCA) and P-ANCA are commonly used as indicators, with a positivity rate of only 30% [2, 3] in EGPA patients. ANCA has played a crucial role in the evolution of diagnostic criteria for EGPA and was once considered a key supportive criterion in previous standards [4]. The American College of Rheumatology 2022 guidelines for the diagnosis of EPGA uses a scoring system as the basis for assessment [5]. Overall, the nonspecific

[1]Department of Thoracic Surgery, Chung Shan Medical University Hospital, [2]Department of Chest Medicine, Chung Shan Medical University Hospital, [3]School of Medicine, Chung Shan Medical University.
Address reprint requests to: Dr. Frank Cheau-Feng Lin, Department of Thoracic Surgery, Chung Shan Medical University Hospital, No. 110, Sec. 1, Jianguo N. Rd., South Dist., Taichung City 402, Taiwan (R.O.C.).

nature of its presentation often leads to diagnostic delays. Here, we report the case of a patient with seronegative ANCA, diagnosed as EGPA after surgery for right middle lobe (RML) syndrome.

Case Presentation

The patient was a 64-year-old female without a history of smoking or alcohol consumption, and no significant history of cancer or specific genetic diseases. She has not traveled abroad and has had no known exposure to infectious diseases. The patient had a long history of asthma, managed with a combination inhaler consisting of inhaled corticosteroids and long-acting beta-agonist. She was admitted to our ward for RML lobectomy due to a mass shadow of an unknown nature. A series of imaging follow-ups revealed RML infiltration, which progressed to collapse with enlargement of the mediastinal lymph nodes (Fig. 1).

The patient's initial hospital admission revealed a white blood cell count of 20940/uL (normal range: <11000/uL), with 80% segmented neutrophils. The C-reactive protein (CRP) level was 1.14 mg/dl; creatinine level was 0.55; alanine transaminase (ALT) was 10 IU/L; and electrolyte levels were sodium 144 mg/dl and potassium 3.7 mg/dl.

C-ANCAs were monitored, but remained negative in serology. In addition, to rule out other tumors, endocrine issues, allergies, etc., the patient underwent further blood tests. Among these, there was no elevation in creatine kinase levels. Tumor markers, including carcinoembryonic antigen, carbohydrate antigen-125, and carbohydrate antigen-199, were within normal ranges. Thyroid function tests indicated normal levels of T3, free T4, and thyroid-stimulating hormone. IgE levels were within normal limits (52.8 KU/L; normal <114 KU/L). Allergy tests for 10 allergens conducted at our institution returned negative results. Sputum culture, fungal culture, and acid-fast staining were negative. Computed tomography (CT) scans of the chest and abdomen revealed no significant signs of malignancy.

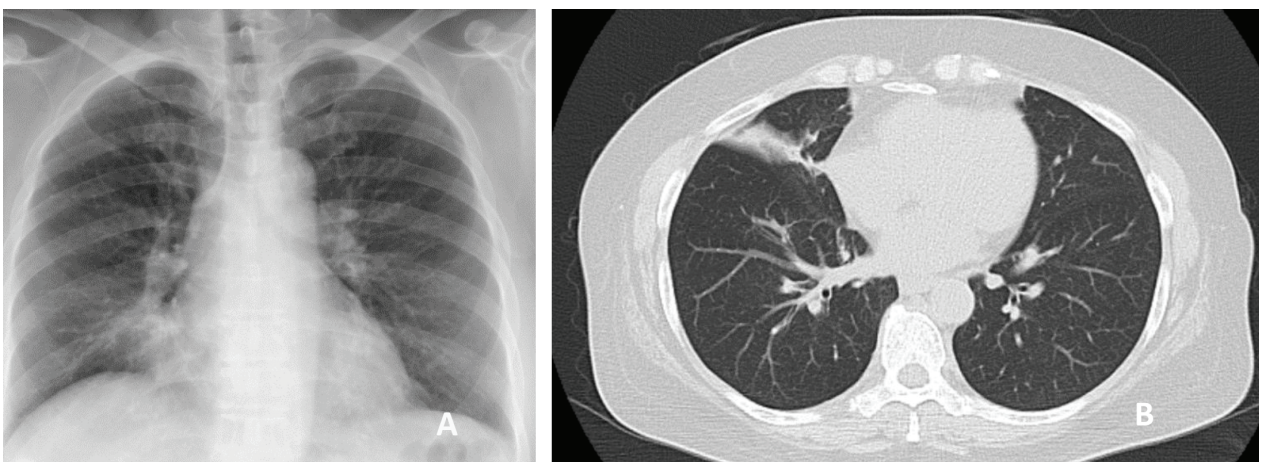

Fig. 1. Initial chest image during early follow-up.
A. There is a noticeable collapse in the right middle lobe, and subsequent follow-ups continue to show varying degrees of this phenomenon.
B. The chest computed tomography (CT) reveals a notable collapse of the right middle lobe.

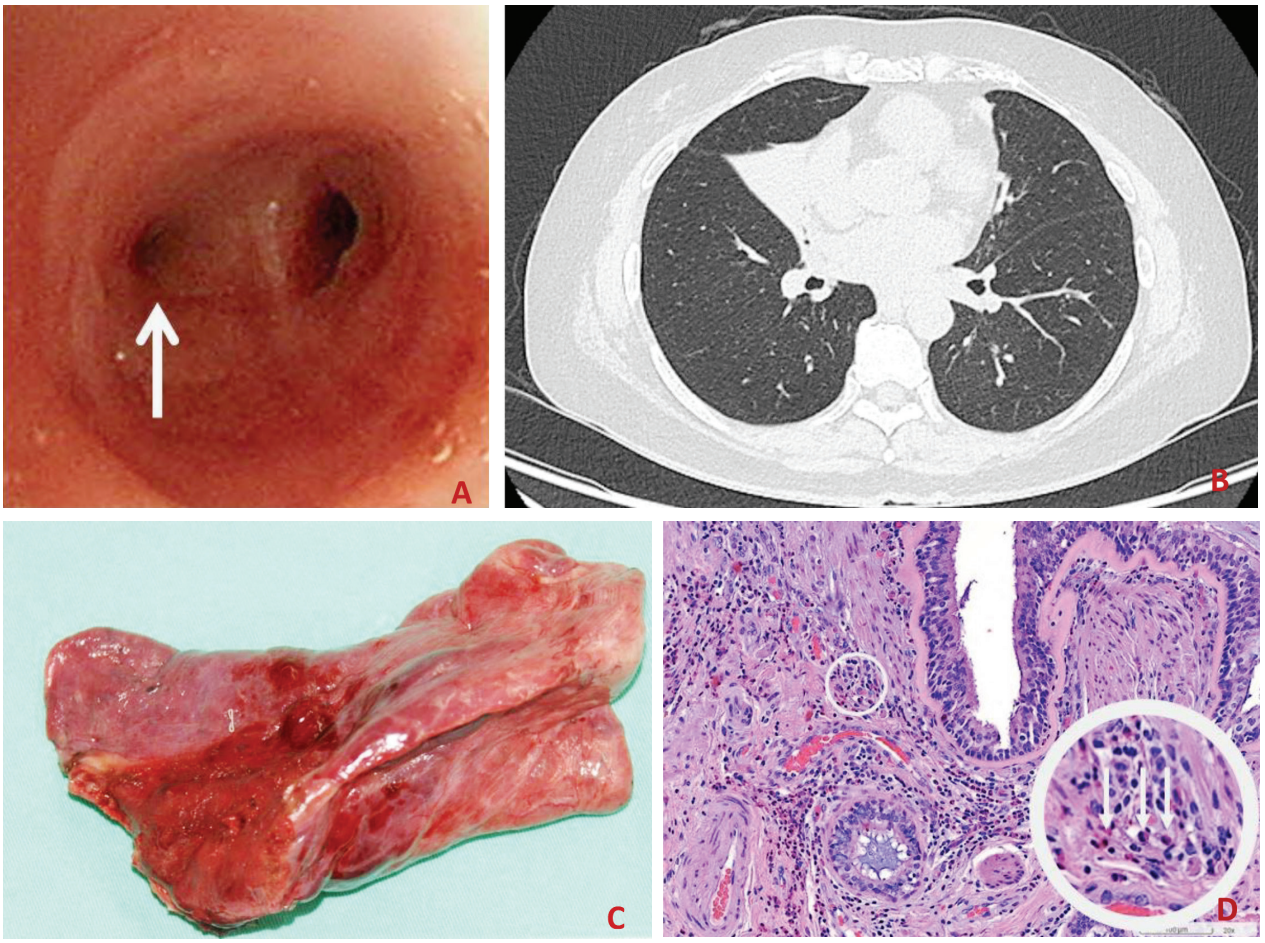

Fig. 2. Preoperation thoracic survey and operation specimen.
A. Polyps within the right truncus intermediate, close to the inlet of the right middle lobe. Biopsy results indicate inflammation. The left side of the picture indicates stenosis of the bronchus (white arrow).
B. Preoperative CT scans for monitoring show a more conspicuous collapse of the right middle lobe.
C. The specimen itself is relatively soft, with only a small amount of secretion. In the present view, the cross-section appears uniform, lacking any local hard masses.
D. Pathology: Eosinophil white blood cell infiltration is present around the blood vessels, indicating eosinophilic vasculitis. The white arrow in the white circle indicates a significant presence of lymphocytes and eosinophils.

Following initial assessment, a bronchoscopy showed excessive vascularization and narrowing of the RML bronchus, but no intrabronchial lesions were found. Ultrasound-guided bronchoscopic biopsy showed signs of inflammation with no malignant cells. Diagnostic thoracic surgery was subsequently scheduled for RML resection and lymph node dissection. Surprisingly, the histopathological examination of the specimen revealed findings consistent with eosinophilic vasculitis and eosinophilic bronchitis, along with non-caseating granulomatous inflammation in the lymph nodes (Fig. 3). Combining these findings with the clinical presentation, the final diagnosis was confirmed as EGPA.

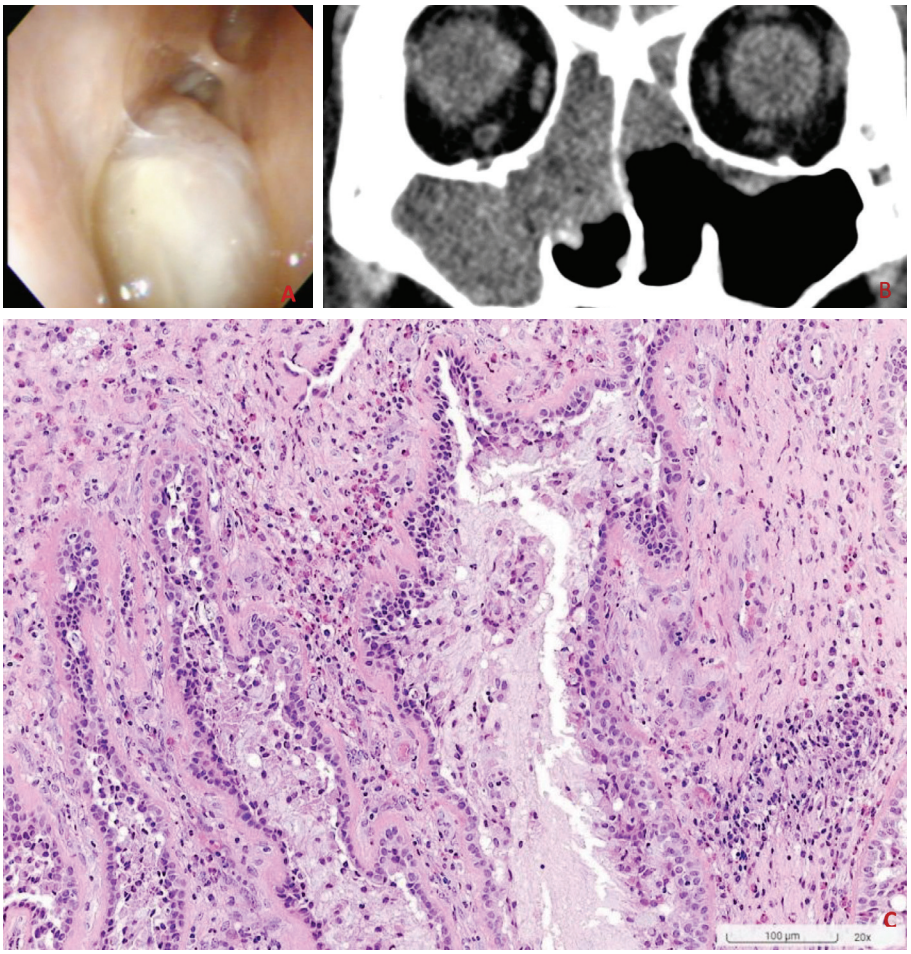

Fig. 3. Otorhinology images.
A. Otoscopy revealed an accumulation of pus within the tympanic membrane.
B. Bilateral nasal cavities show fluid accumulation, with the right side exhibiting more pronounced symptoms.
C. Functional endoscopic sinus surgery pathology: lymphocyte infiltration within the interstitium of the septum epithelium.

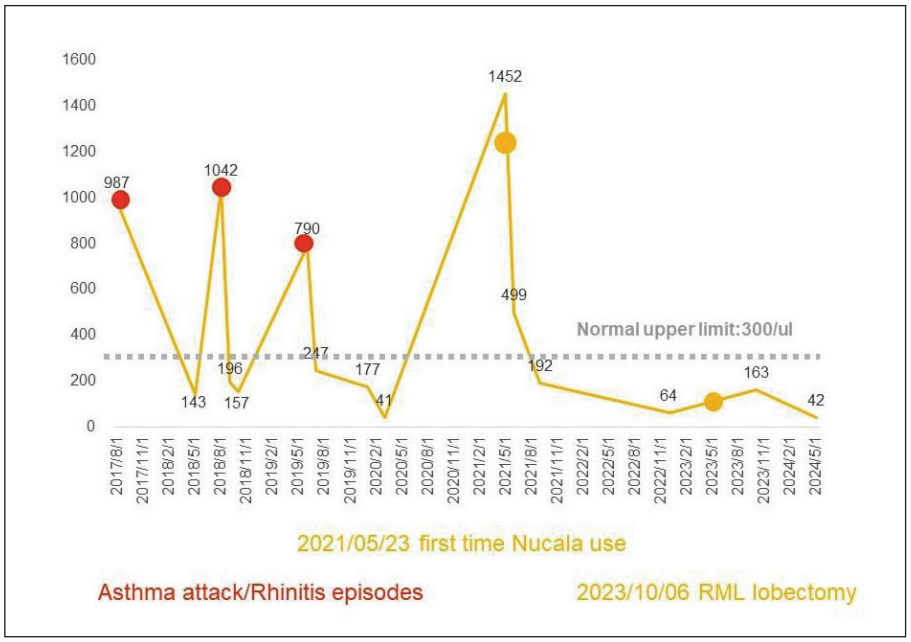

Fig. 4. Eosinophil count change during each hospitalization.
The image shows the eosinophil count at each follow-up and treatment time point. The horizontal grey dashed line at 300 represents the upper limit of the normal reference range. Peaks in the count are often associated with significant events, such as asthma attacks. Yellow dots indicate the times when Nucala was administered, with the exact dates labeled below. Following these administrations, the eosinophil count was generally maintained within the normal range. Surgery was performed when the clinical condition was stable. [[[use "Normal upper limit: 300/ul" in the figure]]]

Clinical physicians started reviewing the medical records for several significant events. Nine years ago, during an episode of pancreatitis, blood tests revealed an elevation in eosinophils, with the eosinophil proportion ranging from 11.6% to 12.0% (count of 636/μL). At that time, immunological diseases were suspected, prompting antinuclear antibody testing, which returned negative, indicating no specific immune issues. Then, 6 years ago, the patient experienced respiratory failure due to exacerbation of asthma, necessitating intubation. Five years ago, she sought treatment at an external facility for intermittent nasal discharge and ear fullness, and was diagnosed with sinusitis and otitis media. She underwent a total of 4 functional endoscopic sinus surgeries, with pathological findings consistent with chronic sinusitis. Notably, pathological specimens also revealed infiltration of eosinophils (as depicted in Fig. 3C). For otitis media, she underwent tympanostomy tube placement and grommet insertion. During treatment, her total white blood cell count peaked at 9.74×10^9/L, with elevated eosinophils (absolute eosinophil count of 1.04×10^9/L; 10.7%). The eosinophil count returned to normal levels during outpatient observation (Fig. 4).

Following thorough review, the patient was prescribed short-term oral prednisone and subcutaneous injection of the anti-IL-5 medication mepolizumab during outpatient visits. During follow-up appointments, the patient reported good control of her asthma with inhalers. There was noticeable improvement in rhinitis and skin rash.

Discussion

Without pathological confirmation, early diagnosis is crucial for EGPA, particularly when there are only clinical manifestations and images. EGPA manifests in 3 stages: the prodromal period, the eosinophilic phase, and the vasculitis phase [6]. According to the American College of Rheumatology 2022 diagnostic criteria, an elevated proportion of eosinophils in the blood and local tissue is a key indicator, and multi-organ involvement occurs throughout the body, including the sinus, lung, pancreas, kidney and brain. It is important to note that ANCA positivity is not a necessary criterion for diagnosing EGPA, based on the American College of Rheumatology 2022 standards; rather, it is considered a negative point, which differs from previous diagnostic criteria (Table 1). The symptoms of these patients are often subtle, making it difficult for clinicians to recognize them, and leading to a delayed diagnosis. Hence, reports of EGPA combined with RML syndrome are extremely limited.

In reviewing this patient's diagnosis and treatment, we can see that the time span from diagnosing RML syndrome to confirming EGPA was 9 years, consistent with previous cases [7]. During a period prior to her surgery, she endured various symptoms, including asthma, sinusitis, dermatitis, otitis media, pancreatitis, and even respiratory failure caused by acute exacerbation of asthma. Due to clinical uncertainty, relevant medications were administered just 2 years before surgery, following a suspicion of EGPA. By the time of admission, she was already in the vasculitic phase, with damage to the RML of the lung requiring surgery. Our case received a score of 7 points, based on the new diagnostic criteria. Despite losing a lung lobe, the diagnosis of EGPA was confirmed, fortunately, by an experienced pathologist.

Epidemiological studies of EGPA in Tai-

Table 1. The 2022 American College of Rheumatology/European Alliance of Associations for Rheumatology Classification Criteria for Eosinophilic Granulomatosis with Polyangiitis.

Criteria applying considerations	
Eosinophilic granulomatosis with polyangiitis when a small/medium vessel vasculitis diagnosis is made Exclusion of alternate diagnosis	
Clinical criteria	
Obstructive airway disease	+3
Nasal polyps	+3
Mononeuritis multiplex	+1
Laboratory and biopsy criteria	
Blood eosinophil count >= 1x 10^9 / Liter	+5
Extravascular eosinophilic-predominant inflammation on biopsy	+2
Positive test for cytoplasmic antineutrophil cytoplasmic antibodies or antiproteinase 3 antibodies	-3
Hematuria	-1

*A score greater than 6 is required to diagnose EGPA, sensitivity of 85% and a specificity of 99%

wan remain unclear. In the Japanese population, EGPA typically occurs between the ages of 49 and 59, with a higher prevalence among females [8]. Over 90% of patients have a history of asthma in the 5-9 years preceding EGPA diagnosis [9]. Clinically, asthma is the most common respiratory disease, present in nearly 90% of patients [10]. Chronic rhinosinusitis is the most common non-thoracic manifestation in 75% of these patients. Cutaneous manifestations occur in two-thirds of patients. Pancreatitis is a rare manifestation in terms of gastrointestinal symptoms. Other commonly discussed systemic diseases involve the cardiovascular, nervous, and lymphatic systems [11-13].

Due to the nonspecific nature of the symptoms, radiological signs may become relatively important in guiding the diagnostic process. Taking the lungs as an example, on high-resolution CT the disease may present as migratory ground-glass opacities (GGOs), transient consolidation, irregular bronchial wall thickening, or small nodules distributed around the bronchi and in the middle lobe area, as well as pleural effusion [14]. The changes observed on consecutive CT scans in this patient may indicate potential progression or evolution of the disease. In a literature review, an Italian report also presented a case similar to RML syndrome, with serum negativity, ultimately diagnosed and treated as RML syndrome [15].

The recommended initial medications for treatment of severe manifestations of EGPA are corticosteroids [16]. In addition, it is recommended to add disease-modifying antirheumatic drugs (DMARDs) during remission. Medication usage should be adjusted based on clinical changes during follow-up [17-18]. Nevertheless, a new choice of therapy has been identified recently -- an anti–interleukin-5 monoclonal antibody known as mepolizumab -- as a therapeutic for people living with EGPA [19-20]. Cases

from Japan reported approximately 50% of patients with EGPA achieved a corticosteroid-free status and protection from organ damage after 3 years of treatment with mepolizumab [21]. Retrospective analysis of our patient's clinical visits for combination inhaler and mepolizumab once a month after surgery found that she had a normal eosinophil count and stable asthmatic condition without further suspicion of a more systemic disease such as recurrent sinusitis, otitis media, or dermatitis issues.

Conclusion

In summary, EGPA is a rare disease that can affect multiple systems and is associated with significant morbidity. It has diverse and non-specific clinical manifestations. The rate of ANCA positivity for this disease is not high, nevertheless the role of eosinophil counts might be a biomarker for EGPA phenotyping. A multidisciplinary approach and appropriate management are critical, and failure to achieve that may result in devastating long-term consequences.

References

1. Abril A, Calamia KT, Cohen MD. The Churg Strauss syndrome (allergic granulomatous angiitis): review and update. Semin Arthritis Rheum 2003; 33(2): 106-14.
2. Vaglio A, Buzio C, Zwerina J. Eosinophilic granulomatosis with polyangiitis (Churg-Strauss): state of the art. Allergy 2013; 68(3): 261-73.
3. Moiseev S, Kronbichler A, Makarov E, *et al*. Association of venous thromboembolic events with skin, pulmonary and kidney involvement in ANCA-associated vasculitis: a multinational study. Rheumatology (Oxford) 2021; 60(10): 4654-4661.
4. Liu LJ, Chen M, Yu F, *et al*. Evaluation of a new algorithm in classification of systemic vasculitis. Rheumatology (Oxford) 2008; 47(5): 708-12.
5. Emmi G, Bettiol A, Gelain E, *et al*. Evidence-Based Guideline for the diagnosis and management of eosinophilic granulomatosis with polyangiitis. Nat Rev Rheumatol 2023; 19(6): 378-393.
6. Yilmaz I, Tutar N, Şimşek AO, *et al*. Clinical and serological features of eosinophilic and vasculitic phases of eosinophilic granulomatosis with poliangiitis: a case series of 15 patients. Turk Thorac J 2017; 18(3): 72-77.
7. Burtson KM, Bishop J. Prevasculitic eosinophilic granulomatosis with polyangiitis. Cureus 2021; 13(4): e14649.
8. Furuta S, Iwamoto T, Nakajima H. Update on eosinophilic granulomatosis with polyangiitis. Allergol Int 2019; 68(4): 430-436.
9. Cottin V, Bel E, Bottero P, *et al*. Respiratory manifestations of eosinophilic granulomatosis with polyangiitis (Churg-Strauss). Eur Respir J 2016; 48(5): 1429-1441.
10. Guillevin L, Cohen P, Gayraud M, *et al*. Churg-Strauss syndrome. Clinical study and long-term follow-up of 96 patients. Medicine (Baltimore) 1999; 78(1): 26-37.
11. Cho WC, Ramlal B, Fiel-Gan M, *et al*. Rare manifestations of Churg-Strauss syndrome with mediastinal and hilar lymphadenopathies: report of an autopsy case. J Pathol Transl Med 2019; 53(1): 66-69.
12. Boggi U, Mosca M, Giulianotti PC, *et al*. Surviving catastrophic gastrointestinal involvement due to Churg-Strauss syndrome: report of a case. Hepatogastroenterology 1997; 44(16): 1169-71.
13. Gerster M, Peker E, Nagel E, *et al*. Deciphering cardiac involvement in systemic inflammatory diseases: noninvasive tissue characterisation using cardiac magnetic resonance is key to improved patients' care. Expert Rev Cardiovasc Ther 2016; 14(11): 1283-1295.
14. Palmucci S, Ini C, Cosentino S, *et al*. Pulmonary vasculitides: a radiological review emphasizing parenchymal HRCT features. Diagnostics (Basel) 2021; 11(12): 2318.
15. Maranini B, Guzzinati I, Casoni GL, *et al*. Case Report: Middle lobe syndrome: a rare presentation in eosinophilic granulomatosis with polyangiitis. Front Immunol 2023; 14: 1222431.
16. Terrier B, Charles P, Aumaitre O, *et al*. ANCA-associated vasculitides: recommendations of the French Vasculitis Study Group on the use of immunosuppressants and

biotherapies for remission induction and maintenance. Presse Med 2020; 49(3): 104031.
17. Ribi C, Cohen P, Pagnoux C, *et al*. Treatment of Churg-Strauss syndrome without poor-prognosis factors: a multicenter, prospective, randomized, open-label study of seventy-two patients. Arthritis Rheum 2008; 58(2): 586-94.
18. Ito, K., Kanemitsu Y, Fukumitsu K, *et al*. Targeting the interleukin-5 pathway improves cough hypersensitivity in patients with severe uncontrolled asthma. Ann Allergy Asthma Immunol 2023; 131(2): 203-208 e1.
19. Ushio Y, Wakiya R, Kato M, *et al*. Two cases of refractory eosinophilic granulomatosis with polyangiitis wherein mepolizumab was effective against pulmonary and ear lesions. Mod Rheumatol Case Rep 2021; 5(2): 327-332.
20. Nara M, Saito M, Abe F, *et al*. A pediatric case of relapsing eosinophilic granulomatosis with polyangiitis successfully treated with mepolizumab. Intern Med 2019; 58(24): 3583-3587.
21. Ueno, M., Miyagawa I, Kawabe A, *et al*. A patient with eosinophilic granulomatosis with polyangiitis successfully weaned from corticosteroids through remission induction therapy with mepolizumab. Mod Rheumatol Case Rep 2022; 6(2): 243-247.

Adenoid Cystic Carcinoma Arising from A Rare Site: A Case Report

Chin-Hua Yo[1], Jing-Quan Zheng[2]

Adenoid cystic carcinoma (ACC) is a rare type of cancer that most commonly arises in the salivary glands but can also occur in other locations, including the nasopharynx, larynx, trachea, lung, liver, and cervix, although less frequently. Patients with ACC are initially asymptomatic, which impedes early detection. No study tool is of clinical value. The diagnosis is confirmed by tissue biopsy. In most cases, ACC patients are treated with surgery first, and this may be followed with postoperative radiotherapy. Patients with locoregional or distant metastases should consider systemic therapy, such as chemotherapy with a single agent or in combination. In this case report, we presented a patient diagnosed with ACC arising from a rare site, found after comprehensive study. Systemic therapy was considered for distant metastases upon diagnosis of this disease. ***(Thorac Med 2025; 40: 125-129)***

Key words: adenoid cystic carcinoma, larynx

Introduction

Adenoid cystic carcinoma (ACC), a rare malignancy that arises mostly from the salivary glands, presents with varying clinical presentations depending on its origin. Its clinical course is indolent. Diagnosis of this disease is mainly based on histopathology. Currently, surgery and/or postoperative radiotherapy is the primary treatment, while chemotherapy is used for palliative care in patients with locoregional and distant metastases. In our case report, the patient's ACC arose from a rare origin, which made our assessment and final diagnosis difficult.

Case Report

This 47-year-old woman was a patient with non-radiographic ankylosing arthritis under daily treatment with sulfasalazine 1000 mg, and reflux esophagitis (GERD grade A) controlled by lansoprazole. She was also a current smoker with an approximately 15-year history of 1 pack per day.

[1]Division of Pulmonary Medicine, Department of Internal Medicine, Shuang Ho Hospital, Taipei Medical University, New Taipei City 23561, Taiwan. [2]Division of Pulmonary Medicine, Department of Internal Medicine, Shuang Ho Hospital, Taipei Medical University, New Taipei City 23561, Taiwan.
Address reprint requests to: Dr. Chin-Hua Yo, Division of Pulmonary Medicine, Department of Internal Medicine, Shuang Ho Hospital, Taipei Medical University, New Taipei City 23561, Taiwan.

She suffered from a dry cough with hoarseness for about 2 months and sought medical attention in our outpatient department. No fever, sputum, rhinorrhea, dyspnea, chest tightness, night sweating, unintentional body weight loss, aspiration, burning sensation in the retrosternal region, or post-nasal drip was reported. In reviewing her medication, no aspirin, angiotensin-converting enzyme inhibitors, or other drugs that may cause this symptom were being used. No environmental exposure or other irritants were mentioned. Physical examination showed no injected throat, barrel chest, stridor, wheezing, or use of an accessory muscle. Chest x-ray was normal. Medication for symptomatic relief was prescribed but failed to control her symptoms.

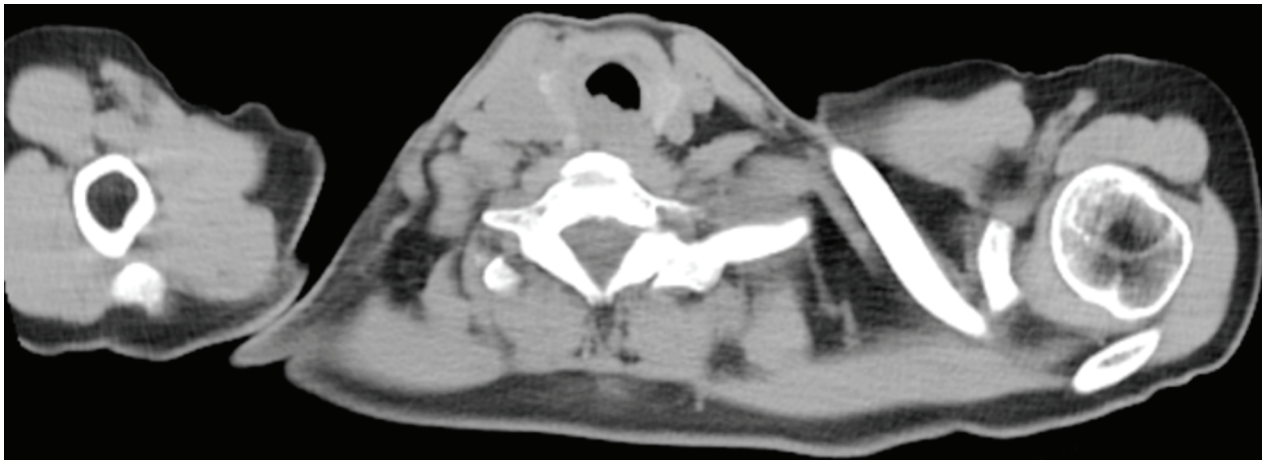

Fig. 1. A tumor in the subglottic region is noted on contrast-enhanced CT of the chest and heart.

Then, she was referred to the Department of Otolaryngology. Laryngoscopy showed normal vocal cord mobility without a visualized tumor. Further studies were arranged. A pulmonary function test with bronchodilator was within normal limits. Computed tomography (CT) of the chest and heart with contrast medium incidentally revealed a tumor in the subglottic region (Fig. 1) with multiple small nodules in the right lung (Fig. 2). Bronchoscopy (Fig. 3) confirmed a subglottic tumor with biopsy of chronic inflammation with focal squamous hyperplasia and mild dysplasia. Surgical biopsy revealed ACC (Fig. 4). Her final diagnosis was ACC with distant metastases. Due to postoperative acute respiratory failure, tracheostomy was performed. Systemic therapy with lenvatinib was initiated. However, she was lost to follow-up in our department and sought a second opinion at another hospital.

Discussion

Adenoid cystic carcinoma (ACC) is a rare malignancy primarily arising from the salivary glands. ACC can also arise from other sites, including the nasopharynx, larynx, lung, skin, breast, liver, and even the cervix, although rarely. It can affect patients of all ages, but is mostly

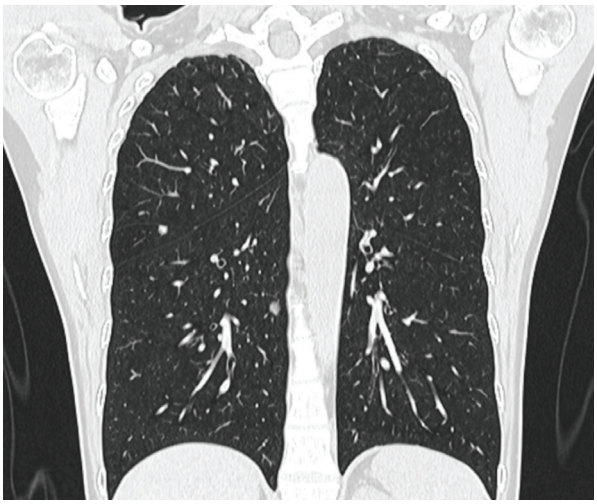

Fig. 2. Multiple small nodules in the right lung are shown in the lung window of CT of the chest and heart.

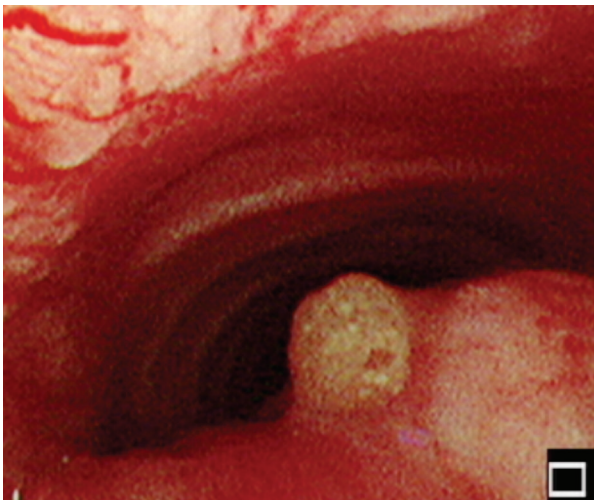

Fig. 3. Under bronchoscopy, a tumor is noted in the subglottic region with partial obstruction of the trachea.

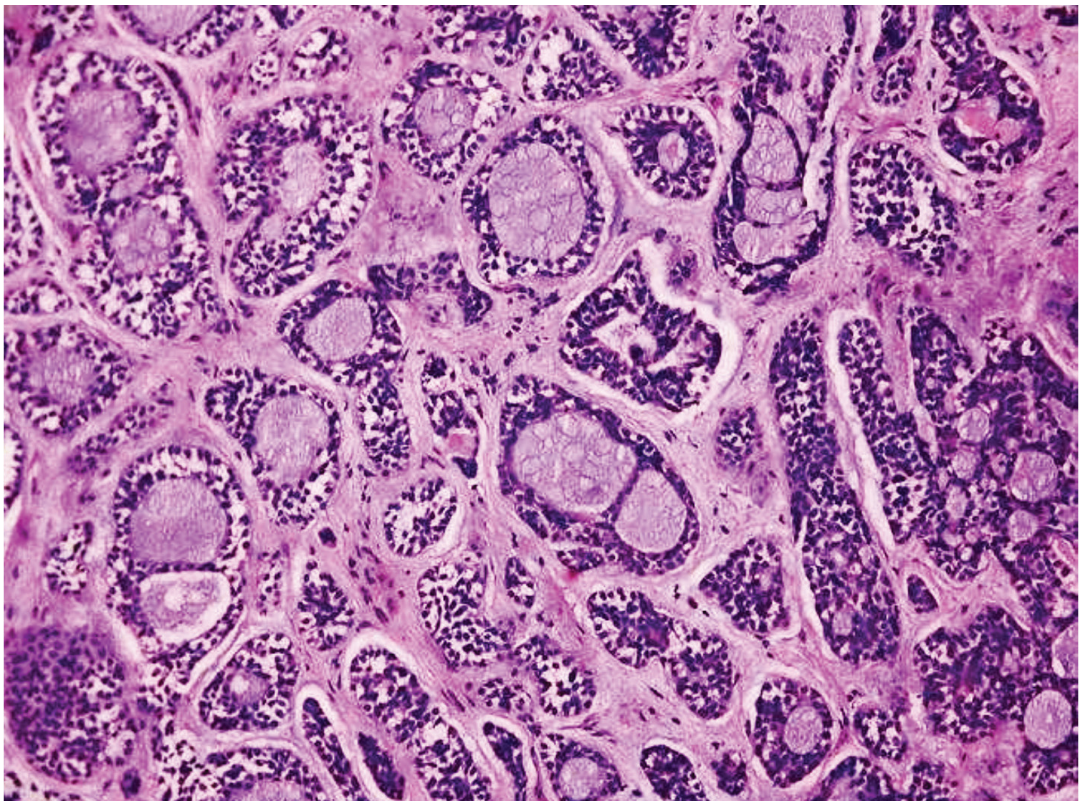

Fig. 4. Adenoid cystic carcinoma with a cribriform pattern.

diagnosed in the fifth or sixth decade of life. It is more common in women [1]. The etiology of this disease is unknown. ACC is also characterized by its indolence, frequent local recurrence and distant metastases. In a retrospective study, the rates of local control, regional control, distant metastases-free and overall survival after 10 years were 78%, 87%, 67%, and 50%, respectively [2].

Clinical presentation in ACC varies with its origin and is always asymptomatic in the early stage. Physical examination, laboratory examination, and radiograph may have no significant value, but CT can be helpful for early detection. However, tissue proof is the gold standard. Histologically, ACC is composed of small basaloid epithelial tumor cells with small to moderate amounts of cytoplasm. Its growth pattern can be classified into cribriform, tubular, and solid growth patterns. Of these 3 growth patterns, the solid growth pattern has been recognized as being of a high grade and having a poorer prognosis [3].

Many cytogenetic studies have revealed that t(6, 9) translocation in ACC results in a fusion of the MYB oncogene to the transcription factor gene NFIB, which can be a potential therapeutic target and a marker for diagnosis [4-5]. A recent proteogenomic analysis divides ACC into cluster I (37%) and II (63%). ACC-I has a worse prognosis with upregulation of MYC and enrichment of NOTCH activating mutations, whereas ACC-II has a better prognosis with upregulation of TP63 and receptor tyrosine kinases [6].

Surgical resection alone and surgery with postoperative radiotherapy are mainstay treatments. Chemotherapy is reserved for palliative treatment in patients with locally recurrent or metastatic ACC. However, there is no consensus on effective treatment, due to the rarity of ACC and the lack of comprehensive studies. A systematic review published in Lancet Oncology in 2011 reported that either single-agent mitoxantrone or vinorelbine can be a reasonable first-line option due to their objective responses and less toxicity. Cisplatin and anthracycline are alternatives for combination chemotherapy [7]. Lymphovascular invasion and a high T classification are independent predictors for prognosis of locoregional control, distant metastases, and survival in patients with ACC [8].

The clinical presentation of our patient was not obvious and became symptomatic with disease progression to the terminal stage. It was difficult for us to get an early and easy diagnosis. Furthermore, her ACC arose from a rare origin with metastases. There is insufficient clinical evidence and consensus for treatment, and there are only a few case reports. Clinically, her treatment followed that of the salivary glands.

Conclusion

ACC is a rare and indolent malignancy. Early detection and timely treatment are difficult for our clinicians. We should always keep in mind that this disease is one of our differential diagnoses. Clinical consensus for its treatment is required to improve patient outcome.

References

1. Zupancic M, Näsman A, Friesland S, *et al*. Adenoid cystic carcinoma, clinical presentation, current treatment and approaches towards novel therapies. Anticancer Res 2024 Apr 1; 44(4): 1325-34.
2. Terhaard CH, Lubsen H, Van der Tweel I, *et al*. Salivary gland carcinoma: independent prognostic factors for locoregional control, distant metastases, and overall survival: results of the Dutch head and neck oncology

cooperative group. Head Neck 2004 Aug; 26(8): 681-93.
3. Moskaluk CA. Adenoid cystic carcinoma: clinical and molecular features. Head Neck Pathol USA 2013 Mar; 7: 17-22.
4. Nordkvist A, Mark J, Gustafsson H, *et al*. Non-random chromosome rearrangements in adenoid cystic carcinoma of the salivary glands. Genes Chromosomes Cancer 1994 Jun; 10(2): 115-21.
5. Persson M, Andrén Y, Mark J, *et al*. Recurrent fusion of MYB and NFIB transcription factor genes in carcinomas of the breast and head and neck. Proc Natl Acad Sci 2009 Nov 3; 106(44): 18740-4.
6. Ferrarotto R, Mitani Y, McGrail DJ, *et al*. Proteogenomic analysis of salivary adenoid cystic carcinomas defines molecular subtypes and identifies therapeutic targets. Clin Cancer Res 2023 Feb 1; 27(3): 852-64.
7. Laurie SA, Ho AL, Fury MG, *et al*. Systemic therapy in the management of metastatic or locally recurrent adenoid cystic carcinoma of the salivary glands: a systematic review. Lancet Oncol 2011 Aug 1; 12(8): 815-24.
8. Ouyang DQ, Liang LZ, Zheng GS, *et al*. Risk factors and prognosis for salivary gland adenoid cystic carcinoma in southern China: a 25-year retrospective study. Medicine 2017 Feb 1; 96(5): e5964.

Anti-synthetase Syndrome with Isolated Pulmonary Manifestation: A Case Report of Rapidly Progressive Respiratory Failure

Yen-Chen Lee[1], Chieh-Jen Wang[2], Wen-Hsiu Wang[3], Chang-Yi Lin[4]

A 77-year-old male diagnosed with anti-synthetase syndrome presented with rapid respiratory failure without musculoskeletal features. Anti-synthetase syndrome is a rare autoimmune disease with a wide spectrum of clinical manifestations involving the lungs, skin, joints and muscles. Eight autoantibodies are associated with the disease, and each has different clinical manifestations that vary slightly based on different anti-aminoacyl-tRNA-synthetase antibodies. Most individuals exhibit musculoskeletal features with varying degrees of interstitial lung disease, but some may exhibit isolated organ involvement only. These presentations pose unique challenges and considerations in the diagnosis and management. ***(Thorac Med 2025; 40: 130-137)***

Key words: Anti-synthetase syndrome, interstitial lung disease, autoantibodies, OJ (isoleucyl)

Introduction

Anti-synthetase syndrome (ASS) is an autoimmune disease characterized by the presence of autoantibodies targeting 1 of several aminoacyl t-RNA synthetases (ARS), along with clinical features including interstitial lung disease (ILD), myositis, Raynaud's phenomenon, arthritis, mechanic's hands and fever [1]. ASS belongs to the family of diseases known as idiopathic inflammatory myopathies, which include polymyositis, dermatomyositis immune-mediated necrotizing myopathy, inclusion body myositis, and myositis overlap syndrome [2]. Among these diseases, ASS is distinguished by the presence of autoantibodies that target the ARS. The ARS play an important role in RNA transcription and protein synthesis. They not only participate in immune system activation as antigens, but also serve in chemo-attractive and cytokine-resembling roles that initiate innate and adaptive pathways [3].

[1]Division of Pulmonary Medicine, Department of Internal Medicine, MacKay Memorial Hospital, Taipei City, Taiwan. Division of Thoracic Medicine, Hsinchu MacKay Memorial Hospital. [2]Division of Pulmonary and Critical Care Medicine, Mackay Memorial Hospital, Taipei, Taiwan. [3]Division of Allergy, Immunology and Rheumatology, Mackay Memorial Hospital, Taipei, Taiwan. [4]Division of Pulmonary and Critical Care Medicine, Mackay Memorial Hospital, Taipei, Taiwan.
Address reprint requests to: Dr. Chieh-Jen Wang, Department of Pulmonary and Critical Care Medicine, Taipei MacKay Memorial Hospital, No.92, Section 2, Zhongshan N Rd, Zhongshan District, Taipei City, 104, Taiwan.

Autoantibodies directed to 8 different ARS have been described: Jo-1 (histidyl), PL-7 (threonyl), PL-12 (alanyl), OJ (isoleucyl), EJ (glycyl), KS (asparaginyl), Zo (phenylalanyl) and Ha (tyrosyl) [4]. Among these 8 ARS, anti-Jo-1 is the most common (30-60%) and anti-OJ is the rarest (<5%) [5]. Despite the sharing of several clinical features among different ARS, there are still considerable differences seen among them. The Jo-1 antibody tends to present musculoskeletal features, and its pulmonary involvement is less pronounced. PL-7 and PL-12 are more prevalent in severe ILD. The OJ antibody tends to be particularly severe in myositis, with higher CK values, more necrosis in muscle biopsy and more profound muscle weakness [3]. However, our case presented a totally opposite clinical manifestation, with ILD as the sole manifestation.

Idiopathic pulmonary fibrosis is more common in men than in women, with adjusted prevalence estimates ranging from 0.33 to 2.51 per 10,000 persons in Europe and 2.40–2.98 per 10,000 persons in North America [6]. The incidence of idiopathic pulmonary fibrosis increases with age [7]. The mean age of patients at diagnosis is around 65–70 years, and it rarely occurs in individuals under 50 years of age; as such, age itself can be a diagnostic criterion [6]. In patients testing positive for anti-OJ antibodies, myositis and ILD can overlap in the clinical presentation. However, conventionally, the disease tends to commence with myositis and ultimately end up with ILD as the sole manifestation [8]. Here, we present the case of a 77-year-old male who had acute respiratory failure and a radiographic pattern consistent with ILD.

Case Presentation

A 77-year-old male presented to the emergency department with shortness of breath persisting for 2 weeks. The patient was born in Taiwan and lived in Taichung City. He had a 60-year history of smoking 1 pack of cigarettes daily, and had a past medical history of hypertension and regular use of anti-hypertensive medication. He did not vape, consume alcohol or use intravenous drugs. The patient was an animal breeder and had a long exposure to sheep and their wool. A week prior to this presentation, he developed a productive cough and labored breathing. Despite receiving symptomatic medication, his symptoms did not improve, but rather deteriorated over time.

At the emergency department, his vital signs were a body temperature of 36.0°C, heart rate of 130 beats per minute, respiratory rate of 30 breaths per minute, and blood pressure of 131/86 mmHg. Chest radiography (Figure 1A) revealed lung consolidation in the right middle lobe, with ground-glass opacities (GGO) in both lungs, that were more pronounced in the lower and peripheral regions. High-resolution computed tomography (HRCT) (Figure 1B) showed diffuse peribronchial infiltration, GGO, and bilateral lower lung consolidations. Laboratory tests indicated leukocytosis (13.3 10^3/uL), and elevated C-reactive protein (4.23 mg/dL), lactate (28.0 mg/dl), and NT-proBNP (5710 pg/ml) levels. Despite receiving oxygen via a mask at 10 L/min, he continued to have shortness of breath with the use of an accessory muscle. Consequently, an endotracheal tube was inserted, and respiration was supported with a mechanical ventilator.

He was admitted to the intensive care unit under the impression of acute respiratory distress syndrome. Owing to high oxygen demand under mechanical ventilation and a poor arterial

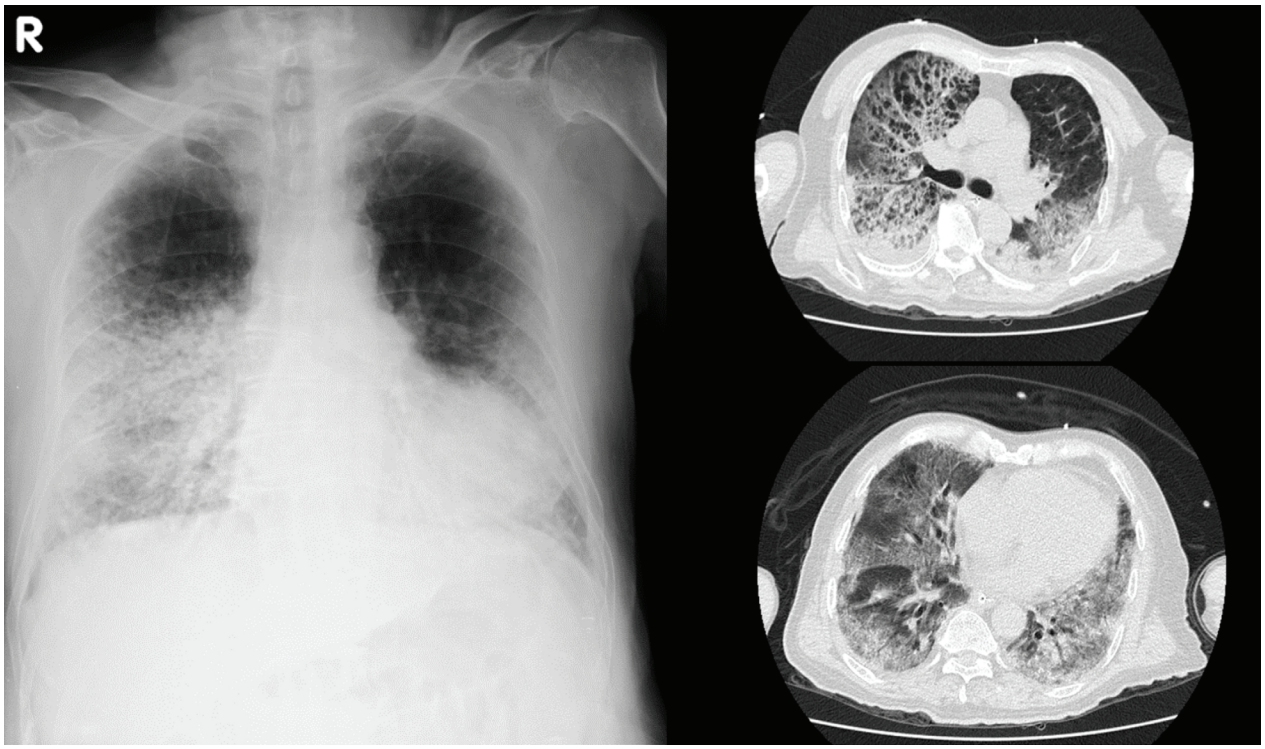

Fig. 1. (A.) Chest radiography showed consolidation in the right middle lung field with GGO in the peripheral and lower lung dominant. (B.) HRCT showed diffuse peribronchial infiltration with GGO plus consolidation in the bilateral lung that was more pronounced in the lower, posterior part of the lung.

oxygen partial pressure to fractional inspired oxygen ratio (131.76), he was placed in the prone position and treated with ceftaroline and levofloxacin. Methylprednisolone 40 mg Q12H and enoxaparin 40 mg QD were administered under the impression of SARS-CoV-2. Bronchoalveolar lavage was performed in order to obtain evidence of the infection. The FilmArray respiratory panel, that included SARS-CoV-2, herpes simplex virus, cytomegalovirus, respiratory synthetial virus, and influenza A and B, reported negative findings. We repeated the SARS-CoV-2 and influenza A and B antigen tests, but the results were still negative.

Since there was no evidence of an infection focus, autoimmune markers including antinuclear factor, anti-double-strand-DNA, anti-cardiolipin IgG/M, anti-SSA, anti-SSB, complement 3, complement 4 (Figure 2A) and autoimmune inflammatory myopathy panels were examined. The result was positive for the OJ antigen (Figure 2B), and therefore ASS was strongly suspected based on the positive serologic test for anti-OJ antibody and the ILD finding. After confirmation, methylprednisolone was kept at 40 mg Q12H as the clinical symptoms and radiographic pattern improved. The patient was returned to the supine position 3 days after being placed in the prone position and was successfully weaned from the ventilator on day 12. He was then transferred to an ordinary ward.

Resolution of the GGO was seen in the follow-up chest radiography on day 16 and in HRCT on day 46 (Figure 3). We gradually tapered down the steroids, and the patient was

Investigation	Results	
Rheumatoid Factor	<10	IU/mL
C3	88	mg/dL
C4	16	mg/dL
Lupus Anticoagulant.	1.10	
Anti-Cardiolipin IGG	<9.4	GPL/mL
Anti-Cardiolipin IGM	17.6	MPL/mL
Anti-β2 glycoprotein 1 IgG	<9.4	SGU/mL
Anti-β2 glycoprotein 1 IgM	<9.4	SMU/mL
Antinuclear Factor	1:80	
Anti-ds-DNA	<1:10	
Anti-ENA Ro52(SSA)	<2.3	CU
Anti-ENA Ro60(SSA)	<4.9	CU
Anti-ENA(SSB)	<3.3	CU

Autoimmune Inflammatory Myopathies 16 Ag (IgG)		
Ro-52	-	-
OJ	++	-
EJ	-	-
PL-12	-	-
PL-7	-	-
SRP	-	-
Jo-1	-	-
PM-Scl75	-	-
PM-Scl100	-	-
Ku	-	-
SAE1	-	-
NXP2	-	-
MDA5	-	-
TIF1 Gamma	-	-
Mi-2 Beta	-	-
Mi-2 Alpha	-	-

備註：
- \- Negative
- +/- Borderline 可疑
- +, ++ Positive 陽性
- +++ Strong Positive 強陽性

Fig. 2. (A.) The autoimmune markers. (B.) The autoimmune inflammatory myopathy panel was positive for the OJ antigene.

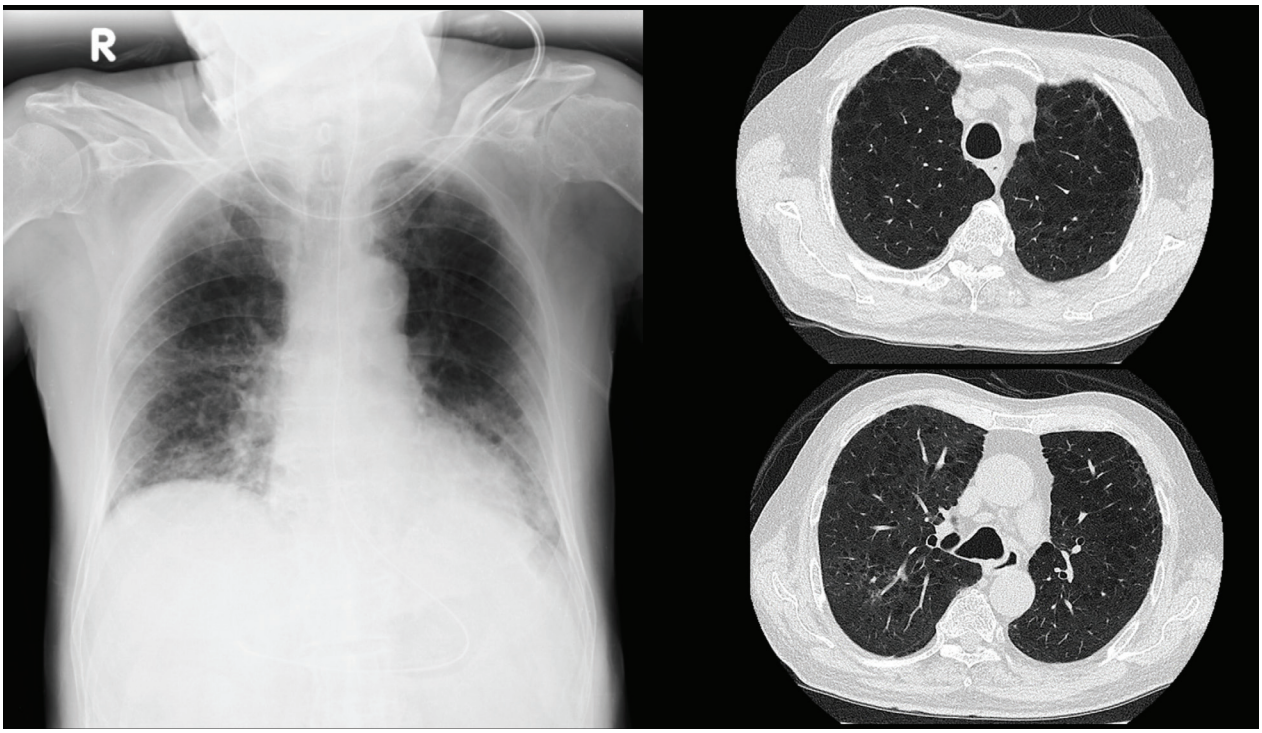

Fig. 3. (A.) Chest radiography showed improvement in the bilateral lung infiltration. (B.) Follow-up HRCT showed improvement in bilateral GGO and consolidation in the bilateral lung field.

discharged 20 days later with methylprednisolone and mycophenolic acid. After discharge, the maintenance dose of 24 mg methylprednisolone and 720 mg mycophenolic acid were continued. We found difficulty in making a slight dose reduction since it caused him to suffer from dyspnea. He was able to undertake light daily activity and occasionally needed oxygen supply. The treatment continued for the next 4 months, until 1 day, the patient developed severe community-acquired pneumonia and passed away soon after admission.

Discussion

Anti-synthetase syndrome (ASS) is a rare clinical condition characterized by the occurrence of a classic clinical triad encompassing myositis, arthritis, and ILD, along with specific autoantibodies that are addressed to different ARS [8]. The ARS family consists of highly conserved cytoplasmic and mitochondrial enzymes, 1 for each amino acid, which are essential for the RNA translation machinery and protein synthesis. Along with their main functions, ARS are involved in the development of immune responses, regulation of transcription, and gene-specific silencing of translation [1]. Although the typical "triad" of arthritis, myositis, and ILD is observed in up to 90% of cases, clinically, the concomitant occurrence of all 3 as the initial presentation is uncommon [9]. In the AENEAS study, the onset was predominantly a single triad feature in all included antibody subgroups, suggesting that the condition can frequently present as isolated ILD, myopathy, or arthritis [10].

The characteristics of disease presentation are slightly different between the 8 ARS. At disease onset, isolated arthritis is the most common presentation in patients with anti-Jo-1, and isolated ILD is the most common presentation in those with anti-PL-7, anti-PL-12, and anti-EJ. The complete triad is the most common pattern in anti-Jo-1, anti-PL7, and anti-EJ; isolated ILD is the most common presentation in those patients with anti-PL-12, and isolated myositis is the most common in those with anti-OJ [8].

There are currently 2 criteria for ASS (Table 1). The first was introduced by Connor *et al*. in 2010, and requires a positive serological test for an ARS in association with at least 1 of the following conditions: evidence of myositis according to the Bohan and Peter criteria; evidence of ILD; evidence of arthritis; persistent unexplained fever; the presence of Raynaud's phenomenon; or the presence of mechanic's hands. Solomon *et al*. proposed other alternative, stricter criteria in 2011 (Table 1) that also require a positive serologic test for ARS plus 2 major (ILD and myositis by Bohan and Peter criteria) or 1 major plus 2 minors (arthritis, Raynaud's phenomenon and mechanic's hands).

Our case was diagnosed based on Connor *et al*.'s criteria, as the patient presented with ILD and was positive for anti-OJ antibodies. There are 4 radiological patterns described in ASS-associated ILD. The most common pattern is non-specific interstitial pneumonia followed by organizing pneumonia, usual interstitial pneumonia and acute interstitial pneumonia [11]. Among those with ILD, the characteristics of CT findings are predominantly lower lobe peripheral opacities, peribronchovascular opacities, lung volume loss, interlobular septal thickening, and thickening of bronchovascular bundles, which correspond to the initial diagnostic CT findings [12]. The development of diffuse ILD is associated with a ventilatory restrictive pattern and a reduction in carbon

Table 3.

Proposed criteria for the diagnosis of ASyS.
ASA: antisynthetase autoantibody; ILD: interstitial lung disease

	Conners *et al*. (2010)	Conners *et al*. (2011)
Serology	Required: Positive serologic testing for an ASA	Required: Positive serologic testing for an ASA
Clinical features	Plus one more of the following: Myositis by the Bohan and Peter criteria; ILD; evidence of arthritis by clinical examination, radiographic findings, or patient self-report; unexplained, persistent fever;Raynaud's phenomenon; mechanic's hands	Plus two major or one major and two minor criteria. Major: ILD; myositis by Bohan and Peter criteria. Minor: arthritis; Raynaud's phenomenon; mechanic's hands

Conners *et al*. in 2010 and Solomon *et al*.(2011) both introduced diagnostic criteria for anti-synthetase syndrome which including positive serological finding and other clinical manifestations.

monoxide diffusion capacity [13]. Furthermore, patients with ASS-associated-ILD tend to have worse pulmonary functioning and radiographic manifestations of ILD than patients with other myositides [14]. Unfortunately, our patient was too weak to undergo a spirometry examination.

Although there is currently no standardized method for treating ASS-associated-ILD, previous retrospective studies have shown that most ASS-associated-ILD patients have a positive response to steroid treatment [15]. Our patient showed great improvement under steroid treatment (methylprednisolone 40 mg Q12H), not just in the clinical picture but also in radiographic features (Figure 3A, B). Frequently used immunosuppressive agents include azathioprine, mycophenolate mofetil, tacrolimus, rituximab, and cyclophosphamide. However, there is little consensus about which agent is preferred, and the use of these agents to treat ASS-associated-ILD is off-label [16-17]. As there are currently no FDA-approved drugs, most regimens are based on retrospective studies and expert opinion. Treatment should be based on the patient's clinical manifestations, focusing on severity and the organs involved [13].

Most ASS-associated-ILD patients generally have a good prognosis in the short term; however, in the long term, 33.3% of patients undergo relapse or deterioration, and their 5-year survival rate is 72.0% to 97.0% [18]. Identifying the cause of acute respiratory failure is a crucial step in initiating a targeted treatment and in improving the diagnosis. Therefore, ASS should be considered among the possible causes, and in cases in which it is suspected, serologic tests should be included in the diagnostic work-up [19].

Conclusion

Anti-synthetase syndrome (ASS) is a rare autoimmune disease with a wide spectrum of clinical presentations. Eight autoantibodies are associated with ASS, each with a slightly different clinical manifestation. Our case illustrates an atypical presentation of anti-OJ antibody with predominant pulmonary involvement and an absence of classical musculoskeletal symp-

toms. However, pulmonary involvement carries higher mortality and morbidity compared to the presentations of musculoskeletal symptoms alone, Furthermore, in cases of ILD with acute respiratory failure, the serologic test for ASS should be taken into consideration, since early diagnosis and treatment are crucial to prevent unfavorable sequelae.

To date, immunosuppression with prednisone and various steroid-sparing agents is the mainstay of therapy. However, convincing data supporting the use of 1 agent over another are lacking. There is no clear evidence for the optimal duration of immunosuppressive therapy, but agreement on limiting long-term steroid use through the use of steroid-sparing agents has been reached. The physician should evaluate the symptoms, the pulmonary function test and radiographs before adjusting the medication.

Finally, further investigation into ASS is warranted to provide insights into the etiological and pathogenetic mechanisms of ILD and ultimately, better outcomes.

Abbreviations

Aminoacyl t-RNA synthetase (ARS)
Anti-synthetase syndrome (ASS)
Interstitial lung disease (ILD)
Ground-glass opacities (GGO)

References

1. Galindo-Feria AS, Notarnicola A, Lundberg IE, *et al*. Aminoacyl-tRNA synthetases: on anti-synthetase syndrome and beyond. Front Immunol 2022 May 13; 13:866087. doi: 10.3389/fimmu.2022.866087. PMID: 35634293; PMCID: PMC9136399.
2. Opinc AH, Makowska JS. Antisynthetase syndrome - much more than just a myopathy. Semin Arthritis Rheum 2021 Feb; 51(1): 72-83. doi: 10.1016/j.semarthrit.2020.09.020. Epub 2020 Dec 22. PMID: 33360231.
3. Patel P, Marinock JM, Ajmeri A, *et al*. A review of antisynthetase syndrome-associated interstitial lung disease. Int J Mol Sci 2024 Apr 18; 25(8):4453. doi: 10.3390/ijms25084453. PMID: 38674039; PMCID: PMC11050089.
4. Mahler M, Miller FW, Fritzler MJ. Idiopathic inflammatory myopathies and the anti-synthetase syndrome: a comprehensive review. Autoimmun Rev 2014 Apr-May; 13(4-5): 367-71. doi: 10.1016/j.autrev.2014.01.022. Epub 2014 Jan 11. PMID: 24424190; PMCID: PMC3970575.
5. Marco JL, Collins BF. Clinical manifestations and treatment of antisynthetase syndrome. Best Pract Res Clin Rheumatol 2020 Aug; 34(4):101503. doi: 10.1016/j.berh.2020.101503. Epub 2020 Apr 11. PMID: 32284267.
6. Pergolizzi JV Jr, LeQuang JA, Varrassi M, *et al*. What do we need to know about rising rates of idiopathic pulmonary fibrosis? A narrative review and update. Adv Ther 2023 Apr; 40(4): 1334-1346. doi: 10.1007/s12325-022-02395-9. Epub 2023 Jan 24. PMID: 36692679; PMCID: PMC9872080.
7. Jo HE, Randhawa S, Corte TJ , *et al*. Idiopathic pulmonary fibrosis and the elderly: diagnosis and management considerations. Drugs Aging 2016 May; 33(5): 321-34. doi: 10.1007/s40266-016-0366-1. PMID: 27083934.
8. Cavagna L, Trallero-Araguás E, Meloni F, *et al*. Influence of antisynthetase antibodies specificities on antisynthetase syndrome clinical spectrum time course. J Clin Med 2019 Nov 18; 8(11):2013. doi: 10.3390/jcm8112013. PMID: 31752231; PMCID: PMC6912490.
9. Huang K, Aggarwal R. Antisynthetase syndrome: a distinct disease spectrum. J Scleroderma Relat Disord 2020 Oct; 5(3): 178-191. doi: 10.1177/2397198320902667. Epub 2020 Feb 18. PMID: 35382516; PMCID: PMC8922626.
10. Wells M, Alawi S, Thin KYM, *et al*. A multidisciplinary approach to the diagnosis of antisynthetase syndrome. Front Med (Lausanne) 2022 Sep 14; 9:959653. doi: 10.3389/fmed.2022.959653. PMID: 36186825; PMCID: PMC9515890.

11. Baratella E, Marrocchio C, Cifaldi R, *et al*. Interstitial lung disease in patients with antisynthetase syndrome: a retrospective case series study. Jpn J Radiol 2021 Jan; 39(1): 40-46. doi: 10.1007/s11604-020-01030-3. Epub 2020 Sep 2. PMID: 32876818; PMCID: PMC7813732.
12. Waseda Y, Johkoh T, Egashira R, *et al*. Antisynthetase syndrome: pulmonary computed tomography findings of adult patients with antibodies to aminoacyl-tRNA synthetases. Eur J Radiol 2016 Aug; 85(8): 1421-6. doi: 10.1016/j.ejrad.2016.05.012. Epub 2016 May 24. PMID: 27423682.
13. Dei G, Rebora P, Catalano M, *et al*. Functional progression in patients with interstitial lung disease resulted positive to antisynthetase antibodies: a multicenter, retrospective analysis. J Clin Med 2020 Sep 21; 9(9):3033. doi: 10.3390/jcm9093033. PMID: 32967131; PMCID: PMC7565737.
14. Marco JL, Collins BF. Clinical manifestations and treatment of antisynthetase syndrome. Best Pract Res Clin Rheumatol 2020 Aug; 34(4): 101503. doi: 10.1016/j.berh.2020.101503. Epub 2020 Apr 11. PMID: 32284267.
15. Zhan X, Yan W, Wang Y, *et al*. Clinical features of anti-synthetase syndrome associated interstitial lung disease: a retrospective cohort in China. BMC Pulm Med 2021 Feb 12; 21(1): 57. doi: 10.1186/s12890-021-01399-5. PMID: 33579248; PMCID: PMC7881640.
16. Witt LJ, Curran JJ, Strek ME. The diagnosis and treatment of antisynthetase syndrome. Clin Pulm Med 2016 Sep; 23(5): 218-226. doi: 10.1097/CPM.0000000000000171. PMID: 27594777; PMCID: PMC5006392.
17. Kannappan R, Kumar R, Cichelli K, *et al*. A review of myositis-associated interstitial lung disease. J Clin Med 2024 Jul 11; 13(14): 4055. doi: 10.3390/jcm13144055. PMID: 39064092; PMCID: PMC11278012.
18. Yamakawa H, Hagiwara E, Kitamura H, *et al*. Predictive factors for the long-term deterioration of pulmonary function in interstitial lung disease associated with anti-aminoacyl-tRNA synthetase antibodies. Respiration 2018; 96(3): 210-221. doi: 10.1159/000488358. Epub 2018 May 16. PMID: 29768275.
19. Vuillard C, Pineton de Chambrun M, de Prost N, *et al*. Clinical features and outcome of patients with acute respiratory failure revealing anti-synthetase or anti-MDA-5 dermato-pulmonary syndrome: a French multicenter retrospective study. Ann Intensive Care 2018 Sep 11; 8(1): 87. doi: 10.1186/s13613-018-0433-3. PMID: 30203297; PMCID: PMC6131681.

Ectopic Intrapericardial Thymoma With Refractory Myasthenia Gravis: Case Report and Review of Literature

Cheng-Jung Lin[1,2], Tsai-Wang Huang[1]

Thymomas, primarily located in the anterior mediastinum, rarely occur in the intrapericardial region. We reported a 31-year-old male who was diagnosed with thymoma with myasthenia gravis (MG). Initial robotic-assisted thoracic surgery with thymectomy was performed, but refractory MG symptoms persisted. Due to the residual tumor, the patient underwent sternotomy, and an ectopic intrapericardial thymoma was resected. The postoperative course was uneventful, and the MG symptoms were under control. Accurate imaging, particularly magnetic resonance imaging, is crucial for diagnosis, while fluorodeoxyglucose-positron emission tomography is ineffective for ectopic thymoma detection. Minimally invasive surgery is commonly used for early thymomas, but open surgery may be preferable for cases with suspected pericardial invasion. Our experience underscored the importance of meticulous imaging and surgical planning to avoid missed diagnoses and incomplete resections of ectopic thymomas, particularly in refractory MG cases. ***(Thorac Med 2025; 40: 138-143)***

Key words: Ectopic intrapericardial thymoma, refractory myasthenia gravis, robotic-assisted thoracic surgery, sternotomy

Introduction

Thymoma is an epithelial tumor that originates from the thymus, and 96% of thymomas are in the anterior mediastinum. Ectopic thymomas are thought to originate from aberrant thymic tissue that migrated during embryologic development, and are found most commonly in the cervical region, followed by the lungs and pleura [1]. Ectopic thymomas described as intrapericardial are rare. To date, according to literature reviews, 9 cases of pericardial thymomas have been reported [2-10], and only 2 have been documented with myasthenia gravis (MG) [5, 10].

Case Report

Our patient was a 31-year-old male with a history of coronary artery disease. He visited

[1]Division of Thoracic Surgery, Department of Surgery, Tri-Service General Hospital, National Defense Medical Center, Taipei, Taiwan, Republic of China. [2]Division of Thoracic Surgery, Department of Surgery, Kaohsiung Armed Forces General Hospital, Kaohsiung, Taiwan, Republic of China.
Address reprint requests to: Dr. Tsai-Wang Huang, Division of Thoracic Surgery, Department of Surgery, Tri-Service General Hospital, 325, Cheng-Kung Road, Section 2, Taipei 114, Taiwan, Republic of China.

our outpatient department in the neurology division in March 2023 due to vertical diplopia, numbness of the right face, and ptosis for 1 week. After excluding a brain lesion, admission was arranged for detailed examination. The repetitive stimulation test of the right facial nerve showed decremental change with a more than 9% reduction, which is suggestive of MG. The follow-up positive result of an acetylcholine receptor antibody supported the impression of MG. Owing to the high level of correspondence between MG and thymoma, contrast-enhanced computed tomography (CT) of the chest was arranged. The CT of the chest revealed an enhancing mass (size: about 3.2 cm) in the left anterior mediastinum, initially suspected to be a typical thymoma. However, the possibility of an ectopic thymoma was not recognized at that time (Fig. 1). Physical examinations were unremarkable, and laboratory examinations were within normal ranges.

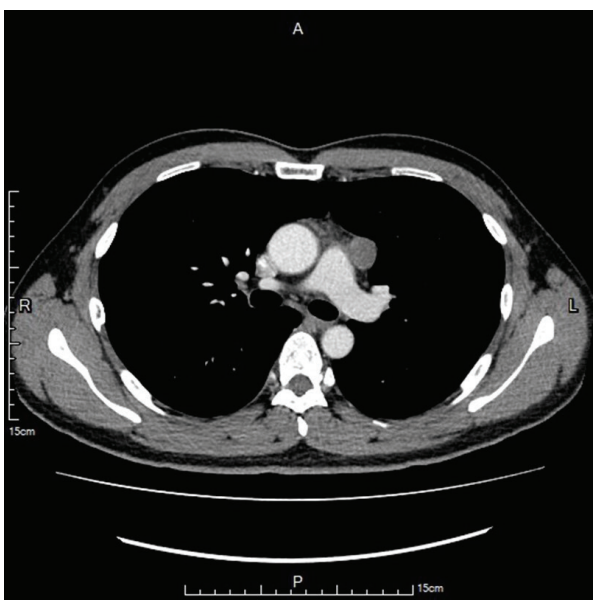

Fig. 1. Chest CT showed an enhancing mass over the left anterior mediastinum, initially presumed to be a typical thymoma.

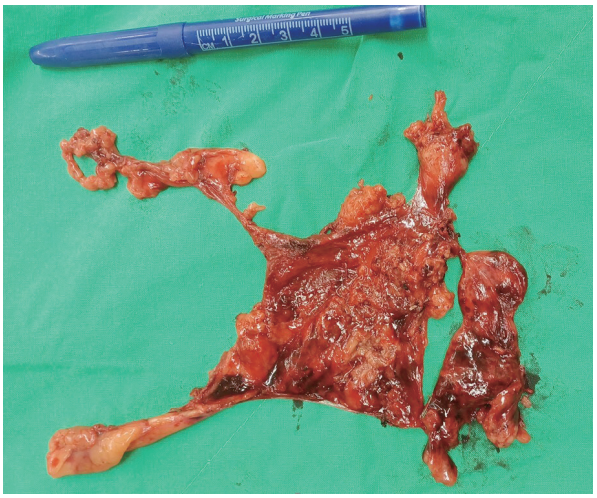

Fig. 2. Thymic tissue resected by robot-assisted thoracic surgery, yellow to brown in color and soft in consistence.

Robot-assisted thoracic surgery with thymectomy then was performed under general anesthesia. After entering the thoracic cavity, the protruding thymic tissue was observed with severe adhesion to the peripheral great vessels, and was removed carefully. The thymic tissue measured 9.8 x 6.5 x 1.8 cm in size, and was 59 gm in weight, yellow to brown in color and soft in consistence (Fig. 2). The specimen was sent for pathological evaluation. The pathology report indicated thymic lymphoid hyperplasia, with no evidence of thymoma, meaning an R0 resection was not achieved. However, we initially believed that the tumor had been fully resected during the robotic-assisted thymectomy, as the entire thymic tissue was removed. The postoperative course was uneventful. After 5 courses of plasma exchange therapy, his symptoms of MG improved, and the patient was discharged 2 weeks after surgery.

Post-surgery, the patient had regular medication with cholinesterase inhibitors, immune modulators, and steroids. However, the patient's symptoms of MG appeared off and on.

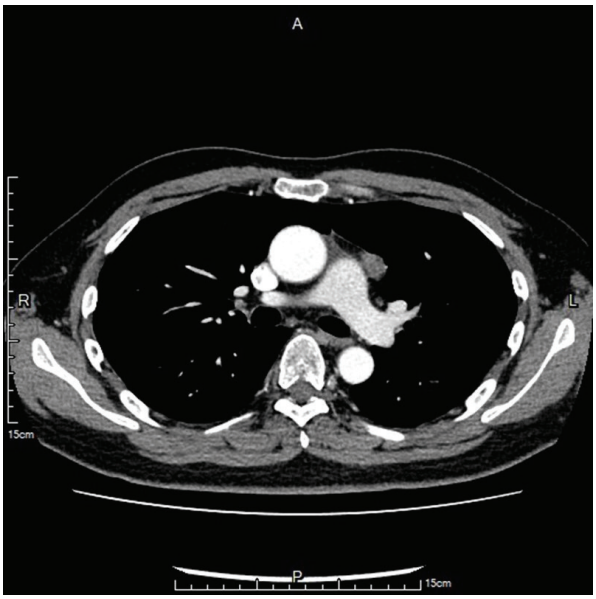

Fig. 3. Follow-up chest CT showed a smaller tumor at the same site, suggesting incomplete removal and residual thymoma.

The patient was admitted twice, in May and August 2023, due to severe ptosis and general weakness. Each time, after plasma exchange therapy, his symptoms resolved, but recurred a few months later. In October 2023, the patient's symptoms of MG exacerbated. He suffered from dysphagia and dyspnea other than ptosis. Plasma exchange therapy was arranged but showed limited response. Due to refractory MG, he received contrast-enhanced CT of the chest, which revealed an enhancing nodule (size: about 2.05 cm) in the left anterior mediastinum. This tumor was smaller than the previous tumor, and appeared at the original surgical site with similar imaging characteristics. Based on the image, incomplete removal was suggested and a residual thymoma was initially considered (Fig. 3).

A chest surgeon was consulted for evaluation of surgical intervention. After discussion, we decided to perform median sternotomy to manage the possibility of adhesion and explore the residual thymic lesion. After median sternotomy, a soft mass was noted left lateral to the heart (Fig. 4) and was then resected. We carefully checked the anterior mediastinal space through inspection and palpation. Another hard mass was found within the pericardium. Pericardiotomy was done, and an intrapericardial tumor then was resected, along with a part of the pericardium (Figs. 5, 6). The pericardium defect was repaired by artificial graft. The 2 specimens were sent for pathological evaluation. The first resected tumor was compatible with stiches granuloma.

Microscopically, the intrapericardial tumor was encapsuled, measuring 3.6 x 3.1 cm in size,

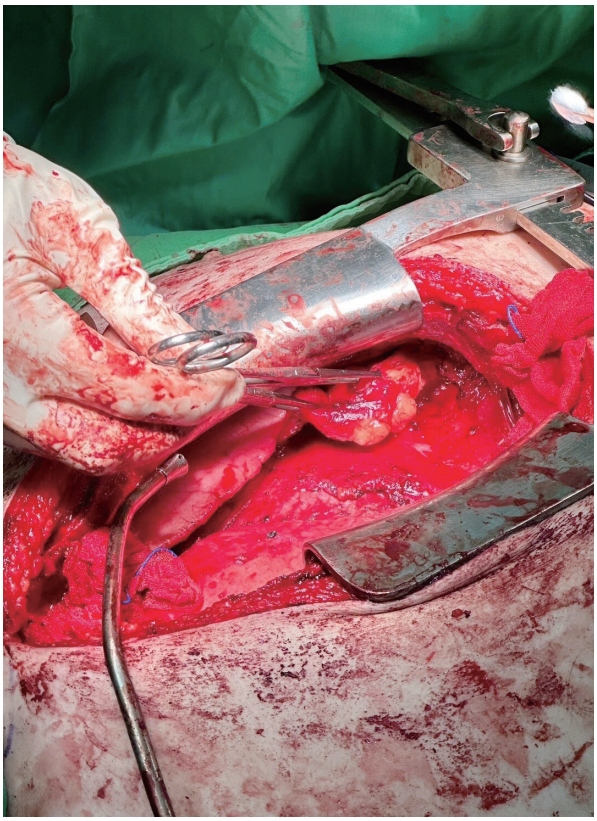

Fig. 4. After median sternotomy, a soft mass was found left lateral to the heart.

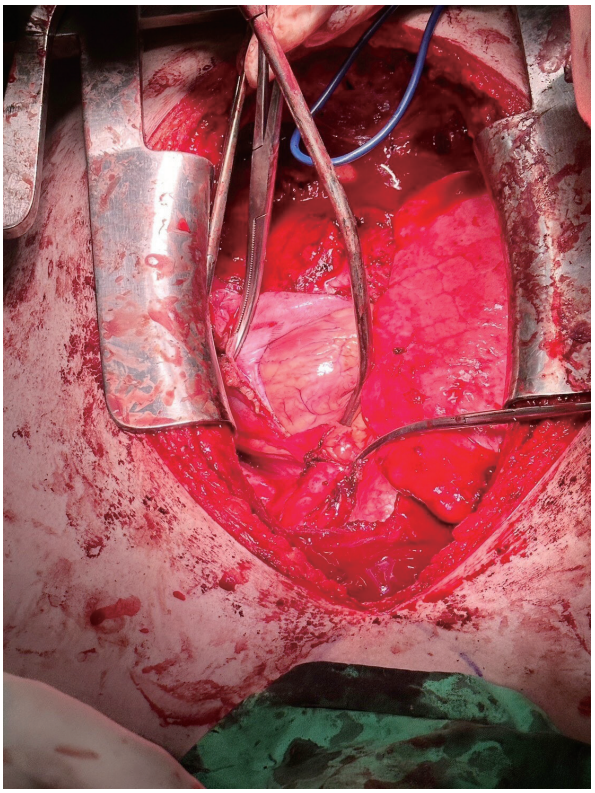

Fig. 5. After opening the pericardium, an intrapericardial tumor was found.

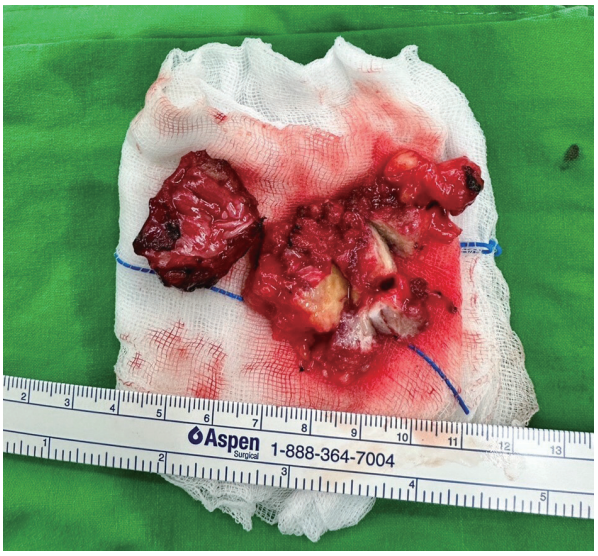

Fig. 6. The intrapericardial tumor was resected with partial pericardium.

within the ectopic thymic tissue. The pathology of the intrapericardial tumor confirmed the diagnosis of ectopic intrapericardial thymoma, WHO type B3, pT1aN0M0, stage I, Masaoka stage I. The patient was discharged uneventfully 2 weeks after the surgery. His condition was stable, with a regular follow-up every 3 months.

Discussion

Thymoma is a rare epithelial tumor, with an incidence of 0.13 per 100,000 persons [11]. The vast majority of thymomas are found within the anterior mediastinum; ectopic thymomas have been documented in merely 4% of cases [1]. This uncommon tumor sometimes involves the heart, usually as metastatic growth originating from the mediastinum. Thymomas infrequently arise from the intrapericardial space, and account for only 7% of all ectopic thymomas. Its presentation can range from being asymptomatic to experiencing chest pain, weight loss, fever, and cardiac symptoms. Because of the limited space of the pericardium, cardiac symptoms including cardiac enlargement, pericardial effusion, heart failure, and cardiac tamponade sometimes can be fatal or require emergency surgical intervention. However, preoperative diagnosis is seldom achieved, and metastatic carcinoma or lymphoma is more frequently considered, particularly in cases featuring a pericardial mass lesion and concomitant pericardial effusion [1].

Accurate imaging of the thymic tumor is crucial for diagnosis. Identification of a possible invasion to surrounding tissues and the presence of ectopic thymoma play important roles in complete resection. The diagnostic information provided by the radiologist will absolutely predict the decision of the chest sur-

geon [12]. Although CT is commonly used for diagnosing thymomas, it can have limitations in detecting ectopic lesions, as was the case here. In hindsight, magnetic resonance imaging (MRI) might have better delineated the tumor's intrapericardial location. Initially, we did not perform MRI, as the lesion was presumed to be a typical thymoma, based on CT findings. In young patients, chemical shift MRI has been superior to CT and conventional MRI in differentiating thymoma and identifying the precise tumor margin. In older patients, thymic tissue is replaced predominantly by fat. Therefore, in elderly patients, fat suppression MRI should be considered to define exact tumor margins [13, 14]. With regard to fluorodeoxyglucose-positron emission tomography (FDG-PET), El-Bawab *et al*. confirmed that it was ineffective in detecting ectopic thymoma [15]. (Dr., El-Bawab is not the name used in reference number 15. Please check.)

In a recent review and meta-analysis of published literature, minimally invasive surgery was widely utilized for early-stage thymomas. Minimally invasive surgery offers comparable oncological outcomes and a lower incidence of complications [16]. Robotic-assisted surgery, compared with other minimally invasive techniques, provides a high-resolution 3-dimensional view and improved dexterity that allows for a safe dissection around vulnerable structures, such as nerves and vessels [17]. However, the robot lacks tactile feedback, and the surgeon is placed far from the patient, in a nonsterile fashion [18]. Cheng and colleagues have compiled a list of criteria for selecting candidates for minimally invasive thymoma resection: a location in the anterior mediastinum, tumor encapsulation, a distinct fat plane between the tumor and vital organs, the existence of residual, normal appearing thymic tissue, no mass compression effect, and unilateral tumor predominance [19].

In our case, the pre-operative chest CT could only hint at the existence of a left anterior mediastinal mass adjacent to the pericardium. We performed robotic-assisted surgery at first, and believed the tumor was adequately resected with total thymectomy. However, the ectopic intrapericardial thymoma was missed, and presented refractory MG. The limitations of preoperative imaging, which did not clearly identify the ectopic intrapericardial thymoma, and the absence of tactile feedback with the robotic system, led to the missed diagnosis.

During the second procedure, we choose sternotomy to explore the residual thymic lesion. Based on inspection and palpation, the ectopic intrapericardial thymoma was found and resected smoothly. In our opinion, MRI should be always considered, particularly for those thymomas without a clear margin or clinical staging. For thymomas with confirmed or potential pericardial invasion, the open method should be considered first, rather than minimally invasive surgery. The lack of tactile feedback may cause the ectopic lesion to be missed and result in an inadequate resection.

Conclusion

This case emphasizes the complexities of diagnosing of ectopic intrapericardial thymomas and highlights the importance of preoperative imaging, particularly MRI, for accurate tumor delineation. This case also suggests that open surgical approaches may be more effective than minimally invasive techniques for ensuring complete resection in cases with potential pericardial invasion. Ongoing management with immunosuppressive therapy and careful follow-

up is crucial for patients with MG and thymic tumors.

References

1. Weissferdt A, Moran CA. The spectrum of ectopic thymomas. Virchows Arch 2016; 469(3): 245-54.
2. Iliceto S, Quagliara D, Calabrese P, *et al*. Visualization of pericardial thymoma and evaluation of chemotherapy by two-dimensional echocardiography. Am Heart J 1984; 107(3): 605-6.
3. Salih Deveci M, Ceyhan K, Deveci G, *et al*. Pericardial rhabdomyomatous spindle cell thymoma with mucinous cystic degeneration. Histopathology 2001; 38(5): 479-81.
4. Theodore S, Parija C, Neelakandhan KS. Giant ectopic pericardial thymoma. Indian J Thorac Cardiovasc Surg 2004; 20: 102-103.
5. Azoulay S, Adem C, Gatineau M, *et al*. Pericardial ectopic thymoma. Virchows Archiv 2005; 446: 185-188.
6. Arai H, Rino Y, Fushimi K, *et al*. Pericardial ectopic thymoma presenting with cardiac tamponade: report of a case. Surg Today 2015; 45: 1200-1204.
7. Zoroufian A, Shirzad M, Shahbazi N, *et al*. Bloody pericardial effusion with a huge pericardial mass: a case report. J Tehran Heart Cent 2020; 15(1): p. 35.
8. Mirra M, Zanella M, Bussani R, *et al*. Intrapericardial thymoma. Arch Pathol Lab Med 1997; 121(1): 59.
9. Tormoehlen LM, Pascuzzi RM. Thymoma, myasthenia gravis, and other paraneoplastic syndromes. Hematol Oncol Clin North Am 2008; 22(3): 509-526.
10. Tsai Y-H, Ko K-H, Yen H, *et al*. Intrapericardial thymoma presented as pericardial tamponade with post-operative myasthenia gravis. Medicina 2022; 58(5): 609.
11. Engels EA. Epidemiology of thymoma and associated malignancies. J Thorac Oncol 2010; 5(10): S260-S265.
12. Ottlakan A, Borda B, Morvay Z, *et al*. The effect of diagnostic imaging on surgical treatment planning in diseases of the thymus. Contrast Media Mol Imaging 2017 Jan 10; 2017: 9307292.
13. Popa GA, Preda EM, Scheau C, *et al*. Updates in MRI characterization of the thymus in myasthenic patients. J Med Life 2012; 5(2): 206.
14. Li K, Yang D-W, Hou S-F, *et al*. Chemical shift and fat suppression magnetic resonance imaging of thymus in myasthenia gravis. Can J Neurolog Sci 2014; 41(6): 782-786.
15. Akamine T, Nakagawa K, Ito K, *et al*. Role of flourine-18 fluorodeoxyglucose positron emission tomography in thymic pathology. Eur J Cardiothorac Surg 2007; 31(4): 731-736.
16. Friedant AJ, Handorf EA, Su S, *et al*. Minimally invasive versus open thymectomy for thymic malignancies: systematic review and meta-analysis. J Thorac Oncol 2016; 11(1): 30-38.
17. Marulli G, Maessen J, Melfi F, *et al*. Multi-institutional European experience of robotic thymectomy for thymoma. Ann Cardiothorac Surg 2016; 5(1): 18.
18. Augustin F, Schmid T, Sieb M, *et al*. Video-assisted thoracoscopic surgery versus robotic-assisted thoracoscopic surgery thymectomy. Ann Thorac Surg 2008; 85(2): S768-S771.
19. Cheng Y-J, Hsu J-S, Kao E-L. Characteristics of thymoma successfully resected by video thoracoscopic surgery. Surg Today 2007; 37: 92-196.

Pulmonary Melioidosis Mimicking Lung Cancer Diagnosed by Surgical Resection and Cured by Adequate Antibiotic Eradication Therapy: A Case Report and Literature Review

Kai-Yu Huang[1], En-Kuei Tang[2], Herng-Sheng Lee[3], I-Yuan Chen[1], Kuo-An Chu[1,4]

Melioidosis is an infectious disease caused by the Gram-negative bacterium *Burkholderia pseudomallei*, which is prevalent in Southeast Asia and northern Australia. Several risk factors have been identified for melioidosis infection, but its diagnosis remains challenging due to the wide variation of its clinical manifestations. Treatment of melioidosis requires appropriate antibiotics therapy, and, if necessary, surgical interventions for diagnosis or treatment should be considered. Here, we report a rare case of pulmonary melioidosis in a patient with a previous history of resected early-stage non-small cell lung cancer, presenting as an incidentally found asymptomatic, solitary pulmonary nodule. Due to a suspicion of recurrent metastatic malignancy, surgical removal of the lesion was arranged. Surprisingly, *Burkholderia pseudomallei*, rather than malignancy, was detected in tissue bacterial culture. Treatment with trimethoprim-sulfamethoxazole, and later, doxycycline plus amoxicillin-clavulanate, was prescribed for a total of 5 months, resulting in successful resolution without recurrence. ***(Thorac Med 2025; 40: 144-149)***

Key words: *Burkholderia pseudomallei*, COPD, lung cancer, melioidosis

Introduction

Melioidosis is an infectious disease prevalent in Southeast Asia and northern Australia [1] that is caused by the Gram-negative bacterium *Burkholderia pseudomallei*. Previous studies have identified several risk factors for developing melioidosis, including chronic lung diseases and cancer [2]. Common clinical presentations include pneumonia, and genitourinary and skin infections. Melioidosis can also cause severe infection such as bacteremia or even tissue abscesses with multi-organ involvement [3]. Early diagnosis is crucial for a better prognosis,

[1]Division of Chest Medicine, Kaohsiung Veterans General Hospital, Kaohsiung, Taiwan. [2]Division of Thoracic Surgery, Kaohsiung Veterans General Hospital, Kaohsiung, Taiwan. [3]Department of Pathology and Laboratory Medicine, Kaohsiung Veterans General Hospital, Kaohsiung, Taiwan. [4]School of Medicine, College of Medicine, National Sun Yat-sen University, Kaohsiung, Taiwan.
Address reprint requests to: Dr. Kuo-An Chu, Division of Chest Medicine, Kaohsiung Veterans General Hospital, Kaohsiung, Taiwan, No. 386, Dazhong 1st Rd., Zuoying Dist., Kaohsiung City 813, Taiwan (R.O.C.).

since traditional empirical antibiotic regimens for suspected bacterial sepsis seldom cover *Burkholderia pseudomallei* [4]. Diagnosis of melioidosis can be challenging because of its varied and non-specific clinical manifestations mimicking many other diseases, including lung malignancy [5].

Here, we report a case of pulmonary melioidosis presenting as a single nodular lesion mimicking metastatic lung cancer. The final diagnosis was confirmed through surgical biopsy and tissue culture.

Case Description

The patient was a 71-year-old male with a smoking history of more than 30 years, who received regular follow-up at the pulmonology outpatient department for chronic obstructive pulmonary disease and bronchiolitis obliterans with organizing pneumonia. He had been diagnosed as having pulmonary squamous cell carcinoma (SCC) of the right upper lobe (RUL), pT1bN0M0, stage IA2, through video-assisted thoracoscopic surgery (VATS) wedge resection (WR) of the RUL in June 2019. No further adjuvant chemoradiotherapy was arranged for the patient. A routine chest computed tomography (CT) scan for pulmonary SCC follow-up in November 2021 revealed a 9.9mm nodule in the right middle lobe (RML) (Fig. 1). After discussing the CT findings with the patient and his family, they decided to maintain regular imaging follow-up first.

In May 2022, a subsequent positron emission tomography–computed tomography (PET-CT) scan revealed that the RML nodule had low glucose metabolism, despite an increase in size (Fig. 2). The patient remained asymptomatic during this period. Due to suspected lung cancer recurrence or metastasis, he was referred to the thoracic surgery OPD and was admitted for

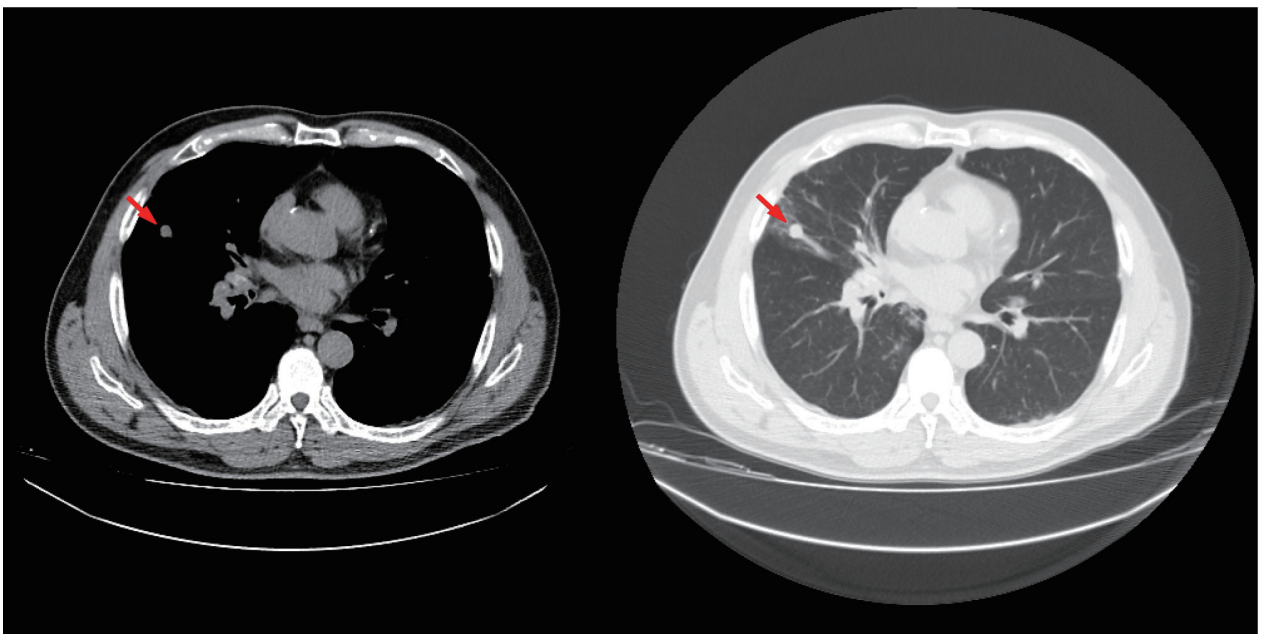

Fig. 1. Non-contrast chest CT scan in November 2021, revealing a faint 9.9mm nodule (red arrow) in the RML. The left-side image is a soft tissue window and the right-side image is the lung window.

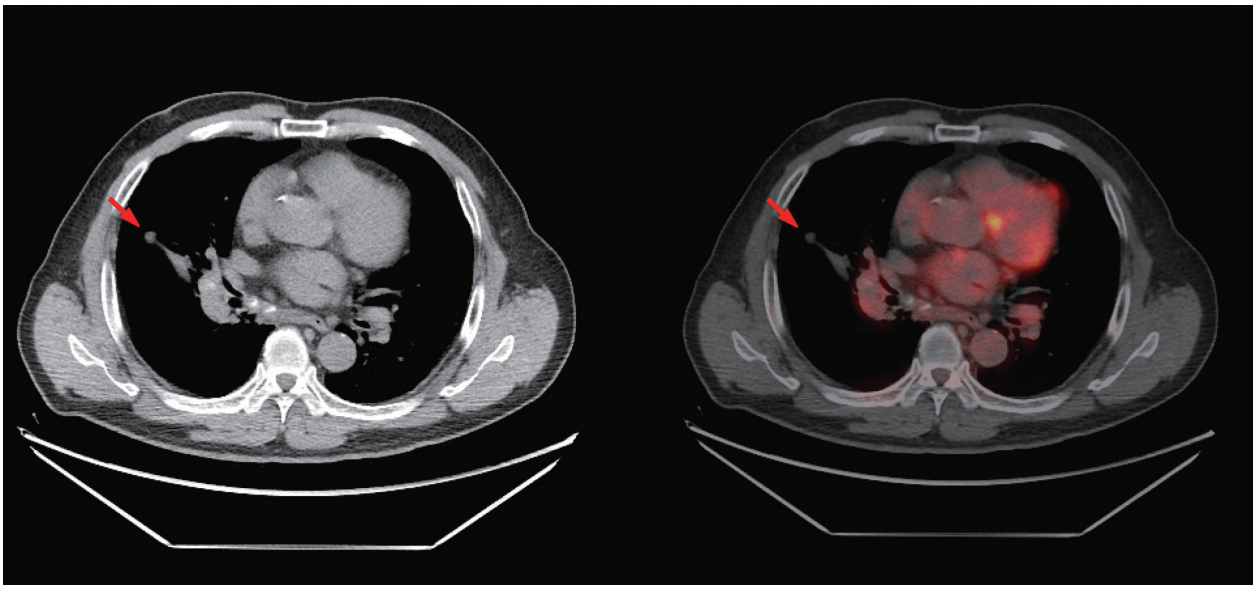

Fig. 2. PET-CT scan in May 2022, revealing the nodule (red arrow) had a low glucose metabolism with an increase in size.

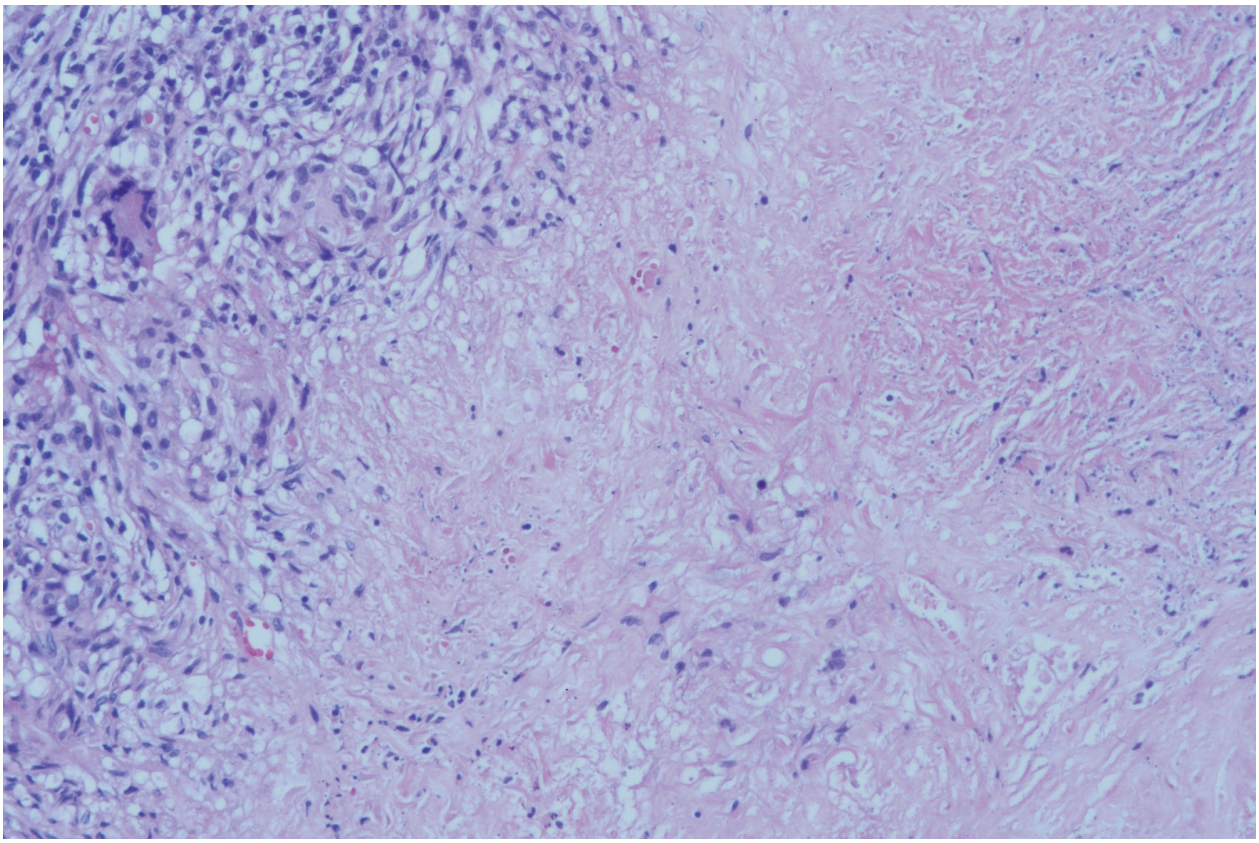

Fig. 3. Pathologic section of the nodule showing chronic granulomatous inflammation with necrosis.

surgical intervention in October, 2022. VATS WR of the RML was performed and the specimen was sent for surgical pathology, bacterial culture, fungal culture, and tuberculosis (TB) culture. The patient was discharged on day 4.

Five days after discharge, the pathology report showed chronic granulomatous inflammation with necrosis (Fig. 3). No mycobacteria, cryptococcus or fungi were identified. Both fungal culture and TB culture showed negative results, but *Burkholderia pseudomallei* infection was proved through tissue bacterial culture. Under the diagnosis of pulmonary melioidosis, trimethoprim-sulfamethoxazole (TMP-SMX) was prescribed. Later it was shifted to doxycycline plus amoxicillin-clavulanate due to side effects such as lethargy, nausea, and vomiting. The 5-month antibiotics treatment course was completed on April 2nd, 2023, and a serial follow-up chest CT on April 10th, 2023, showed complete remission without local recurrence.

Discussion

Melioidosis was first described by pathologist Alfred Whitmore and his assistant C. S. Krishnaswami in 1911 as a "glanders-like" disease found among morphia addicts in Rangoon, Burma [6-7]. The pathogen of melioidosis, *Burkholderia pseudomallei*, is a Gram-negative, aerobic bacillus widely found in soil and water in tropical and subtropical regions, particularly in Southeast Asia and northern Australia [8]. Melioidosis mainly affects people who are in frequent contact with soil and water in these regions, through inhalation, ingestion, or percutaneous inoculation, with the latter being the most common mode of transmission [9].

Many host risk factors for melioidosis have been identified in previous studies, including diabetes mellitus, alcoholism, chronic kidney disease and lung disease [10]. Currie *et al*. found that 434 (80%) of 540 cases in their Darwin prospective study had identified risk factors for melioidosis, such as chronic lung disease (26%), immunosuppressive status (6%), and malignancy (6%). Among these risk factors, chronic respiratory disease was the only individual risk factor predictive of mortality (19% vs 13%; risk ratio=1.5 (95% CI 1.1–2.4); p=0.048) [3].

Melioidosis was thought to be underdiagnosed due to its varied clinical manifestations [11]. The clinical spectrum of melioidosis ranges from nonspecific symptoms such as fever, cough, headache, and myalgia, to fatal septicemia with multi-organ involvement. Pneumonia was found to be the most common presenting feature in previous studies [3]. The classic radiological findings of acute or subacute pulmonary melioidosis are multiple nodular opacities or multiple patches of alveolar infiltration, which may progress rapidly to a coalescence of lesions or cavitation [12]. Chronic pulmonary melioidosis commonly shows cavities, nodules, and fibroreticular and patchy alveolar infiltrates mainly affecting the upper lobes on chest radiograph [13].

A definite diagnosis of melioidosis requires a positive culture of *Burkholderia pseudomallei* from any clinical sample obtained from a symptomatic at-risk patient [14]. Pus from lung abscesses or sputum in patients with pneumonia are proper culture samples. Blood cultures are recommended in all cases of suspected melioidosis as bacteremia is common [11].

Successful management of melioidosis involves prolonged courses of antibiotics, typically consisting of an initial intensive therapy followed by eradication therapy [15]. For initial intensive therapy, intravenous ceftazidime or

meropenem is preferred, and the duration of initial intensive therapy shouldbe a minimum of 10–14 days. Oral eradication therapy with drugs like TMP-SMX or doxycycline for 3- 6 months is usually suitable. Adjunctive therapies such as surgical drainage of abscesses may be necessary for localized infection [16].

The mortality rate of patients with melioidosis can range from 10% to as high as 40%, depending on whether rapid diagnosis and early implementation of optimal antibiotic therapy are available [15]. However, bacterial culture, which is the current gold standard for diagnosis, has low sensitivity (60%) [17]. Some serologic assays have been developed, but there has been only limited clinical use due to high background antibody positivity in endemic regions and false negative results in early disease [18]. As a result, developing non-culture-based diagnostic methods may be a top-priority issue in the future in order to improve prognosis.

Conclusion

We report a rare case of pulmonary melioidosis presenting as an asymptomatic solitary pulmonary nodule detected by chest CT scan in a patient with a history of chronic pulmonary disease and lung cancer, which are known to be risk factors for melioidosis infection. The definite diagnosis was confirmed by bacterial culture of lung tissue obtained during VATS WR. The patient underwent an effective 5-month treatment course with oral TMP-SMX initially, followed by doxycycline plus amoxicillin-clavulanate, instead of initial ceftazidime or meropenem, due to resected mild disease. Raising clinical awareness and arranging proper bacteriological diagnosis of melioidosis in suspected patients are important for early diagnosis of this rare disease.

References

1. Cheng AC, Currie BJ. Melioidosis: epidemiology, pathophysiology, and management. Clin Microbiol Rev 2005; 18(2): 383-416.
2. Currie BJ, Jacups SP. Intensity of rainfall and severity of melioidosis, Australia. Emerg Infect Dis 2003; 9(12): 1538-42.
3. Currie BJ, Ward L, Cheng AC. The epidemiology and clinical spectrum of melioidosis: 540 cases from the 20-year Darwin prospective study. PLoS Negl Trop Dis 2010; 4(11): e900.
4. Wiersinga WJ, Currie BJ, Peacock SJ. Melioidosis. N Engl J Med 2012; 367(11): 1035-44.
5. Chakravorty A, Heath CH. Melioidosis: an updated review. Aust J Gen Pract 2019; 48(5): 327-32.
6. Whitmore A, Krishnaswami CS. A hitherto undescribed infective disease in Rangoon. Ind Med Gaz 1912; 47(7): 262-7.
7. Whitmore A. An account of a glanders-like disease occurring in Rangoon. J Hyg (Lond) 1913; 13(1): 1-34.31.
8. Currie BJ, Dance DA, Cheng AC. The global distribution of *Burkholderia pseudomallei* and melioidosis: an update. Trans R Soc Trop Med Hyg 2008; 102 Suppl 1: S1-4.
9. White NJ. Melioidosis. Lancet 2003; 361(9370): 1715-22.
10. Suputtamongkol Y, Chaowagul W, Chetchotisakd P, *et al*. Risk factors for melioidosis and bacteremic melioidosis. Clin Infect Dis 1999; 29(2): 408-13.
11. Wiersinga WJ, Virk HS, Torres AG, *et al*. Melioidosis. Nat Rev Dis Primers 2018; 4:17107.
12. Bateson EM, Webling DD. The radiological appearances of pulmonary melioidosis: a report on twenty-three cases. Australas Radiol 1981; 25(3): 239-45.
13. Reechaipichitkul W. Clinical manifestation of pulmonary melioidosis in adults. Southeast Asian J Trop Med Public Health 2004; 35(3): 664-9.
14. Hoffmaster A, AuCoin D, Baccam P, *et al*. Melioidosis diagnostic workshop, 2013. Emerg Infect Dis J 2015; 21(2).
15. Currie BJ. Melioidosis: evolving concepts in

epidemiology, pathogenesis, and treatment. Semin Respir Crit Care Med 2015; 36(1): 111-25.

16. Lipsitz R, Garges S, Aurigemma R, *et al*. Workshop on treatment of and postexposure prophylaxis for *Burkholderia pseudomallei* and B. mallei infection, 2010. Emerg Infect Dis 2012;18(12): e2.
17. Limmathurotsakul D, Jamsen K, Arayawichanont A, *et al*. Defining the true sensitivity of culture for the diagnosis of melioidosis using Bayesian latent class models. PLoS One 2010; 5(8): e12485.
18. Robertson G, Sorenson A, Govan B, *et al*. Rapid diagnostics for melioidosis: a comparative study of a novel lateral flow antigen detection assay. J Med Microbiol 2015; 64(8): 845-8.

Multiple Mass-Like Lesions as a Rare Radiologic Finding of Pulmonary Syphilis: A Case Report

Yi-Chen Wang[1], Shu-Fang Huang[2]

Syphilis affects several organs and can lead to secondary conditions. However, pulmonary masses secondary to syphilis infection are rare. Here, we report a case in which a pulmonary mass with a cavity was incidentally detected.

A 68-year-old Taiwanese man with chronic kidney disease presented to our hospital complaining of general malaise and chronic axillary ulcers that had persisted for 1 month. Chest imaging incidentally revealed multiple masses with cavities in both lungs. Serial studies of the pulmonary lesions were performed without definitive findings. The patient was diagnosed with syphilis based on positive serological tests. During benzathine penicillin treatment, follow-up chest imaging and skin ulcers showed a therapeutic response to penicillin. A biopsy of the skin lesion revealed growth of *Treponema pallidum*. Gummatous syphilis was also confirmed in the skin and lungs. However, the serologic response and gummas had not completely resolved by the annual observation. Here, we discuss the potential etiology and further treatment of residual syphilis infections. ***(Thorac Med 2025; 40: 150-157)***

Key words: Case report, lung neoplasms, cavitation, *Treponema pallidum*, Spirochaetales infections, treatment outcome

Introduction

Syphilis is a sexually transmitted infection caused by the spirochete bacterium *Treponema pallidum*. If left untreated, it can result in extensive organ impairment, such as in the skin and the cardiovascular, neurological, ocular, and musculoskeletal systems, precipitating systemic symptoms.

Pulmonary syphilis represents a manifestation of this disease, although it may manifest as a mild symptom or remain asymptomatic. The detection of T. pallidum in collected samples can pose significant challenges. Therefore, the diagnosis of pulmonary syphilis is complicated. Here, we describe a rare case of secondary syphilis infection associated with pulmonary involvement in a Taiwanese man.

[1]Department of Internal Medicine, Kaohsiung Armed Forces General Hospital, Kaohsiung, Taiwan. [2]Department of Internal Medicine, Kaohsiung Armed Forces General Hospital, Kaohsiung, Taiwan & Department of Thoracic Medicine, Kaohsiung Armed Forces General Hospital, Kaohsiung, Taiwan.
Address reprint requests to: Dr. Yi-Chen Wang, Department of Internal Medicine Kaohsiung Armed Forces General Hospital, No. 2, Zhongzheng 1st Rd., Lingya Dist., Kaohsiung City, 80284 Taiwan (R.O.C.).

Case Report

A 68-year-old man visited our hospital complaining of general malaise and chronic bilateral axillary ulcers that had persisted for 1 month. Besides a dry cough for a month, he had no fever, sputum production, or weight loss. His medical history included end-stage renal disease, atrial fibrillation, and urinary tuberculosis infection after left-sided nephrectomy. He was a non-smoker and had neither unsafe sexual exposure nor had he travelled overseas in the past few months. The patient reported no recent exposure to water or soil related to the chronic wounds. He denied any relevant insect or animal bites and did not acknowledge a history of trauma near the wound site.

Upon arrival at the hospital, the patient presented with normal consciousness. His physical examination results were as follows: height, 170 cm; weight, 62.3 kg; body mass index, 21.55 kg/m2; body temperature, 36°C; pulse, 119 beats/min (irregular); blood pressure, 124/68 mmHg; and SpO_2, 100% (indoors). Initially, no skin rashes or lymph node enlargement was observed.

Laboratory test results on initial examination

The patient's white blood cell count was 10,780 /μL (Table 1). Serum biochemical tests

Table 1. Laboratory Findings on Admission

	On presentation	Reference range
<Blood cell count>		
White blood cells (10^3/uL)	10.78	4~11
Differential count (%)		
Neutrophils	82.7	40–75
Lymphocytes	6.5	20–45
Monocytes	6.3	2~10
Hemoglobin (g/dL)	7.2	13.5–17.5
Hematocrit (%)	22.5	40–52
Platelets (10^3/μL)	272	150–400
<Serum chemistry>		
Blood urea nitrogen (mg/dl)	155	7~25
Creatinine (mg/dl)	12.8	0.7–1.3
Alanine transaminase (U/L)	9	13–39
Glucose (mg/dL)	106	70–100
Natrium (mmol/L)	132	136–145
Potassium (mmol/L)	4.7	3.5–5.1
C-reactive protein (mg/dL)	5.29	< 1.0
<Immunology>		
Erythrocyte sedimentation (mm/1 h)	115	2~15
IgG4 (mg/dL)	189	8–140
Anti-ENA	0.14	< 0.7

IgE (IU/mL)	1880	< 100
C-ANCA	Negative	< 0.2
P-ANCA	Negative	< 0.2
Anti-DNA (IU/ml)	Negative (63)	< 200
ANA	< 1:40	< 1:40
C3 (mg/dL)	79.6	90–180
C4 (mg/dL)	20.1	10~40
<Infection>		
RPR/VDRL	Reactive (1:64)	
TPPA/TPHA	Positive (> 1:20480)	Negative (< 1:80)
Hepatitis B surface antigen	Non-reactive	
Hepatitis C virus antibody	Non-reactive	
HIV-Ag/Ab	Non-reactive	
Bacterial (blood)	Negative	
Acid-fast bacilli (urine)	Negative	
Acid-fast bacilli (sputum)	Negative	
Fungus (bronchial wash)	Negative	
Bacteria (bronchial wash)	Negative	
Acid-fast bacilli (bronchial wash)	Negative	
Aspergillus antigen (serum)	Negative	
Cryptococcus antigen (serum and bronchial wash)	Negative	
<Tumor marker>		
Carcinoembryonic antigen (ng/mL)	13.3	< 5

revealed impaired kidney function (blood urea nitrogen level, 155 mg/dL; creatinine, 12.8 mg/dL). The serum C-reactive protein level was 5.29 mg/dL. A predialysis evaluation was performed for end-stage renal disease, and a positive syphilis test result was incidentally revealed. The rapid plasma reagin card test (RPR) and *Treponema pallidum* hemagglutination test (TPHA) revealed titers of 1:64 and ≥ 1:20480, respectively. An elevated carcinoembryonic antigen (13.3 ng/mL) (CEA) level was noted. The results of the human immunodeficiency virus (HIV) antibody test were negative. Rheumatoid factor and antineutrophil cytoplasmic antibody test results were normal.

Imaging and pathology findings

Chest radiography revealed multiple masses in the right lung (Fig. 1a). Contrast-enhanced thoracic computed tomography (CT) revealed multiple ill-defined consolidations in both lungs, with cavity changes (Fig. 2a, 2b). Abdominal CT revealed no malignancy of the gastrointestinal tract. Pathological tests of a

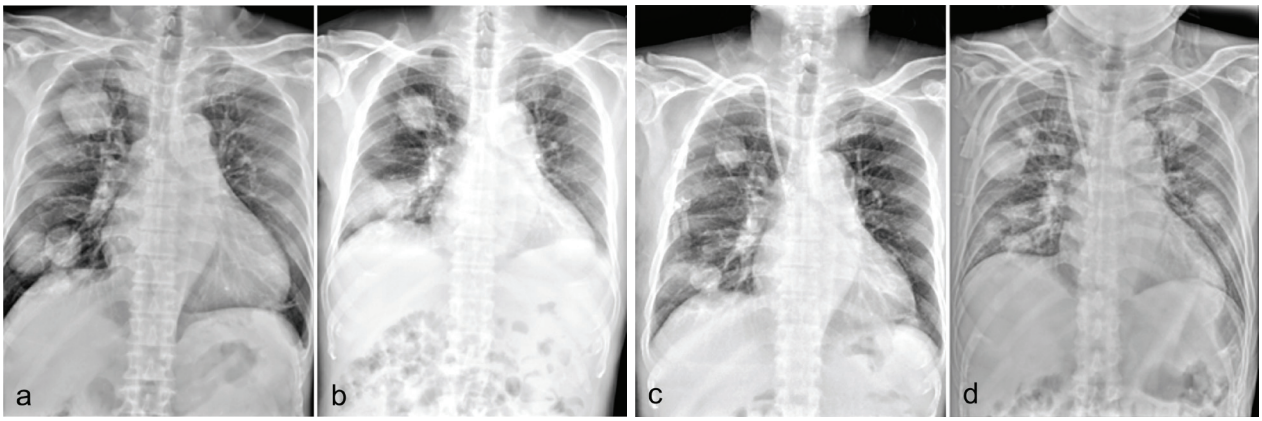

Fig. 1. Serial Chest Films of the Patient. a. Chest radiograph revealed several masses in the right lung field. b. One month later, the patient's chest film showed improvement after weekly intramuscular (IM) injections of benzathine penicillin G 2.4 million units IM, for 3 weeks. c. Two months later, the right lung mass was contracted. d. Four months later, recurrence of the mass was observed in the bilateral lungs.

CT-guided biopsy of the lung mass revealed necrotic tissue and reactive alveolar cell hyperplasia, whereas bronchial washing revealed the presence of bronchial epithelial cells, neutrophils, and lymphocytes. The bacterial culture/smear, acid-fast bacilli, mycobacterial culture, and periodic acid-Schiff stain (PAS stain) of the CT-guided biopsy, and bronchial wash, were all negative, as was the *Treponema pallidum* test.

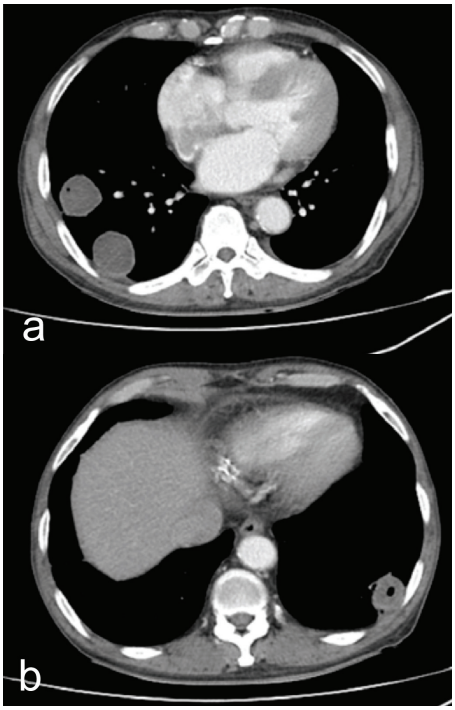

Fig. 2. Chest Computed Tomography. The pre-treatment image shows a bilateral lobe mass with a cavitary lesion.

Clinical course

As the timing of infection was unknown, we presumed that the patient had secondary syphilis. The patient was started on benzathine penicillin (240M IU, once a week, for 3 doses). Empirically, antibiotics with piperacillin-tazobactam are administered to treat chronic ulcers. During the first 3 months after the administration of antibiotics, we noticed a decreased serum RPR titer (1:64 to 1:32) and partial regression of the chest film lesions (Fig. 1b, 1c).

However, poor healing of the skin ulcer on the legs (Fig. 3) persisted, with suspicious recurrence of the lung mass 6 months after the initial penicillin treatment (Fig. 1d). The patient was then readmitted to our hospital. All microbiological studies, including those for Mycobacterium, fungi, and neoplasms, were performed, and no pathogens were identified.

A second dose of benzathine penicillin (240M IU, once a week, for 3 doses) was ad-

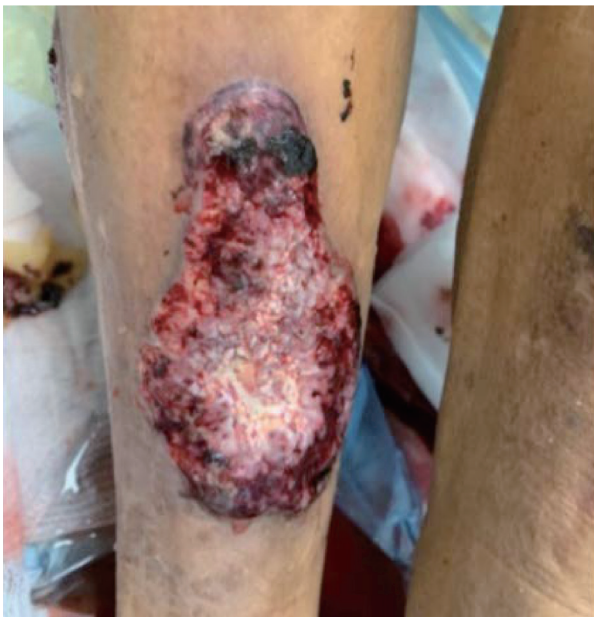

Fig. 3. Syphilis Gummas Manifest Tumor-Like Growths on the Leg.

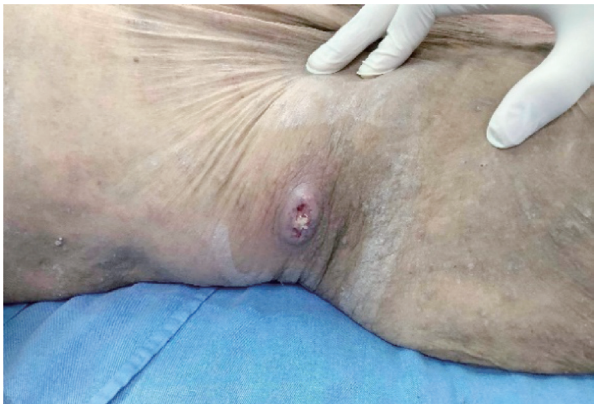

Fig. 4. Syphilis Gummas Lead to the Formation of Ulcerated Lesions on the Scrotum.

ministered based on suspicious secondary skin and pulmonary changes caused by syphilis. The follow-up serum RPR titer became 1:16 at the end of the second admission period. Since some of the ulcers on the patient's legs were not healing, oral minocycline (200 mg/day) with a third course of benzathine penicillin (240M IU, once a week, for 3 doses) was administered in the outpatient department (OPD). Eight months later, new ulcers appeared on the scalp, fingers, and scrotum (Fig. 4), and the RPR titer increased to 1:32. The patient denied having had any recent unprotected sexual exposure. We asked the patient to undergo a lumbar puncture because of concerns regarding a syphilis invasion of the central nervous system; however, the patient refused it and denied any associated neurological symptoms.

Surgery was performed on an unhealed scrotal wound. Full-thickness skin grafts were made, and pathological images revealed acute, chronic inflammation with mild neutrophil invasion, numerous lymph plasma cell infiltrates, and granuloma formation. Immunohistochemical staining revealed the presence of *Treponema pallidum* at the dermo-epidermal junction (Fig. 5a, 5b). Based on the criteria for the clinical diagnosis of pulmonary syphilis and the patho-

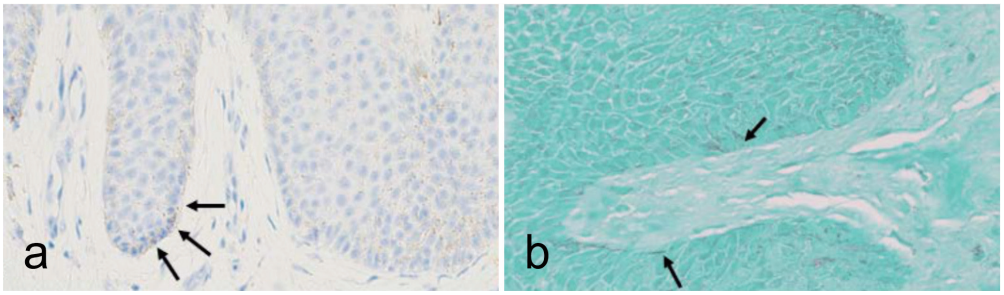

Fig. 5. Pathology of the Scrotum. a. Immunohistochemical stain revealed *Treponema pallidum* in the epidermis. b. Silver impregnation staining revealed *Treponema pallidum* in the epidermis.

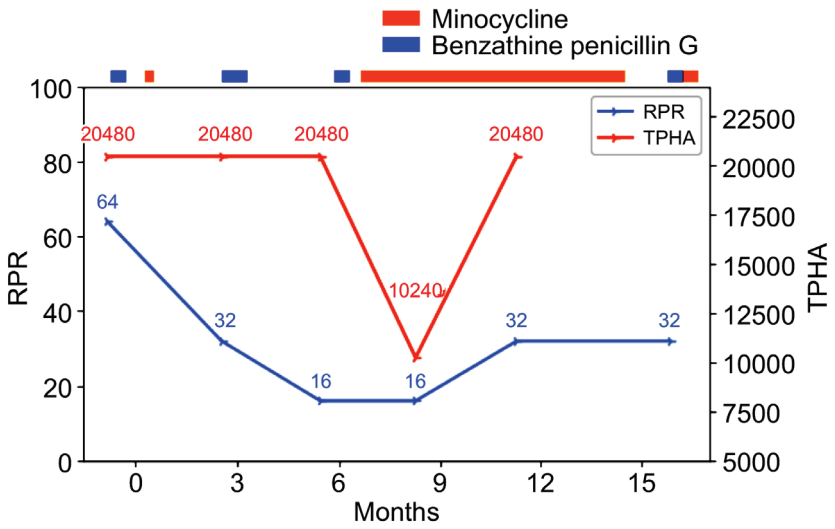

Fig. 6. Clinical Course of the Patient. The figure depicts the clinical progression of the patient. The vertical axis reflects the fluctuation in serum RPR values over time. The types of antibiotics administered during treatment are indicated above the graph. Although there was a transient 4-fold decrease in RPR values, a subsequent rise was noted approximately 1 year after initiating therapy.
RPR: Rapid plasma regain, TPHA: *Treponema pallidum* hemagglutination

logical findings of granulomatous skin ulcers, a final diagnosis of secondary syphilis with pulmonary and skin involvement was made. In addition to the 3 doses of benzathine penicillin (240M IU, once a week), a fourth dose was administered. The patient underwent serial OPD follow-ups for stable disease, and 200 mg/day of oral minocycline also was prescribed. The patient's clinical course is shown in Fig. 6.

Discussion

Pulmonary involvement of syphilis is rare. During the pre-antibiotic era, the prevalence of lung involvement was mainly due to congenital and tertiary syphilis, occurring in 1–12.5% of cases [1]. However, recent reports have indicated an increased incidence of secondary syphilis [2]. The clinical and radiological presentations of pulmonary involvement are nonspecific, and patients are typically asymptomatic or manifest mild symptoms.

Chest imaging reveals the presence of pulmonary lesions. Lung lesions associated with syphilis exhibit variability, ranging from solitary nodules to multiple nodules within a single lobe, and manifestations such as ground-glass opacities, nodular opacities in multiple lobes, and encysted pleural effusion [3-6]. In our case, chest CT revealed multiple ill-defined consolidations involving both lungs, with associated cavity formation. The differential diagnosis of lung masses includes lung abscesses, necrotizing pneumonia, septic emboli, fungal infection, nocardia, tuberculosis, primary or metastatic lung cancer, rheumatoid nodules, and Wegener's granulomatosis [7]. Despite the thorough examination of numerous pulmonary samples, direct visualization of T. pallidum remains infrequently achieved in the context of syphilis. The below criteria have been proposed by Coleman *et al*. for the clinical diagnosis of pulmo-

nary syphilis, and do not include bronchoscopy or lung biopsy [1]:

(a) Historical and physical findings typical of secondary syphilis.

(b) Serological test results positive for syphilis.

(c) Pulmonary abnormalities observed radiographically with or without associated symptoms or signs.

(d) Exclusion of other forms of pulmonary disease when possible, based on the findings of serological tests, sputum smears and cultures, and sputum cytology.

(e) Response to anti-syphilis therapy based on radiological signs.

In the present case, a pulmonary mass with a cavity was incidentally detected. After examination, we excluded bacterial and fungal infections, autoimmune diseases, and malignancies. Syphilis infection was diagnosed based on positive RPR test results. The patient received anti-syphilis therapy for secondary syphilis. The titer decreased 4-fold (1:16) after 6 months. The patient then was diagnosed with secondary syphilis with pulmonary and skin involvement.

However, gummas also developed. The titer increased 2-fold (1:32) at 12 months, and quantitative non-treponemal serological tests were repeated at 6, 12, and 24 months to determine the treatment effects [8]. Re-infection or treatment failure was likely indicated in those patients demonstrating a sustained 4-fold increase in non-treponemal test titers persisting for more than 2 weeks or in those exhibiting signs or symptoms associated with primary or secondary syphilis. Our patient presented no risk factors for re-infection, such as men having sex with men (MSM) or HIV infection. We presume that patients with secondary syphilis have a higher likelihood of treatment failure or re-infection than those with primary syphilis.

Concomitant neurosyphilis is also considered syphilis of unknown duration and should be evaluated. Since our patient refused further study of the cerebrospinal fluid, re-administration of treatment involved weekly injections of 2.4 million intramuscular benzathine penicillin G units for 3 weeks. In cases where treatment failure is suspected to be attributable to a central nervous system infection, cerebrospinal fluid examination should be considered when follow-up remains uncertain or when initial high titers persist beyond 24 months.

Conclusion

In summary, we reported a case of pulmonary syphilis with multiple cavitating round masses detected bilaterally on CT. Diagnostic challenges emerged due to the asymptomatic nature of the condition and the absence of pathological findings in lung pathology tests. The clinical diagnosis of pulmonary syphilis was made based on the criteria established by Coleman *et al*. [1].

This case emphasizes that, in cases of insufficient serological response following treatment, it is essential to consider the possibility of re-infection, treatment failure, and concurrent neurosyphilis. Additionally, it is crucial to conduct regular serological and clinical monitoring at least once a year to detect any sustained increase in nontreponemal titers. This approach aims to ensure timely intervention and effective management of syphilis cases, and to promote optimal patient outcomes.

References

1. Coleman DL, McPhee SJ, Ross TF, *et al*. Secondary

syphilis with pulmonary involvement. West J Med 1983; 138: 875-8.
2. Fenton KA, Lowndes CM. Recent trends in the epidemiology of sexually transmitted infections in the European Union. Sex Transm Infect 2004; 80: 255-63.
3. Goda K, Katsurada M, Doy T, *et al*. Pulmonary syphilis with a cicatricial variant of organizing pneumonia: a case report. BMC Pulm Med 2023; 23: 170.
4. Ohta A, Furusyo N, Kishihara Y, *et al*. Secondary syphilis with pulmonary involvement. Intern Med 2018; 57: 121-6.
5. Reddy RN. Secondary pulmonary syphilis. Chest 2022; 161: A128.
6. Elzouki AN, Al-Kawaaz M, Tafesh Z. Secondary syphilis with pleural effusion: case report and literature review. Case Rep Infect Dis 2012; 2012: 409896.
7. Gafoor K, Patel S, Girvin F, *et al*. Cavitary lung diseases: a clinical-radiologic algorithmic approach. Chest 2018; 153: 1443-65.
8. Workowski KA, Bachmann LH, Chan PA, *et al*. Sexually transmitted infections treatment guidelines, 2021. MMWR Recomm Rep 2021; 70: 1-187.

Delayed Life-Threatening Hemothorax After a Blunt Chest Trauma with Rib Fractures: A Case Report

Ya-Fu Cheng[1], Ching-Yuan Cheng[1]

Delayed hemothorax can occasionally occur following blunt chest trauma. However, life-threatening massive hemothorax that occurs after more than 72 h post-injury is rare. Here, we reported the case of a patient who had suffered blunt chest trauma accompanied with mild rib displacement, and who developed massive hemothorax 14 days after the injury. The patient underwent emergency video-assisted thoracoscopic surgery (VATS), and bleeding from the intercostal artery was successfully controlled. This case highlights the potential of a life-threatening massive hemothorax even after mild thoracic trauma. VATS proved to be a feasible method for diagnosing and managing intercostal artery bleeding. ***(Thorac Med 2025; 40: 158-163)***

Key words: chest trauma; delayed hemothorax; intercostal artery; video-assisted thoracoscopic surgery

Introduction

Patients that visit the emergency departments of hospitals with blunt chest traumas are common. Rib fractures are the most common injury suffered in such chest traumas, and hemothorax is a known complication [1-2]. Hemothorax that occurs immediately after trauma is common and well-documented; however, delayed hemothorax is rare and poses unique diagnostic and therapeutic challenges.

Previously conducted studies have reported that the incidence of delayed hemothorax ranges from 7.4% to 36% [3-5]. The majority of patients suffering from delayed hemothorax can be treated with thoracic drainage. In rare cases, patients suffer from delayed massive hemothorax and require surgical intervention. Such a massive hemothorax typically occurs within 72 h of trauma. According to a previously conducted study that reviewed 1,278 chest trauma patients, the incidence of life-threatening hemothorax that required surgical intervention was only 0.3% (5 patients). The average time to the occurrence of a hemothorax incident was 63.6 h following a trauma, with superficial diaphragmatic lacerations caused by the sharp edges of broken ribs responsible for all cases [6].

Diaphragmatic injuries, pulmonary lacerations, great vessel injuries, or intercostal artery injuries can be responsible for a hemothorax [7]. Here, we report the case of a patient who

[1]Division of Thoracic Surgery, Department of Surgery, Changhua Christian Hospita.
Address reprint requests to: Dr. Ching-Yuan Cheng, Division of Thoracic Surgery, Department of Surgery, Changhua Christian Hospital No. 135 Nanxiao St., Changhua City, Changhua County 500, Taiwan.

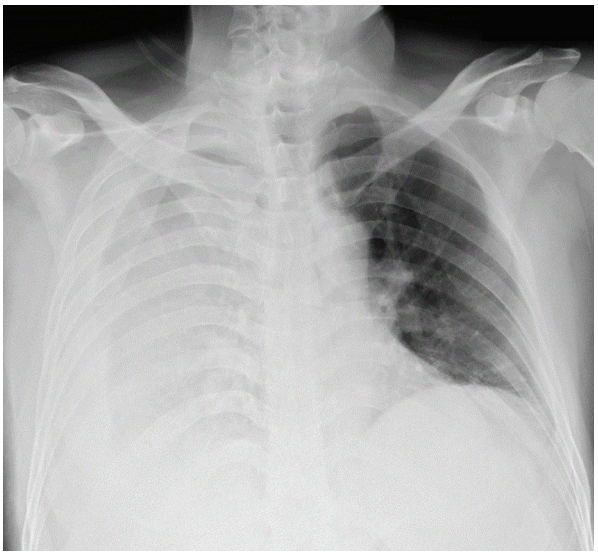

Fig. 1. Chest X-ray revealed massive right pleural effusion.

sustained a right anterior chest injury following a fall that had occurred 14 days back. The patient developed a life-threatening massive hemothorax, which was successfully treated by video-assisted thoracic surgery (VATS) without complications.

Case Presentation

A 59-year-old man presented to the emergency department with a sudden onset of right anterior chest pain and shortness of breath during the previous 1 hour. He had a history of grade II myelofibrosis, for which he was being treated with ruxolitinib. Fourteen days earlier, he had sustained a fall, hitting his chest, which resulted in fractures of the right 4th to 6th ribs without any evidence of pneumothorax or hemothorax, and no further referral or admission was required.

His vital signs upon arrival at the emergency department indicated tachycardia (heart rate: 110 beats/min), early shock (blood pressure: 95/71 mmHg), and oxygen saturation of 92%. Massive right pleural effusion was visible on the chest X-ray (Fig. 1). Laboratory tests indicated leukocytosis. His hemoglobin level was 13.2 g/dL, while the platelet count was 167,000 per microliter of blood. Chest computed to-

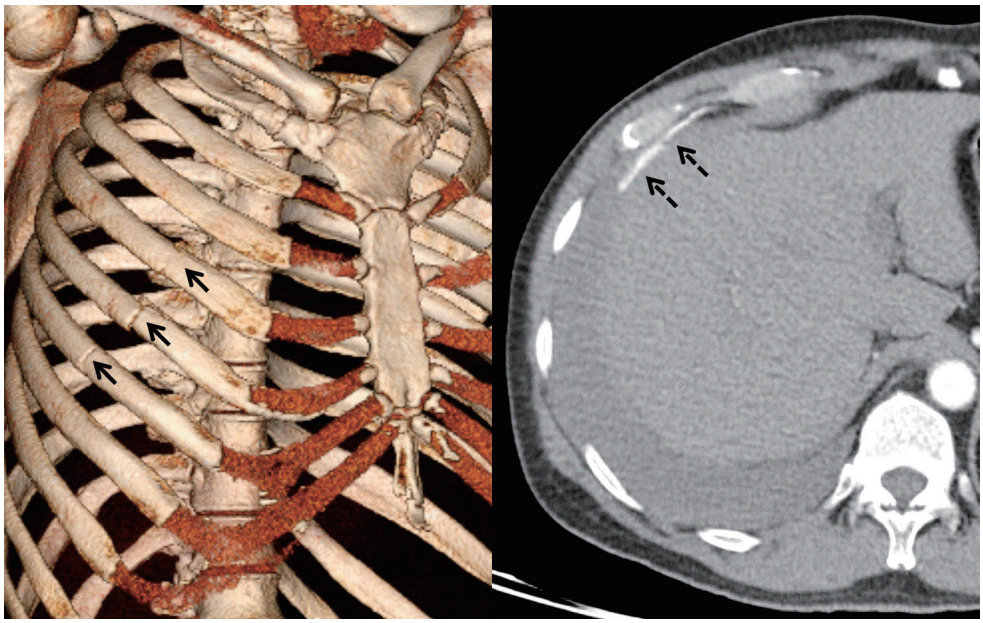

(A) **(B)**

Fig. 2. Chest computed tomography (CT scan) revealed: (A) fractures of the right 4th to 6th ribs (represented with a black straight arrow) with (B) massive right pleural effusion and contrast extravasation at the site of the right anterior 6th rib (black dotted arrow).

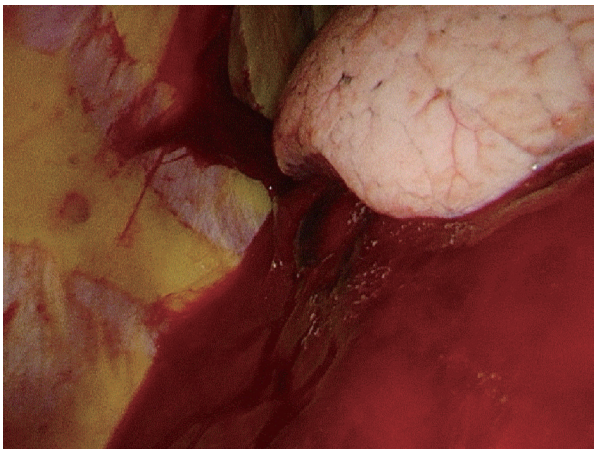

Fig. 3. Massive amounts of bloody fluid and clots were identified and removed using video-assisted thoracoscopic surgery.

mography (CT) revealed fractures of the right 4th to 6th ribs along with massive right pleural effusion and contrast extravasation in the vicinity of the right anterior 6th rib (Fig. 2A & 2B). A chest tube was inserted and 3000 ml of dark blood was drained out. Emergency surgery was scheduled after clamping the chest tube. The patient was immediately administered massive fluid and blood transfusions.

A 2-port VATS approach was performed with the patient, with 1 port positioned at the 5th intercostal space along the anterior axillary line and the 2nd port at the 7th intercostal space along the posterior axillary line. A large amount of bloody fluid and clots were first removed (Fig. 3). Profuse bleeding was identified from the anterior 6th intercostal artery when the diaphragm was pressed down (Fig. 4A). Electrocautery was performed for controlling the bleeding (Fig. 4B). The patient was transferred to the intensive care unit with a 28-Fr chest tube after completion of the surgery. A follow-up chest X-ray showed good bilateral lung expansion and no

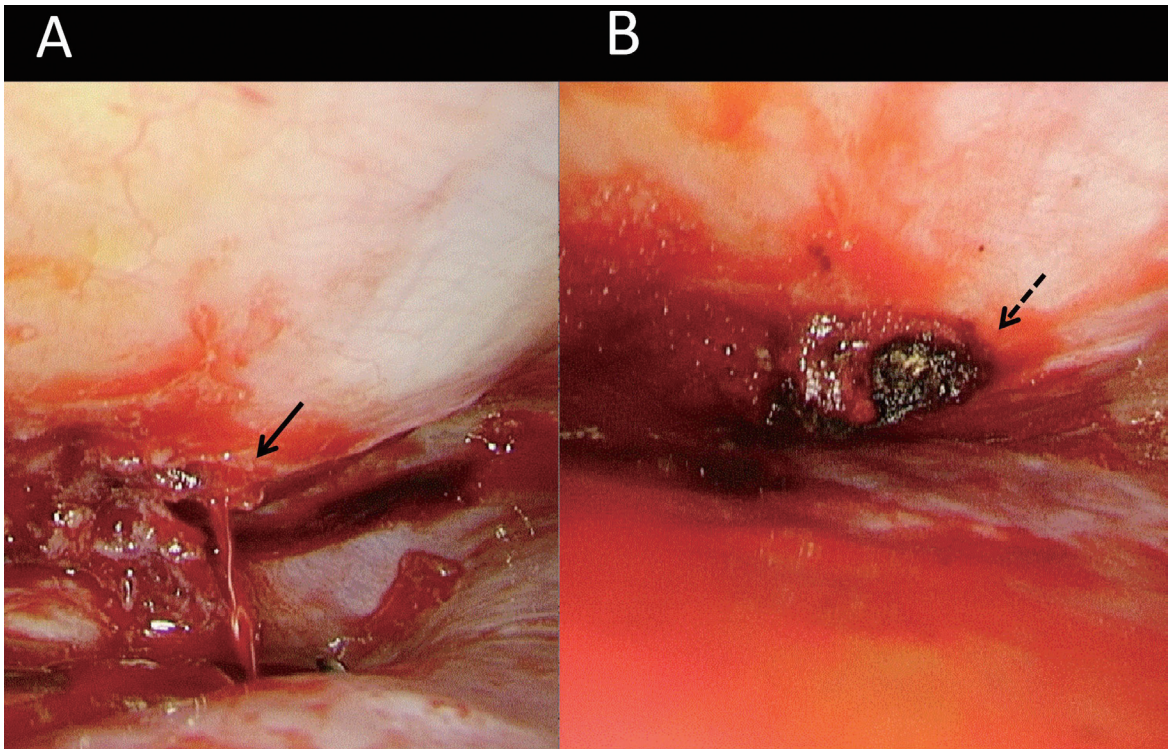

Fig. 4. (A) Profuse bleeding from the anterior 6th intercostal artery was identified (black straight arrow). (B) The bleeding was controlled with electrocautery (black dotted arrow).

evidence of any residual pleural effusion. The chest tube was removed on postoperative day 3. The patient's recovery was uneventful, and he was discharged on the 4th postoperative day.

Discussion

The definition of delayed hemothorax has not been universally established; however, 2 commonly accepted definitions exist. Ritter *et al*. defined delayed hemothorax as the absence of hemothorax on initial examination, with subsequent detection later, which could sometimes be as early as 2 h following the injury [8]. Shorr *et al*. defined delayed hemothorax as hemothorax that occurs 24 h post-injury [9]. There exists no consensus regarding the definition of massive hemothorax, as well. Most researchers define it as blood drainage of 1.5 liters or more immediately following chest tube insertion; or a continuous bleeding of at least 200 ml per hour for 4 hours [6]. Some other researchers report that a presence of blood exceeding 1000 ml in the pleural cavity qualifies as massive hemothorax [10]. Delayed massive hemothorax that requires surgery following blunt chest trauma is an exceedingly rare phenomenon.

The causes of delayed massive hemothorax are diverse. A previous study had compiled data from 20 patients across 11 studies [11]; 13 of the 20 patients had suffered from lower rib fractures (below the 7th rib) with diaphragmatic injury, 5 patients had suffered from intercostal artery bleeding, and the remaining cases were probably caused by extrapleural bleeding or musculophrenic artery injury. In more than 50% of these cases, all patients presented with multiple rib fractures, and symptoms were observed within 72 h after injury. Patients experiencing intercostal artery bleeding were treated by thoracotomy. The current case is the first report of delayed massive hemothorax caused by intercostal artery bleeding that was successfully treated using VATS in the literature.

The pathophysiology of delayed hemothorax associated with intercostal artery bleeding is most likely linked to vessel erosion resulting from displaced rib fragments [12]. Some previously conducted retrospective reviews have identified pseudoaneurysms of the affected intercostal artery as the likely cause. Intercostal arterial bleeding can be controlled using various treatment options. If the bleeding can be identified on CT imaging, angioembolization is a suitable option for treating patients in a stable condition. Surgical intervention is warranted if the patient's condition is unstable, or when the bleeding site is not well-defined. Electrocautery enables us to achieve initial control of the symptoms. Once the bleeding site is identified, hemostatic clips or suture ligation can be used to control the bleeding. In the event of the failure of these methods, ligation of the entire intercostal vascular bundle at the proximal and distal sites can be considered [13].

Most patients who experience delayed massive hemothorax have multiple rib fractures, but predicting which patients are at increased risk is not easy. A previously conducted study that analyzed 109 patients with delayed hemothorax reported that patients with posterior rib displacement were more likely to develop delayed massive hemothorax [[14].---is this correct???]] Another study conducted by Gonzalez G *et al*., identified the number of totally displaced rib fractures as a significant risk factor [14]. this is the Gonzalez reference]] Age over 70 years has also been listed as a predictor of delayed hemothorax [16]. However, the current patient was a 59-year-old man who had suffered mild

displacement fractures of the anterior 4th to 6th ribs, thereby indicating that it is difficult to predict delayed hemothorax after rib fractures. Although most cases have been documented to occur within 72 h of injury, delayed hemothorax can develop as late as 44 days following a trauma [6]. Therefore, patients must be informed about the risks and signs of delayed hemothorax following blunt chest trauma. Patients with more than 2 displaced rib fractures are recommended to undergo close radiographic follow-up within 1 month of the injury [17].

Our patient had a history of myelofibrosis and was being treated with ruxolitinib. Myelofibrosis is a rare disease characterized by anemia, extramedullary lhematopoiesis, and splenomegaly [18]. Momelotinib and ruxolitinib are the medications prescribed for treating myelofibrosis [19]. Inadequately controlled myelofibrosis can cause severe anemia, pallor, petechiae, ecchymosis and bleeding. Association between myelofibrosis and hemothorax has been seldom reported. The myelofibrosis in our patient was well-controlled and the blood cell counts were within normal limits. The relationship between massive hemothorax and myelofibrosis needs to be further investigated.

Conclusion

Delayed massive hemothorax is a life-threatening condition that is very rare and hard to predict. Prompt intervention is warranted, and VATS is a feasible choice for diagnosis and treatment.

Conflict of interest statement

There are no conflicts of interest to declare.

References

1. Sarode AL, Ho VP, Pieracci FM, *et al*. The financial burden of rib fractures: national estimates 2007 to 2016. Injury 2021 Aug; 52(8): 2180-2187.
2. Zeiler J, Idell S, Norwood S, *et al*. Hemothorax: a review of the literature. Clin Pulm Med 2020 Jan; 27(1): 1-12.
3. Misthos P, Kakaris S, Sepsas E, *et al*. A prospective analysis of occult pneumothorax, delayed pneumothorax and delayed hemothorax after minor blunt thoracic trauma. Eur J Cardiothorac Surg 2004 May; 25(5): 859-864.
4. Émond M, Sirois MJ, Guimont C, *et al*. Functional impact of a minor thoracic injury: an investigation of age, delayed hemothorax, and rib fracture effects. Ann Surg 2015 Dec; 262(6): 1115-1122.
5. Plourde M, Émond M, Lavoie A, *et al*. Cohort study on the prevalence and risk factors for delayed pulmonary complications in adults following minor blunt thoracic trauma. CJEM 2014 Mar; 16(2): 136-143.
6. Chang SW, Ryu KM, Ryu JW. Delayed massive hemothorax requiring surgery after blunt thoracic trauma over a 5-year period: complicating rib fracture with sharp edge associated with diaphragm injury. Clin Exp Emerg Med 2018 Mar 30; 5(1): 60-65.
7. Chen CL, Cheng YL. Delayed massive hemothorax complicating simple rib fracture associated with diaphragmatic injury. Am J Emerg Med 2014 Jul; 32(7): 818.e3-818.e4.
8. Ritter DC, Chang FC. Delayed hemothorax resulting from stab wounds to the internal mammary artery. J Trauma 1995 Sep; 39(3): 586-589.
9. Shorr RM, Crittenden M, Indeck M, *et al*. Blunt thoracic trauma. Analysis of 515 patients. Ann Surg 1987 Aug; 206(2): 200-205.
10. Cakmak M, Yuksel M, Kandemir MN. Characteristics of the patients undergoing surgical treatment for pneumothorax: a descriptive study. J Pak Med Assoc 2016 May; 66(5): 554-558.
11. Muronoi T, Kidani A, Oka K, *et al*. Delayed massive hemothorax due to diaphragm injury with rib fracture: a case report. Int J Surg Case Rep 2020; 77: 133-137.
12. Álvarez-Ortega AC, Aranda-Hoyos A, Posso-Nuñez JA, *et al*. Delayed hemothorax following blunt thoracic trauma: a case report. J Cardiothorac Surg 2024 Jun 27;1

9(1): 395.
13. Laugsand EA, Xanthoulis A. Management of a life-threatening intercostal artery bleeding, difficult to visualize in open surgery: a case report. J Surg Case Rep 2020 Oct 31; 2020(10): rjaa444.
14. Gonzalez G, Robert C, Petit L, *et al*. May the initial CT scan predict the occurrence of delayed hemothorax in blunt chest trauma patients? Eur J Trauma Emerg Surg 2021 Feb; 47(1): 71-78.
15. Seok J, Yoon SY, Han J, *et al*. Prediction model of delayed hemothorax in patients with traumatic occult hemothorax using a novel nomogram. J Chest Surg 2024 Sep 27; 57(6): 519-528.
16. Émond M, Guimont C, Chauny JM, *et al*. Clinical prediction rule for delayed hemothorax after minor thoracic injury: a multicentre derivation and validation study. CMAJ Open 2017 Jun 12; 5(2): E444-E453.
17. Ahn S, Lee S, Kim S, *et al*. Risk factors for delayed hemothorax in patients with rib fracture in the emergency department. Am J Emerg Med 2024 Feb; 76: 173-179.
18. Pardanani A, Gotlib JR, Jamieson C, *et al*. Safety and efficacy of TG101348, a selective JAK2 inhibitor, in myelofibrosis. J Clin Oncol 2011 Mar 1; 29(7): 789-796.
19. Mesa RA, Kiladjian JJ, Catalano JV, *et al*. SIMPLIFY-1: A Phase III randomized trial of momelotinib versus ruxolitinib in Janus kinase inhibitor-naïve patients with myelofibrosis. J Clin Oncol 2017 Dec 1; 35(34): 3844-3850.

Bronchiolar Adenoma (BA)/Ciliated Muconodular Papillary Tumor (CMPT) of the Lung: a Case Report and Literature Review

Hsieh-Min Cheng[1], Ting-Chia Chang[1]

Bronchiolar adenoma (BA)/ciliated muconodular papillary tumor (CMPT) is a rare, low-grade malignant neoplasm of the lung's periphery, characterized by the proliferation of ciliated columnar cells, goblet cells, and basaloid cells. We described the case of a 68-year-old female who presented with progressive general malaise and anorexia for 3 months. Initial chest radiographs suggested nodules in the right upper and left lower lungs. Chest computed tomography scan identified multiple subpleural patches in the right upper, right lower, and left lower lobes. The patient underwent video-assisted thoracoscopic surgical wedge resections targeting these lesions in the right upper and right lower lobes. Histopathological examination of the resected right lower lobe confirmed BA/CMPT. This case contributes to the broader understanding of BA/CMPT, discussing its clinical and histological characteristics in the context of existing literature. ***(Thorac Med 2025; 40: 164-170)***

Key words: bronchiolar adenoma, ciliated muconodular papillary tumor

Introduction

Bronchiolar adenoma (BA)/ciliated muconodular papillary tumor (CMPT) is a rare neoplasm initially described by Ishikawa, *et al*. in 2002 [1]. It is characterized by its peripheral lung location and histopathological presence of a mix of mucinous, ciliated, and basal cells. Despite its benign nature, BA/CMPT presents diagnostic and therapeutic challenges due to its infrequency. Here, we report a case of BA/CMPT and discuss its characteristics by reviewing the existing literature.

Case Presentation

A 68-year-old woman presented with a 3-month history of progressive general malaise and anorexia. She denied symptoms of upper respiratory tract infection. On Day 1 of admission, the chest X-ray revealed suspicious nodules in the right upper and left lower lungs (Fig. 1), necessitating further assessment with a chest computed tomography (CT) scan.

[1]Division of Chest Medicine, Department of Internal Medicine, Chi Mei Medical Center.
Address reprint requests to: Dr. Ting-Chia Chang, No. 901, Zhonghua Rd. Yongkang Dist., Tainan City 71004, Taiwan (R.O.C.)

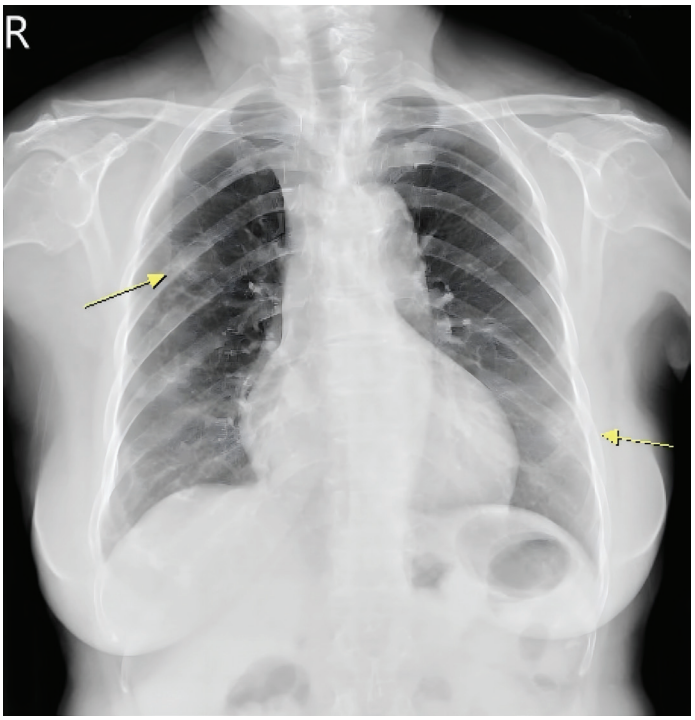

Fig. 1. Chest X-ray on Day 1 of admission showed suspected nodules in the right upper and left lower lobe (yellow arrows).

The chest CT scan (Fig. 2a, Fig. 2b) on Day 3 of admission showed multiple subpleural patches in the right upper, right lower, and left lower lobes (RUL, RLL, and LLL). These findings indicated a differential diagnosis of potential tumor growth or atypical pneumonia, such as tuberculosis (TB), non-tuberculous mycobacterial (NTM) infection, or fungal infection. However, the sputum sample was not available for microbiological testing.

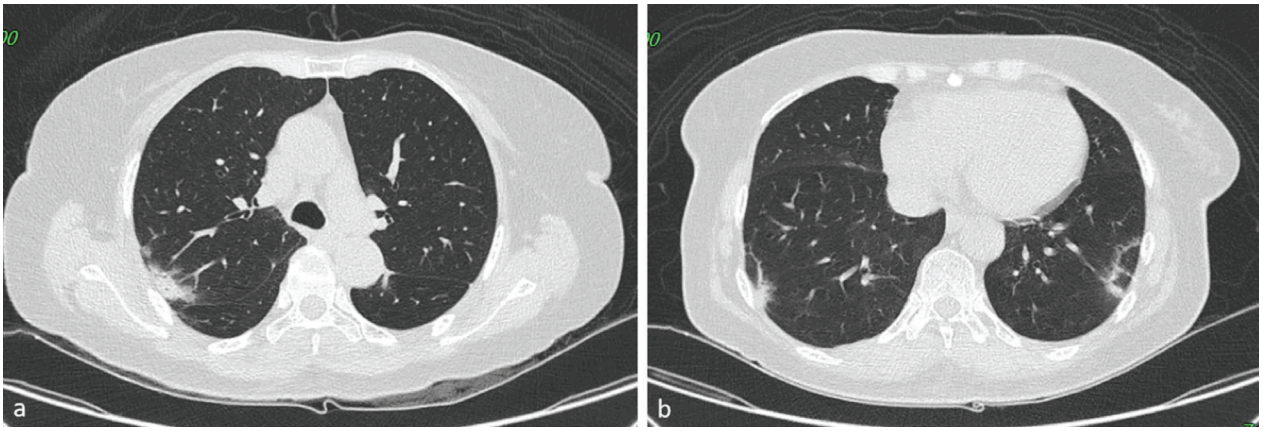

Fig. 2. (a),(b) Chest CT scan on Day 3 of admission displayed multiple subpleural patches in the right upper lobe, right lower lobe, and left lower lobe.

To confirm the diagnosis, we proceeded with video-assisted thoracoscopic surgery (VATS) wedge resection of the lung, targeting lesions in the RUL and RLL. Pathological examination of the RLL specimen uncovered a small nodule featuring glandular architecture characterized by the presence of ciliated and mucinous cells atop a basal cell layer without notable nuclear atypia or mitotic activity. Immunohistochemical assays indicated positivity for CK7 and focal positivity for thyroid transcription factor-1 (TTF-1), whereas CK20 was not expressed (Fig. 3a, Fig. 3b, Fig. 3c, Fig. 3d). These features are indicative of a BA/CMPT, generally recognized as a benign entity.

The patient underwent a follow-up chest CT scan 3 months later, which revealed residual subpleural patches with migratory behavior in the RUL, RLL, and LLL. Some patches showed new development, while others exhibited regression, raising suspicion of chronic active inflammation, possibly due to TB or NTM infection (Fig. 4a, Fig. 4b). Notably, the patient exhibited no symptoms of upper respiratory tract infection, and sputum samples remained unavailable for analysis. A subsequent CT scan performed 9 months later indicated further regression of the migrating subpleural patches in the RUL, RLL, and LLL (Fig. 5a, Fig. 5b).

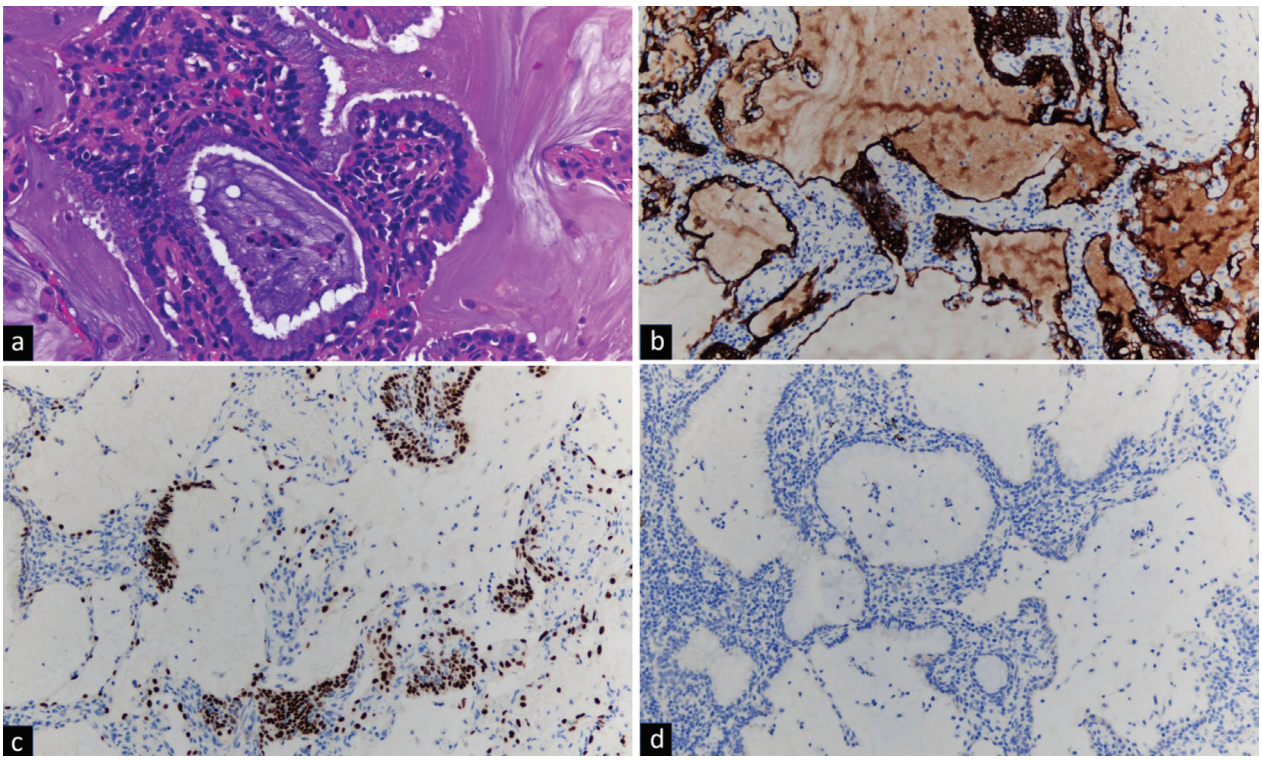

Fig. 3. (a) Hematoxylin and eosin staining at 400x magnification of the right lower lobe specimen revealed glandular architecture, consisting of ciliated and mucinous cells atop a basal cell layer, without significant nuclear atypia or mitotic activity. (b), (c), (d) Immunohistochemical stains demonstrated positivity for CK7, focal positivity for TTF-1, and negative CK20 stain.

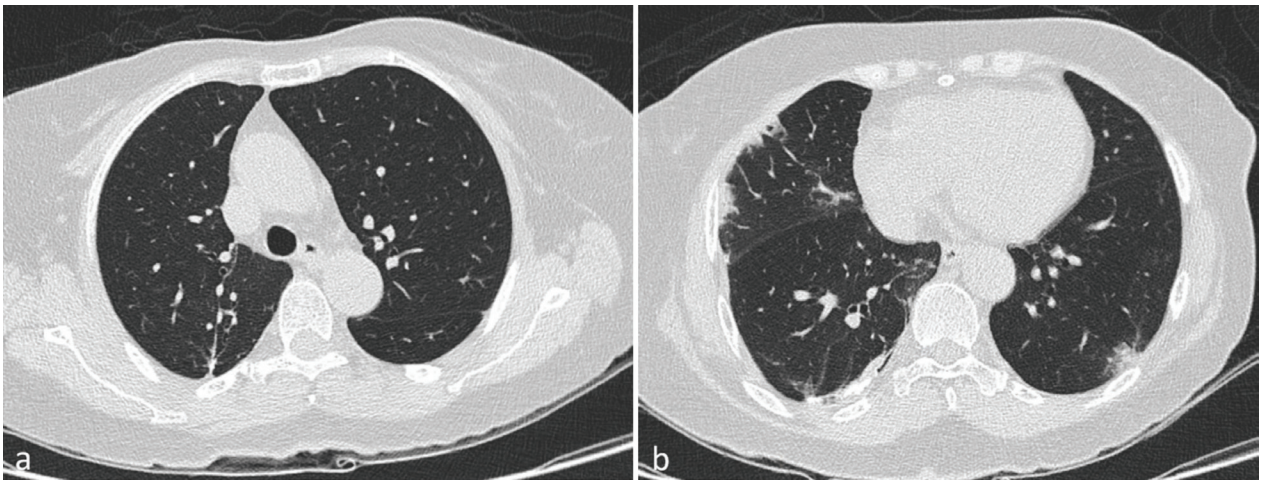

Fig. 4. (a), (b) Follow-up chest CT scan performed 3 months later revealed residual migrating subpleural patches in the right upper lobe, right lower lobe, and left lower lobe.

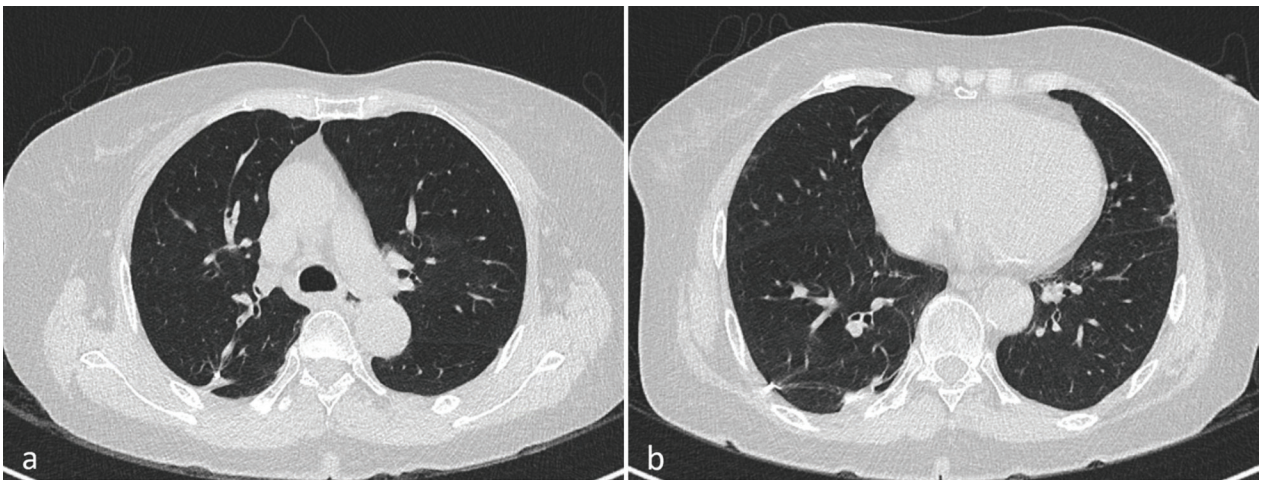

Fig. 5. (a), (b) Follow-up chest CT scan performed 9 months later showed further regression of the subpleural patches in the right upper lobe, right lower lobe, and left lower lobe.

Discussion

BA/CMPT is classified as a benign neoplasm in the 5th edition of the 2021 World Health Organization Classification of Thoracic Tumors. While some patients may exhibit symptoms such as chest pain or productive cough, most individuals with BA/CMPT are asymptomatic [2-3]. Our patient presented only with nonspecific symptoms, such as general malaise and anorexia. BA/CMPT is more commonly found in East Asian populations, with significantly few cases reported in Western populations [2, 4]. BA/CMPT typically occurs between the ages of 55 and 83, with a median age of 72 years [5]. The relationship between BA/CMPT and factors such as gender and smoking habits is still under investigation and requires

further study [3, 6]. The lesions are often discovered incidentally during routine check-ups or unrelated health visits [7].

Regarding imaging features, BA/CMPT usually presents as a solitary lesion, primarily found in the peripheral regions of the lungs, adjacent to the pleura. On CT scans, BA/CMPT can present as irregular solid, partially solid, or ground-glass nodules [8, 9]. It may also appear as cystic or cystoid lesions [10]. A key CT scan finding associated with BA/CMPT is a central or peripheral vacuolar sign within the tumor, with the central vacuolar sign being particularly characteristic [5, 10]. The enhancement patterns of BA/CMPT are more readily evaluated in larger lesions with a predominantly solid component, and often exhibit significant delayed enhancement, peaking during the venous phase. Additionally, some cases display angiographic features in the arterial phase, characterized by a natural alignment of vasculature and smooth margins [6]. In our patient, the CT scan revealed multiple subpleural patches in the RUL, RLL, and LLL, predominantly located in peripheral regions.

Due to its diverse CT manifestations, the diagnosis of BA/CMPT can be significantly challenging: it is often mistaken for non-mucinous adenocarcinoma, nodular mass-type mucinous adenocarcinoma, or inflammatory nodules [2]. When evaluating lung neoplasms, primary lung carcinoma and metastatic disease are most commonly found, with metastases covering a broad range of both epithelial and mesenchymal tumors. Lower-grade carcinomas, such as carcinoid tumors and salivary-type carcinomas, also occur with some frequency. However, benign neoplasms are relatively rare. This diverse histological spectrum can complicate the identification of benign lung neoplasms.

Common benign lung tumors include pulmonary adenomas (including BA/CMPT), bronchial papillomas, and benign mesenchymal tumors. However, BA/CMPT is often misdiagnosed as adenocarcinoma based on preoperative imaging and intraoperative frozen sections [11]. Given that BA/CMPT presents a non-aggressive growth pattern and can be effectively managed through surveillance or localized lobectomy, an accurate diagnosis is crucial to avoid unnecessary interventions.

On gross examination of biopsy specimens, BA/CMPT tumors appear as off-white or grayish-brown, with a soft, mucous-like, or even gelatinous texture [12]. Although both lungs can be involved, the lower lobes, particularly the right, are more commonly involved, as observed in our patient [13-14].

Microscopically, BA/CMPT tumors generally range in size from 2 to 45 mm, with most being between 5 and 15 mm in diameter [15]. They often feature a central unpaired artery, surrounded by acellular mucin and chronic inflammation [13]. BA/CMPT is histologically characterized by a mix of mucinous, ciliated and basal cells, which frequently line fibrovascular cores of true papillae [16]. In rare cases, squamous metaplasia may occur, which should not be mistaken for squamous cell carcinoma arising in a BA/CMPT [11, 17]. All cases exhibit a continuous layer of basal cells that express p40, p63 and CK 5/6 [11, 18], but TTF-1 shows varied expression. It has been noted that BA/CMPT exhibits significant morphological variability, and not all cases display all classical histological features [11]. Some lesions may be flat, lack papillary growth, and contain only some of the epithelial components, such as mucinous or ciliated cells [11].

The growth rate of BA/CMPT is reported to

be around 0.49 mm per year, which aligns with the growth rates seen in benign lung tumors (0.5 to 5 mm per year) [19, 20]. However, follow-up studies have identified morphological changes in BA/CMPT, such as the lobular sign, burr, and vacuolar sign. These observations indicate that BA/CMPT may undergo a natural growth process similar to indolent lung adenocarcinomas, with dynamic morphological changes over time [6, 21].

The scientific literature indicates that the prognosis of BA/CMPT is generally positive. Long-term studies have reported 100% 5-year overall survival and recurrence-free survival rates for patients with BA/CMPT, reinforcing its benign characteristics and favorable long-term outcome [6, 22-23].

The diagnosis of BA/CMPT is rare and primarily depends on pathological examination. However, distinguishing BA/CMPT from other tumors, like lung adenocarcinoma, based solely on microscopic features, can be challenging. Accurate differentiation requires evaluation of clinical factors, the location of the lesion, and imaging characteristics. While the World Health Organization Classification of Lung Histology 2021 (5th edition) categorizes BA/CMPT as benign, the identification of mutations in lung cancer driver genes raises concerns about the potential for malignant transformation [24-25]. This indicates that BA/CMPT may represent a neoplastic process rather than merely a reactive lesion [26-27]. Our patient exhibited nonspecific symptoms including general malaise and anorexia. Imaging studies revealed bilateral lung involvement, with a significant predominance of lower lobe involvement, especially on the right side, in line with epidemiological reports. Histopathological examination indicated glandular architecture composed of ciliated and mucinous epithelial cells overlying a basal cell layer, consistent with the characteristics of BA/CMPT.

Conclusion

BA/CMPT of the lung is an uncommon peripheral lung tumor that presents unique histological features. This case highlights the diagnostic challenges and therapeutic considerations of BA/CMPT. BA/CMPT is often underrecognized, leading to misdiagnosis before surgical intervention and complicating clinical management. Thorough evaluations that incorporate clinical presentation, imaging characteristics, and pathological findings to improve the understanding of BA/CMPT's unique traits and differentiate it from other lung tumors, particularly adenocarcinoma, are necessary. Ultimately, these advances will significantly benefit patients with BA/CMPT. Ongoing research and collaboration are crucial for clarifying the clinical behavior and optimal management strategies for this rare neoplasm.

References

1. Ishikawa Y. Ciliated muconodular papillary tumor of the peripheral lung: benign or malignant. Pathol Clin Med 2002; 20: 964.
2. Gao H, Du XL, Chen CN, *et al*. [Bronchiolar adenoma: a clinicopathological analysis of 15 cases]. Zhonghua Bing Li Xue Za Zhi 2020; 49(6): 556-61.
3. Sun J, Liu K, Tong H, *et al*. CT texture analysis for differentiating bronchiolar adenoma, adenocarcinoma in situ, and minimally invasive adenocarcinoma of the lung. Front Oncol 2021; 11: 634564.
4. Liu L, Aesif SW, Kipp BR, *et al*. Ciliated muconodular papillary tumors of the lung can occur in western patients and show mutations in BRAF and AKT1. Am J Surg Pathol 2016; 40(12): 1631-6.

5. Lau KW, Aubry M-C, San Tan G, *et al*. Ciliated muconodular papillary tumor: a solitary peripheral lung nodule in a teenage girl. Hum Pathol 2016; 49: 22-6.
6. Li F, Qi L, Li L, *et al*. CT imaging features of bronchiolar adenoma. Chinese J Radiol 2022: 62-7.
7. Zhang M, Song P, Zhao L, *et al*. The clinical characteristics and surgical management of ciliated muconodular papillary tumor. Zhonghua Zhong Liu Za Zhi [Chinese J Oncol] 2020; 42(6): 491-4.
8. Yang Y, Xie X, Jiang G, *et al*. Clinicopathological characteristic of ciliated muconodular papillary tumour of the lung. J Clin Pathol 2022; 75(2): 128-32.
9. Ishikawa M, Sumitomo S, Imamura N, *et al*. Ciliated muconodular papillary tumor of the lung: report of five cases. J Surg Case Rep 2016; 2016(8): rjw144.
10. Krishnamurthy K, Kochiyil J, Alghamdi S, *et al*. Bronchiolar adenomas (BA)-A detailed radio-pathologic analysis of six cases and review of literature. Ann Diagn Pathol 2021; 55: 151837.
11. Chang JC, Montecalvo J, Borsu L, *et al*. Bronchiolar adenoma: expansion of the concept of ciliated muconodular papillary tumors with proposal for revised terminology based on morphologic, immunophenotypic, and genomic analysis of 25 cases. Am J Surg Pathol 2018; 42(8): 1010-26.
12. Taguchi R, Higuchi K, Sudo M, *et al*. A case of anaplastic lymphoma kinase (ALK)-positive ciliated muconodular papillary tumor (CMPT) of the lung. Pathol Int 2017; 67(2): 99-104.
13. Ding B, Shang Z, Xiang Z, *et al*. Clinicopathologic features and frozen diagnostic pitfalls of bronchiolar adenoma/ciliated muconodular papillary tumors (BA/CMPTs). Am J Surg Pathol 2023; 47(4): 431-9.
14. Wang Y, Wang D, Wang J, *et al*. Primary ciliated muconodular papillary tumor: a rare pulmonary disease and literature review of 65 cases. Thorac Cancer 2021; 12(12): 1917-22.
15. Qiu Y, Zhang N, Liu L, *et al*. Bronchiolar adenoma: a clinicopathological analysis of 12 cases. Zhonghua Bing Li Xue Za Zhi [Chinese J Pathol] 2021; 50(8): 937-9.
16. Sato S, Koike T, Homma K, *et al*. Ciliated muconodular papillary tumour of the lung: a newly defined low-grade malignant tumour. Interact Cardiovasc Thorac Surg 2010; 11(5): 685-7.
17. Teng X, Chen Z, Zhang L, *et al*. Bronchiolar adenoma with squamous metaplasia: a distinct phenotype. Histopathology 2023; 83(2): 193-201.
18. Minami Y. [III. The Notable Topics of the 5th Edition of WHO Classification for the Thoracic Tumours (2021)]. Gan To Kagaku Ryoho 2022; 49(8): 847-52.
19. Mori K, Saitou Y, Tominaga K, *et al*. Small nodular lesions in the lung periphery: new approach to diagnosis with CT. Radiology 1990; 177(3): 843-9.
20. Onishi Y, Kusumoto M, Motoi N, *et al*. Ciliated muconodular papillary tumor of the lung: thin-section CT findings of 16 cases. Am J Roentgenol 2020; 214(4): 761-5.
21. Matsushima R, Mori T, Saeki S, *et al*. Long-term follow-up of ciliated muconodular papillary tumor of the lung by computed tomography: a case report. J Surg Case Rep 2020; 2020(12): rjaa522.
22. Cao L, Wang Z, Gong T, *et al*. Discriminating between bronchiolar adenoma, adenocarcinoma in situ and minimally invasive adenocarcinoma of the lung with CT. Diagn Interv Imaging 2020; 101(12): 831-7.
23. Tachibana M, Saito M, Kobayashi J, *et al*. Distal-type bronchiolar adenoma of the lung expressing p16INK4a–morphologic, immunohistochemical, ultrastructural and genomic analysis–report of a case and review of the literature. Pathol Int 2020; 70(3): 179-85.
24. Li X, Wu Y, Hui D, *et al*. Multiple bronchiolar adenomas with malignant transformation and CCNE1 mutation: a case report and literature review. J Cardiothorac Surg 2021; 16: 1-6.
25. Liu X-L, Miao C-F, Li M, *et al*. Malignant transformation of pulmonary bronchiolar adenoma into mucinous adenocarcinoma: a case report. World J Clin Cases 2023; 11(1): 233.
26. Jin Y, Shen X, Shen L, *et al*. Ciliated muconodular papillary tumor of the lung harboring ALK gene rearrangement: case report and review of the literature. Pathol Int 2017; 67(3): 171-5.
27. Chen F, Ren F, Zhao H, *et al*. Mucinous adenocarcinoma caused by cancerization from a ciliated multinodular papilloma tumor: a case report. Thorac Cancer 2021; 12(10): 1629-33.

Iatrogenic Tracheal Rupture Caused by Inadvertent Use of Airway Exchange Catheter for Double-Lumen Tube Replacement

Li-Yen Chang[1], Yu-Heng Li[2], Chen-Hsiang Chi[3], Yung-Wei Tung[4], Che-Hao Hsu[5]

Tracheobronchial rupture during double-lumen tube (DLT) placement is a rare, but potentially life-threatening complication. This complication is mostly due to direct trauma by the DLT. However, injury caused by the airway exchange catheter (AEC) during exchanging of the DLT is usually neglected. The AEC is widely used to increase the safety of changing endotracheal tubes (ETTs). An AEC is a long, small diameter, hollow, semi-rigid catheter that is inserted through an in situ ETT as a stylet guided for tracheal extubation and new intubation. After the ETT is withdrawn over the AEC, the AEC can also serve as a temporary conduit to administer oxygen manually through its hollow conduit during the exchange process. In the operation room setting, the AEC is commonly used for the exchange of a DLT. It avoids the risks of re-intubation and shortens the time for airway management. Although the AEC is considered a safe device, inadvertent use can cause catastrophic complications. Here, we reported the case of a 64-year-old woman who suffered from adenocarcinoma of the right middle lobe of the lung and received video-assisted thoracic surgery. After an atraumatic intubation of a DLT, an AEC was used to replace the DLT with an ETT at the conclusion of the surgery. A partial disruption of the membranous trachea, which may have resulted from the use of an AEC, was identified after operation. ***(Thorac Med 2025; 40: 171-176)***

Key words: Tracheal rupture, double-lumen tube, airway exchange catheters

Introduction

Tracheobronchial rupture during double-lumen tube (DLT) placement is a rare, but potentially life-threatening complication. This complication is mostly due to direct trauma by the DLT. However, injury caused by the airway exchange catheter (AEC) during exchange of

[1]Department of Anesthesiology, Taichung Armed Forces General Hospital, National Defense Medical Center, Taichung 41169, Taiwan. [2]Department of Anesthesiology, Tungs' Taichung MetroHarbor Hospital, Taichung 43503, Taiwan. [3]Department of Anesthesiology, Tungs' Taichung MetroHarbor Hospital, Taichung 43503, Taiwan. [4]Department of Thoracic Surgery, Tungs' Taichung MetroHarbor Hospital, Taichung 43503, Taiwan. [5]Department of Anesthesiology, Tungs' Taichung MetroHarbor Hospital, Taichung 43503, Taiwan.

*Correspondence: Dr. Che-Hao Hsu, No.699,Section 8, Taiwan Boulevard,Wuqi District,Taichung City 435403 Taiwan.

Address reprint requests to: Dr. Yu-Heng Li, No.699,Section 8, Taiwan Boulevard,Wuqi District,Taichung City 435403 Taiwan.

the DLT is usually neglected. AEC are widely used to increase the safety of changing endotracheal tubes (ETTs) [1]. An AEC is a long, small diameter, hollow, semi-rigid catheter that is inserted through an in situ ETT as a stylet guided for tracheal extubation and new intubation. After the ETT is withdrawn over the AEC, the AEC can also serve as a temporary conduit to administer oxygen manually during the exchange process. In the intensive care unit (ICU), the repeated intubation rate is as high as 19% in extubated patients [2]. The AEC provides a convenient and safe airway management device for re-intubated patients [3] and is well recognized by the American Society of Anesthesiologists [4-5]. In the operation room setting, the AEC is commonly used for the exchange of the DLT. It helps in avoiding the risks of re-intubation and shortens the time for airway management.

Although the AEC is considered a safe device, inadvertent use can cause catastrophic complications [6-7]. Here, we report the case of a 64-year-old woman who suffered from adenocarcinoma of the lung and right middle lobe and received video-assisted thoracic surgery (VATS). After an atraumatic intubation of the DLT, an AEC was used to replace the DLT with an ETT at the conclusion of the surgery. A partial disruption of the membranous trachea, which may have resulted from the use of the AEC, was identified after the operation.

Case Report

A 64-year-old woman underwent VATS for right middle lung lobectomy and extended lymph nodes dissection due to lung adenocarcinoma. She had no other significant medical or surgical history. She was 155 cm tall and weighed 51 kg. At preoperative evaluation, she presented with normal functional capacity, unremarkable physical examination, and no evidence of a difficult airway. General anesthesia was induced and her trachea was intubated smoothly with a left-sided double-lumen tracheal tube, size 35F, using a laryngoscopy Macintosh (MAC) 3 blade. Proper placement of the bronchial lumen of the tube in the left main bronchus was confirmed with fiberoptic bronchoscopy, and no signs of trachea abnormalities were found at that time. The patient was placed in the lateral position for the surgical procedure, and the position of the DLT was checked once again. No blood or signs of bronchial or tracheal trauma were ever observed. One-lung ventilation was established. The surgery was performed smoothly and her vital signs were maintained well.

At the conclusion of the surgery, and for respiratory care in the ICU, we exchanged the DLT for an ETT. The bronchial balloon of the DLT was deflated and withdrawn to 21 cm in depth. The AEC (Cook® Airway Exchange Catheter) (Fig. 1) was lubricated and passed through the bronchial lumen of the DLT, after

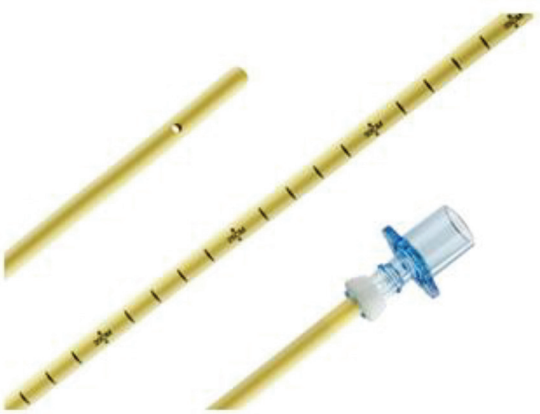

Fig. 1. Cook® Airway Exchange Catheter made by Cook Critical Care (Bloomington, IN, USA).

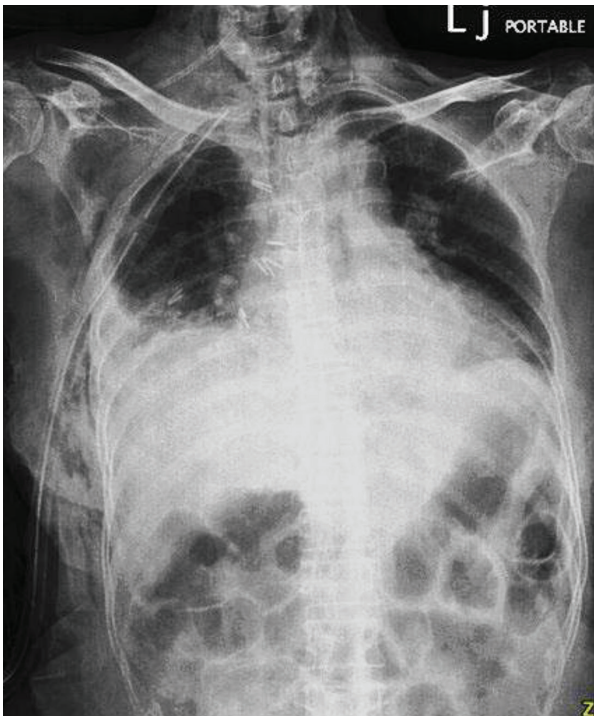

Fig. 2. First-day postoperative chest radiograph showed subcutaneous emphysema, pleural effusion at the right lung.

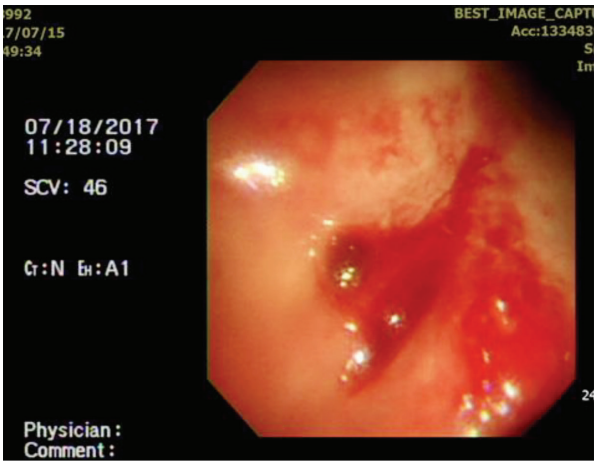

Fig. 3. A linear 1.5-cm partial-thickness laceration of the membranous trachea was found in the postoperative bronchoscopy.

suctioning the trachea and adequate oxygenation was provided. The DLT was then removed, with the AEC remaining in place. A 7.0-size ETT was inserted over the AEC. The whole procedure was done smoothly, except some resistance was encountered during AEC insertion. The patient was transferred to the ICU. Due to stable vital signs, weaning from ventilator was begun. Extubation at the ICU was successful at 12-hours postoperatively. On the second day, subcutaneous emphysema in the bilateral neck region developed. Chest radiograph showed the subcutaneous emphysema and lung collapse at the right lower lobe (Fig. 2). The immediate bronchoscopy revealed a 1.5-cm linear mucosal laceration located at the lower trachea, 2 cm above the carina (Fig. 3).

Due to persistent and massive air leakage from the chest tube, emergency thoracotomy with repair of the trachea, and use of tissue glue for sealing were undertaken without complication, and no further cardiopulmonary events occurred. The remainder of the hospital course was uneventful and the patient was discharged.

Discussion

Airway trauma during endotracheal intubation is a well-known complication. The injuries that result from mucosal injury are mostly minor [8]. However, serious damage such as tracheal rupture may occur, causing catastrophic complications. These injuries usually are left undetected or have delayed diagnosis due to their non-specific symptoms. Complications include pneumothorax, mediastinal emphysema, and prolapse of the esophagus into the trachea causing respirator insufficiency [9]. Clinical presentations of tracheal rupture include hemoptysis, dysphagia, dyspnea and subcutaneous emphysema. In extreme cases, respiratory distress can develop [10]. The first symptom of tracheal injury frequently appears within 12 hours after extubation, although it has been re-

ported to be delayed up to 100 hours following intubation [11]. Imaging studies including chest radiography, computed tomography, and bronchoscopy can aid in diagnosing and locating lesions of a tracheobronchial injury.

Tracheobronchial rupture is more common when using DLTs, because of their larger external diameter and stiff consistency [12, 13]. These ruptures occur rarely, likely in less than 0.2% of DLT intubations [14]. Most commonly, injuries are located at the distal trachea or left main bronchus, usually because of the preference for left-sided DLTs. The injuries usually occur as a longitudinal tear within the membranous portion of the trachea. The risk factors for these injuries include placement by inexperienced personnel, multiple intubation attempts, placement of the stylet through the DLT with its tip protruding, overinflation of the cuff, over-sized DLT, an incompletely anesthetized patient, steroid use or radiation therapy, and previous tracheomalacia [15]. These injuries can occur during intubation or extubation of a DLT [6, 16]. Even during an otherwise uneventful intubation, tracheobronchial laceration may occur, potentially due to trauma caused from the tip of the ETT catching in a fold of membranous tissue in the posterior trachea [10]. In our case, a post-intubation check with bronchoscopy showed no anomalies. The injury most likely occurred when an AEC was used to exchange the DLT, because the physician described encountering stiff resistance during this process.

The use of an AEC is not without risks [1]. These risks can be divided into 2 categories: (1) barotrauma resulting from air entry exceeding air exit and (2) failure to successfully pass the new ETT over the AEC. Moreover, tracheal damage by an AEC is usually an ignored complication because it can only be confirmed by bronchoscopic examination [17]. Airway exchange failure rates and the occurrence of pneumothorax are greatest when using an exchange catheter for DLT insertion [18]. There are case reports in which the AEC caused tracheal laceration during placement of the DLT [7] or when used for re-intubation [19]. The tube exchanger is stiff in consistency so as to serve as an adequate guide for sliding the ETT into the trachea. The tip is also firm and the leading edge can cause trauma. The depth of insertion of the AEC must be watched. An insertion that is too deep can directly increase the risk of perforation of the tracheobronchial tree [19, 20]. When administering oxygen via an AEC, deep insertion may also lead to the risks of barotrauma [21]. Many cases of tracheobronchial perforations have been reported, and in these cases, the location of the tracheal tear usually was beneath the carina [20]. It is prudent not to allow the centimeter calibration on the AEC to exceed a depth of 26 cm in an adult, and never insert an AEC when resistance is encountered [19].

Many types of AECs have been used; 1 of the most widely used is the multiple-sized, appropriately adapted, centimeter-depth-marked, commercial model made by Cook Critical Care (Bloomington, IN). Cook has redesigned the AEC and has made the leading tip soft, whereas the rest of the exchanger is still firm. They emphasize that the catheter has a blunt, soft, and flexible tip and is atraumatic to internal structures. The new model may make tracheal damage less likely [22]. In our case, the reformed model we used did not fully prevent the risks of airway trauma. The inadvertent use of an ACE may lead to tracheal damage.

When a tracheobronchial tear does occur, it can result in life-threatening complications. During anesthesia, abrupt changes in vital

signs, difficulty with ventilation, or onset of an unexplainable ventilatory air leak may be the first signs. If unrecognized, symptoms of tension pneumothorax or subcutaneous emphysema may occur. Thoracic cavity infection or sepsis ensues. Simple airway mucosal tearing is always self-limited without any special treatment. It was believed that if the breach was less than 1 cm, it would gradually stop leaking [23]. However, if patients are in an acute stage with severe air leakage, breathing difficulties and an unstable general condition, rupture of the trachea and bronchus should be operated on as soon as possible. The success rate is high in early repair of healthy tissue, with quick improvement and better long-term outcome. Scar stricture, infection, retraction and adhesion may appear on a broken end that is delayed until the late stage, and this is not conducive to surgical repair [24]. Early recognition of tracheobronchial tear and prompt repair are of paramount importance for optimal patient outcome.

Conclusion

A tracheal rupture after use of an AEC for exchanging of a DLT is very rare. In our case, it was the AEC that was thought to cause the lower tracheal laceration. Tube exchangers have made re-intubation easy and safer, but not without risks. Cautious manipulation, rather than avoidance of this technique, is vital to protecting the airway from the anesthesia-related injury. Immediate inspection of the airway by an experienced surgeon is necessary to check the extent of damage. Prompt recognition and repair of the rupture are important to obtaining an optimal patient outcome and prevention of systemic complications.

References

1. Benumof JL. Airway exchange catheters: simple concept, potentially great danger. Anesthesiology 1999; 91: 342-344.
2. Demling RH, Read T, Lind LJ, *et al*. Incidence and morbidity of extubation failure in surgical intensive care patients. Crit Care Med 1988; 16: 573-577.
3. Mort TC. Continuous airway access for the difficult extubation: the efficacy of the airway exchange catheter. Anesth Analg 2007; 105: 1357-1362.
4. Bedger RC, Jr., Chang JL. A jet-stylet endotracheal catheter for difficult airway management. Anesthesiology 1987; 66: 221-223.
5. Practice guidelines for management of the difficult airway. A report by the American Society of Anesthesiologists Task Force on Management of the Difficult Airway. Anesthesiology 1993; 78: 597-602.
6. Hartman WR, Brown M, Hannon J. Iatrogenic left main bronchus injury following atraumatic double lumen endotracheal tube placement. Case Rep Anesthesiol 2013; 2013:524348.
7. Thomas V, Neustein SM. Tracheal laceration after the use of an airway exchange catheter for double-lumen tube placement. J Cardiothorac Vasc Anesth 2007; 21: 718-719.
8. Mencke T, Echternach M, Kleinschmidt S, *et al*. Laryngeal morbidity and quality of tracheal intubation: a randomized controlled trial. Anesthesiology 2003; 98: 1049-1056.
9. Kaloud H, Smolle-Juettner FM, Prause G, *et al*. Iatrogenic ruptures of the tracheobronchial tree. Chest 1997; 112: 774-778.
10. Jones TS, Sullivan A, Damle S, *et al*. Assessment and management of post-intubation airway injuries. Semin Cardiothorac Vasc Anesth 2017; 21: 99-104.
11. Chamberlain S, Rahman H, Frunza G, *et al*. Massive surgical emphysema secondary to iatrogenic tracheal laceration. BMJ Case Rep 2015; 2015.
12. Knoll H, Ziegeler S, Schreiber JU, *et al*. Airway injuries after one-lung ventilation: a comparison between double-lumen tube and endobronchial blocker: a randomized, prospective, controlled trial. Anesthesiology 2006; 105: 471-477.
13. Liu H, Jahr JS, Sullivan E, *et al*. Tracheobronchial

rupture after double-lumen endotracheal intubation. J Cardiothorac Vasc Anesth 2004; 18: 228-233.
14. Fitzmaurice BG, Brodsky JB. Airway rupture from double-lumen tubes. J Cardiothorac Vasc Anesth 1999; 13: 322-329.
15. Ceylan KC, Kaya SO, Samancilar O, *et al*. Intraoperative management of tracheobronchial rupture after double-lumen tube intubation. Surg Today 2013; 43: 757-762.
16. Benumof JL, Wu D. Tracheal tear caused by extubation of a double-lumen tube. Anesthesiology 2002; 97: 1007-1008.
17. Rashid AM, Williams C, Noble J, *et al*. Pneumothorax, an underappreciated complication with an airway exchange catheter. J Thorac Dis 2012; 4: 659-662.
18. McLean S, Lanam CR, Benedict W, *et al*. Airway exchange failure and complications with the use of the Cook Airway Exchange Catheter(R): a single center cohort study of 1177 patients. Anesthes Analg 2013; 117: 1325-1327.
19. Seitz PA, Gravenstein N. Endobronchial rupture from endotracheal reintubation with an endotracheal tube guide. J Clin Anesthes 1989; 1: 214-217.
20. deLima LG, Bishop MJ. Lung laceration after tracheal extubation over a plastic tube changer. Anesthes Analg 1991; 73: 350-351.
21. Axe R, Middleditch A, Kelly FE, *et al*. Macroscopic barotrauma caused by stiff and soft-tipped airway exchange catheters: an in vitro case series. Anesthes Analg 2015; 120: 355-361.
22. Neustein SM. The safe use of an airway exchange catheter. Anesthes Analg 2014; 119:216.
23. Zhao Z, Zhang T, Yin X, *et al*. Update on the diagnosis and treatment of tracheal and bronchial injury. J Thorac Dis 2017; 9: E50-E56.
24. Lui N, Wright C. Intraoperative tracheal injury. Thorac Surg Clin 2015; 25: 249-254.

Declarations:

Ethics approval and consent to participate: not applicable

Consent for publication: Written informed consent was obtained from the patient for publication of this case report and any accompanying images. A copy of the written consent is available for review by the Editor-in-Chief of this journal.

Availability of supporting data: Not applicable

Competing interests: The authors declare that they have no competing interests in this section.

Funding: not applicable

Author contributions: Conceptualization, C.-H.H.; writing—original draft, L.-Y.C., Y.-H. L.; reviewing and editing, C.-H. C., Y.-W. T.

All authors have read and agreed to the published version of the manuscript.

Acknowledgements: Not applicable.

Segmental Volume Reduction Through Bronchoscopic Thermal Vapor Ablation in Symptomatic Heterogeneous Emphysematous Chronic Obstructive Pulmonary Disease - 4 Case Reports

Szu-Yu Liu[1], Jeng-Shiuan Tsai[1], Chian-Wei Chen[1], Po-Lan Su[1], Yau-Lin Tseng[2], Chang-Wen Chen[1], Chin-Wei Kuo[1]

Bronchoscopic lung volume reduction techniques improve lung function and dyspnea symptoms in chronic obstructive pulmonary disease (COPD) patients with upper lung-dominant heterogeneous emphysema. Bronchoscopic thermal vapor ablation (BTVA) is a treatment with an acceptable safety profile for these patients. However, this technique is rarely performed in Taiwan, and there is a lack of experience using it. We performed BTVA for 4 symptomatic COPD patients with upper lung-predominant heterogeneous emphysema, despite having received adequate bronchodilator treatment between January 2022 and June 2023. These patients were aged between 45 and 69 years, had baseline predicted FEV1 values ranging from 28% to 75%, and exhibited substantial hyperinflation. The baseline COPD Assessment Test (CAT) scores ranged from 10 to 22. Three patients received BTVA once on a unilateral lung, and 1 patient underwent staged BTVA on the ipsilateral lung. Post-BTVA pneumonitis was observed in 1 patient, and there was improvement after steroid and antibiotic treatment. Three of the 4 patients experienced a reduction in emphysema as observed on chest CT scans, improvements in FEV1, reduced residual volume, lower CAT scores, and stable exercise capacity. One patient was lost to follow-up for unknown reasons. BTVA is effective and safe for symptomatic COPD patients with upper lung-predominant heterogeneous emphysema and poor lung function. ***(Thorac Med 2025; 40: 177-183)***

Key words: BTVA, COPD, emphysema

[1]Division of Chest Medicine, Department of Internal Medicine, National Cheng Kung University Hospital, College of Medicine, National Cheng Kung University, Tainan, Taiwan. [2]Division of Chest Surgery, Medicine Department of Surgery, National Cheng Kung University Hospital, College of Medicine, National Cheng Kung University, Tainan, Taiwan.
Address reprint requests to: Dr. Chin-Wei Kuo, National Cheng Kung University Hospital, No.138, Sheng Li Road, Tainan, Taiwan.

Introduction

Chronic obstructive pulmonary disease (COPD) is characterized by progressive airway obstruction and is associated with parenchymal abnormalities in both the airway and the lungs. Emphysema, a common feature of COPD, is linked to hyperinflation, dyspnea, a rapid decline in forced expiratory volume in 1 second (FEV_1), and increased mortality [1]. Standard treatments, including inhaled bronchodilators, inhaled corticosteroids, and pulmonary rehabilitation, partially improve pulmonary function and reduce hyperinflation. However, despite receiving maximal medical therapy, many patients continue to experience significant dyspnea and exercise intolerance.

Lung volume reduction surgery (LVRS) has been shown to improve lung function, alleviate dyspnea, and enhance quality of life in patients with upper lobe-predominant emphysema and low post-rehabilitation exercise capacity [2]. However, the risks of surgery and general anesthesia significantly limit the number of patients eligible for LVRS [3]. To overcome these limitations, bronchoscopic lung volume reduction (BLVR) techniques, including valve or coil implantation, and thermal vapor ablation, have been developed and have demonstrated significant benefits in improving lung function and reducing dyspnea in COPD patients with heterogenous emphysema [4].

Bronchoscopic thermal vapor ablation (BTVA) is a well-established technique within the spectrum of BLVR. It delivers thermal energy through heated water vapor, inducing a localized inflammatory response that leads to lung fibrosis and atelectasis, ultimately resulting in permanent lung volume reduction [5]. Clinical studies have shown significant improvements in lung function and quality of life following BTVA, with an acceptable safety profile for patients with COPD [5, 6]. Moreover, unlike valve- or coil-based BLVR methods, which are unsuitable for patients with interlobar collateral ventilation (CV), BTVA remains a viable option for patients with upper lobe-predominant heterogeneous emphysema, regardless of the presence of interlobar CV [7].

Despite its promise, clinical experience with BTVA remains limited in Taiwan. Here, we present the clinical outcomes of 4 emphysematous COPD patients treated with BTVA at National Cheng Kung University Hospital, providing insights into the feasibility and effectiveness of BTVA in Taiwanese population.

Methods

We performed BTVA on 4 severely symptomatic COPD patients between January 2022 and June 2023. Based on previous study [6], the key eligibility criteria for BTVA included upper lobe-predominant heterogeneous emphysema, an FEV_1 between 20% and 45% of predicted value, a residual volume (RV) exceeding 150% of predicted value, a diffusing capacity of the lungs for carbon monoxide (DLCO) greater than 20% of predicted value, and a modified Medical Research Council (mMRC) score greater than 2, despite optimal medical treatment. Upper lobe-predominant heterogeneous emphysema was confirmed via chest CT imaging, with a calculated heterogeneity index greater than 1.2 used to define heterogeneous emphysema [7]. Since the initial implementation of BTVA in our hospital, we have adjusted the enrollment criteria to reduce the risk of severe complications in patients with high disease severity.

The treatment plan was designed using the InterVapor Personalized Procedure Program (IP3) software. BTVA was performed under deep sedation and neuromuscular blockade in the intensive care unit, with oxygenation and ventilation maintained via invasive mechanical ventilation. The balloon of the InterVapor catheter was inflated to occlude the target bronchus, delivering heated water vapor with a target vapor dose of 8.5 calories/g. Prophylactic antibiotics were administered before the procedure, and tracheal extubation was performed after a few hours of observation. Complications such as pneumothorax, hemoptysis, and pneumonitis were closely monitored post-procedure. Systemic glucocorticosteroids were administered using a tapered regimen for 2 to 4 weeks to mitigate pneumonitis. Pulmonary function tests and symptom scores were documented at 3, 6, and 12 months following the BTVA procedure.

Case Description

The 4 patients were male, aged between 45 and 69 years (Table 1). All were diagnosed with COPD group B and were receiving dual bronchodilator treatment. Their baseline FEV_1 values ranged from 28% to 75% of predicted value, and they exhibited substantial hyperinflation, with RV exceeding 140% of predicted

Table 1. Baseline Characteristics and BTVA Setting of Enrolled Patients

Category	Patient 1	Patient 2	Patient 3	Patient 4
Age, years	45	57	69	67
Sex	Male	Male	Male	Male
Body-mass index (kg/m²)	28.7	20.7	25.1	27.0
Smoking history (pack-years)	60	60	122	160
mMRC	2	2	2	3
CAT	11	10	10	22
FEV1 value (predicted %)	1.22L (36%)	1.49L (55%)	1.55L (75%)	0.71L (28%)
RV value (predicted %)	6.58L (426%)	3.96L (262%)	2.12L (141%)	5.08L (301%)
DLCO (predicted %)	74	53	48	26
VO2 Max/kg (predicted %)	18.6 (61%)	15.7 (51.3%)	14.5 (57%)	9.8 (39.5%)
Inhaled bronchodilator	ICS+LABA+LAMA	LABA+LAMA	LABA+LAMA	ICS+LABA+LAMA
BTVA targeted bronchus, segment volume and treatment dose	1st time: LB1 (419 ml, 365 cal) LB3 (492 ml, 297 cal) 2nd time: LB1 (385 ml, 357 cal) LB3 (341 ml, 255 cal)	LB3 (461 ml, 374 cal)	RB1 (452 ml, 340 cal) RB3 (733 ml, 731 cal)	RB1 (414 ml, 306 cal) RB2 (809 ml, 467 cal)
Complication	Nil	Nil	Pneumonitis	Nil
Hospital stays	1st time: 5 days 2nd time: 6 days	5 days	11 days	6 days

value. Baseline COPD Assessment Test (CAT) scores ranged from 10 to 22, and baseline VO_2 max values ranged from 9.8 to 18.6 mL/kg/min.

The first patient underwent staged BTVA at 6-month intervals for treatment of segmental bronchus of the left upper lung, segment 1 (LB1) and LB3. The other 3 patients received a single BTVA procedure on 1 lung (Table 1). Post-BTVA pneumonitis occurred in the third patient, who showed improvement after a 5-day course of prednisolone at 0.8 mg/kg/day and an antibiotic. This patient, aged 69 years, had a baseline FEV_1 of 75% and a diagnosis of combined pulmonary fibrosis and emphysema (CPFE). Unfortunately, the patient was lost to follow-up for unknown reasons.

No pneumothorax or COPD exacerbations requiring hospitalization were observed in the other 3 patients during the 1-year follow-up period. Chest CT scans showed reductions in emphysema (Fig. 1) See page 181). These patients also demonstrated pulmonary function improvements, with FEV_1 increases ranging from 120 mL to 580 mL at 12 months post-BTVA and RV reductions ranging from 1720 mL to 2580 mL during follow-up (Fig. 2). Additionally, the ratio of inspiratory capacity (IC) to total lung capacity (TLC) improved significantly. Maximal oxygen uptake (VO_2 max) remained stable at the 6-month follow-up (Fig. 2). All 3 patients experienced decreases in CAT and mMRC scores, reflecting symptomatic improvement (Fig. 2).

Discussion

In our case series, most patients reported improvements in symptoms and quality of life following BTVA. These findings are consistent with those of previous studies [5-6, 8, 11]. While VO_2 max did not improve after treatment, it remained stable. VO_2 max is considered the gold standard for assessing aerobic exercise ca-

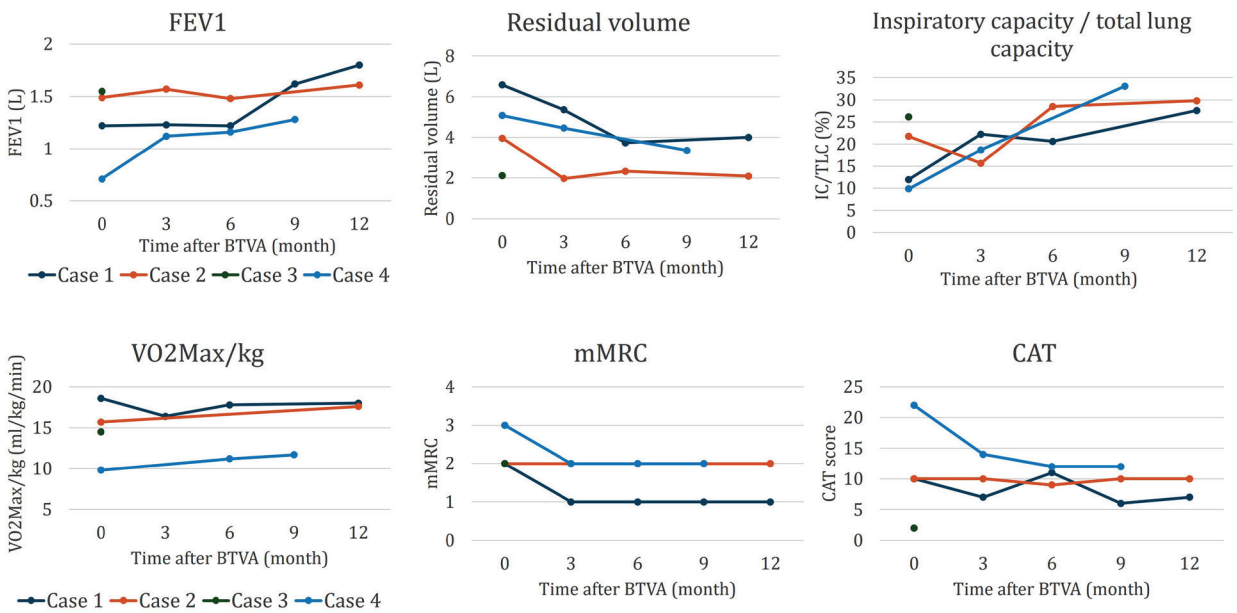

Fig. 2. Changes in Pulmonary Function and Dyspnea Scores Before and After BTVA Treatment.

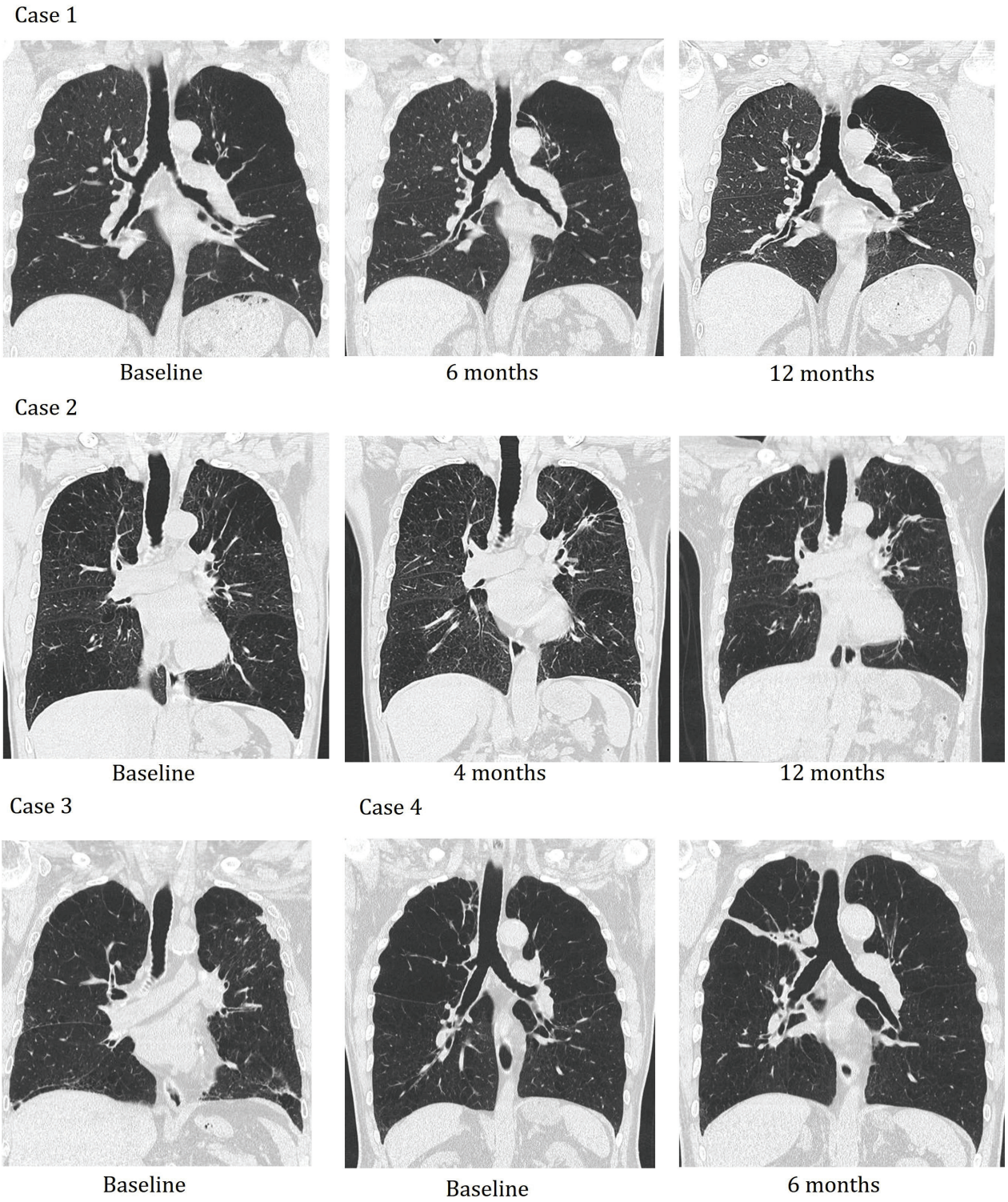

Fig. 1. Chest CT Images Before and After BTVA Treatment.

pacity and is an important measure of exercise intolerance in patients with COPD [12]. However, the cardiopulmonary exercise test (CPET) reflects not only respiratory mechanical factors but also cardiocirculatory and muscle strength factors. During follow-up, we measured the resting inspiratory capacity (IC) and the ratio of IC to total lung capacity (TLC) as indicators of exercise limitation. Resting IC reflects the operating limits of tidal volume expansion during exercise in COPD and is a marker of dynamic hyperinflation and exertional dyspnea [13]. Our patients demonstrated significant improvements in the IC/TLC ratio, with increases of 15%, 8%, and 23% at 12 months post-BTVA.

BTVA has been well-established as an effective and safe treatment option. The pilot study conducted in 2009 by Snell *et al*. confirmed the feasibility of unilateral upper-lobe BTVA and its acceptable safety profile [8]. Subsequently, Snell *et al*. conducted a prospective single-arm study involving 44 patients with upper-lobe predominant emphysema treated with a higher vapor dose of 10 calories/g [5]. This study reported significant improvements, including an increase in FEV_1 of 141 ± 26 mL, a reduction in residual volume by 406 ± 113 mL, and a 48% reduction in target lobar volume as measured by HRCT at 6 months post-treatment.

Furthermore, the STEP-UP study [6] utilized a staged treatment strategy targeting the most diseased emphysematous segments of the bilateral upper lobes using a vapor dose of 8.5 calories/g. The study reported a significant mean increase of 14.7% in FEV_1 and a 9.7-point reduction in the St. George's Respiratory Questionnaire (SGRQ) score at 6 months following bilateral BTVA, compared to the control group. During the 12-month follow-up period, improvements in lung function and quality of life (SGRQ score) were sustained, although the 6-min walk test did not show significant improvement after treatment [11].

Since BTVA delivers thermal energy via heated water vapor, inducing a localized inflammatory reaction [8], common adverse effects include acute COPD exacerbations, pneumonia, and pneumonitis [9]. In the STEP-UP trial, the incidence of pneumonia or pneumonitis was 18%, with a mean hospital stay of 11 days [6]. These complications did not lead to respiratory failure or the need for intensive care. Glucocorticosteroids are recommended to alleviate symptoms of a localized inflammatory reaction (0.5 mg/kg for 2–4 weeks using a tapered regimen). Prophylactic antibiotics are also suggested to reduce the risk of bacterial superinfection [7].

In our study, the third patient, with a baseline FEV_1 of 75%, had CPFE and developed pneumonitis and hemoptysis within 1 week after BTVA. Symptoms resolved after short-term treatment with steroids, antibiotics, and tranexamic acid. The hospital stays lasted 11 days. This patient did not fully meet the eligibility criteria of the STEP-UP trial [6], as the FEV_1 exceeded the threshold of 45%. Although the residual volume precisely met the threshold of 140%, this deviation from eligibility criteria may have contributed to the adverse events and the patient's failure to return for follow-up visits. The other 3 patients remained asymptomatic to the inflammatory reaction. Moving forward, stricter adherence to enrollment criteria will be essential to minimize adverse effects and maximize treatment efficacy.

Summary

In our experience, BTVA is a safe and ef-

fective procedure to improve lung function and quality of life in symptomatic COPD patients with upper lobe-predominant heterogeneous emphysema and impaired lung function. Careful patient selection is crucial to achieving optimal outcomes.

References

1. Davey C, Zoumot Z, Jordan S, *et al*. Bronchoscopic lung volume reduction with endobronchial valves for patients with heterogeneous emphysema and intact interlobar fissures (the BeLieVeR-HIFi study): a randomised controlled trial. Lancet 2015; 386(9998): 1066-73.
2. Fishman A, Martinez F, Naunheim K, *et al*. A randomized trial comparing lung-volume-reduction surgery with medical therapy for severe emphysema. N Engl J Med 2003; 348(21): 2059-2073.
3. Abdelsattar ZM, Allen M, Blackmon S, *et al*. Contemporary practice patterns of lung volume reduction surgery in the United States. Ann Thorac Surg 2021; 112(3): 952-960.
4. Shah PL, Herth FJ, van Geffen WH, **et al**. Lung volume reduction for emphysema. Lancet Respir Med 2017 Feb; 5(2): 147-156.
5. Snell G, Herth FJ, Hopkins P, *et al*. Bronchoscopic thermal vapour ablation therapy in the management of heterogeneous emphysema. Eur Respir J 2012; 39(6): 1326-1333.
6. Herth FJ, *et al*. Segmental volume reduction using thermal vapour ablation in patients with severe emphysema: 6-month results of the multicentre, parallel-group, open-label, randomised controlled STEP-UP trial. Lancet Respir Med 2016 Mar; 4(3): 185-93.
7. Gompelmann D, Shah PL, Valipour A, *et al*. Bronchoscopic thermal vapor ablation: best practice recommendations from an expert panel on endoscopic lung volume reduction. Respiration 2018; 95(6): 392-400.
8. Snell G, Hopkins P, Westall G, *et al*. A feasibility and safety study of bronchoscopic thermal vapor ablation: a novel emphysema therapy. Ann Thorac Surg 2009; 88(6):1993–1998.
9. Gompelmann D, Eberhardt R, Ernst A, *et al*. The localized inflammatory response to bronchoscopic thermal vapor ablation. Respiration 2013; 86: 324-31.
10. Zhi L, Liao L, Wu Z, *et al*. Impact of bronchoscopic thermal vapor ablation on lung volume reduction in patients with emphysema: a meta-analysis. BMC Pulm Med 2023 Oct 26; 23(1): 405.
11. Shah PL, Gompelmann D, Valipour A, *et al*. Thermal vapour ablation to reduce segmental volume in patients with severe emphysema: STEP-UP 12-month results. Lancet Respir Med 2016; 4: e44-e45.
12. Choi H-E, Min E-H, Kim H-K, *et al*. Peak oxygen uptake and respiratory muscle performance in patients with chronic obstructive pulmonary disease: clinical findings and implications. Medicine 2022 Oct 21; 101(42): e31244.
13. O'Donnell DE, Elbehairy AF, Webb KA, *et al*. Canadian Respiratory Research Network. The link between reduced inspiratory capacity and exercise intolerance in chronic obstructive pulmonary disease. Ann Am Thorac Soc 2017 Jul; 14(Supplement_1): S30-S39.

A Rare Presentation of Lung Adenocarcinoma with Duodenal Metastasis

Yu-Mu Chen[1,2], Kuo-Tung Huang[1], Chieh-Hao Lai[1], Meng-Chih Lin[1,3], Sheng-Wei Tu[1]

Lung adenocarcinoma with duodenal metastasis is extremely uncommon. We report a case of duodenal metastasis from primary lung adenocarcinoma that presented with upper gastrointestinal bleeding. Tumor cells showed immunopositivity for thyroid transcription factor 1 and cytokeratin-7 (CK7), and immunonegativity for CK20, synaptophysin and CDX2, suggesting the diagnosis of metastatic adenocarcinoma of lung origin. ***(Thorac Med 2025; 40: 184-188)***

Key words: Lung adenocarcinoma, metastasis

Introduction

Lung cancer is 1 of the most common malignancies of which distant metastasis is usually present when initially diagnosed [1]. Tumor-stromal interactions have replaced seed and soil hypotheses as the main mechanism of distant metastases [2-4]. Lung cancer patients who were younger, female, and with an EGFR mutation or small cell histology were more likely to have distant metastases [1, 5]. Lung cancer patients with de novo distant metastases had a shorter survival period than those without [5-7]. The most common sites of lung cancer metastasis are the lymph node, lung, bone, brain, liver, pleura and adrenal glands [8]. Lung cancer rarely metastasizes to the gastrointestinal (GI) tract, with only a 0.2–1.7% occurrence rate in clinical studies [9-14]. We present the case of a 58-year-old female with a history of adenocarcinoma, who was found to have a duodenal mass on esophagogastroduodenoscopy (EGD) diagnosed as metastatic adenocarcinoma from the lung, based on histological analysis.

Case Report

A 58-year-old female patient was diagnosed with left upper lung adenocarcinoma, T4N2M1b stage IVA, with lung-to-lung and brain metastasis in October 2019. She had a wild-type EGFR mutation, no ALK rearrangement, no ROS mutation, and no BRAF V600 mutation. Due to a high PDL-1 expression, she

[1]Division of Pulmonary and Critical Care Medicine, Department of Internal Medicine, Kaohsiung Chang Gung Memorial Hospital, Kaohsiung, Taiwan. [2]Graduate Institute of Clinical Medical Sciences, College of Medicine, Chang Gung University, Taoyuan 33302, Taiwan. [3]Respiratory Center of Excellence, Chang Gung Medical Institute, Kaohsiung 83301, Taiwan.
Address reprint requests to: Dr. Sheng-Wei Tu, Division of Pulmonary and Critical Care Medicine, Department of Internal Medicine, Kaohsiung Chang Gung Memorial Hospital, Kaohsiung, Taiwan.

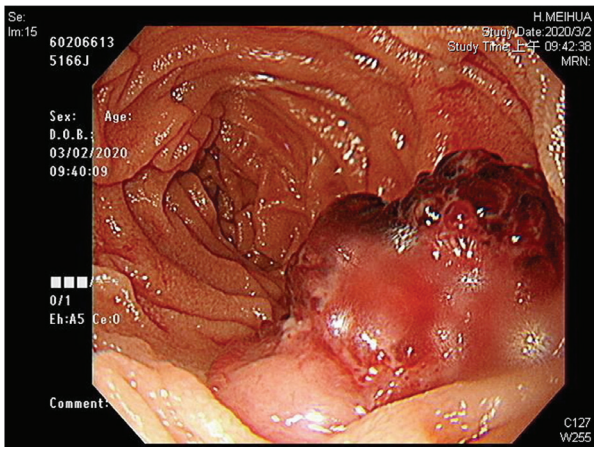

Fig. 1. Tumor mass under esophagogastroduodenoscopy.

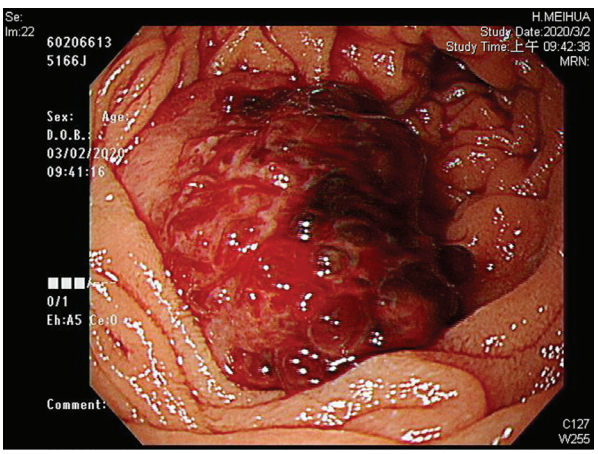

Fig. 2. Tumor mass under esophagogastroduodenoscopy.

began receiving pembrolizumab 200 mg every 3 weeks in January 2020. On 1 March 2020, she suffered from epigastric pain for 2 days, with the accompanying symptoms of nausea, a heartburn sensation and tarry stool passage. So she came to the emergency department, where upper gastrointestinal bleeding was suspected. Her lab data testing revealed hemoglobin 7.8 g/dL. On 2 March, the patient received an EGD, which showed an ulcerative mass about 2 cm in size with recent bleeding at the second portion of the duodenum [Fig.1, 2]. Biopsy was taken from the duodenal mass and the pathology report revealed a positive thyroid transcription factor-1 immunohistochemistry stain, suggestive of metastatic adenocarcinoma from the lung [Fig. 4, 5]. Abdominal computed tomography with contrast on 7 March 2020 showed multiple nodules in the liver, left adrenal gland, pancreatic tail, and right retroperitoneum, suggesting metastasis [Fig. 3]. After the gastrointestinal bleeding had subsided, the patient was discharged, with plans to receive chemotherapy in the near future.

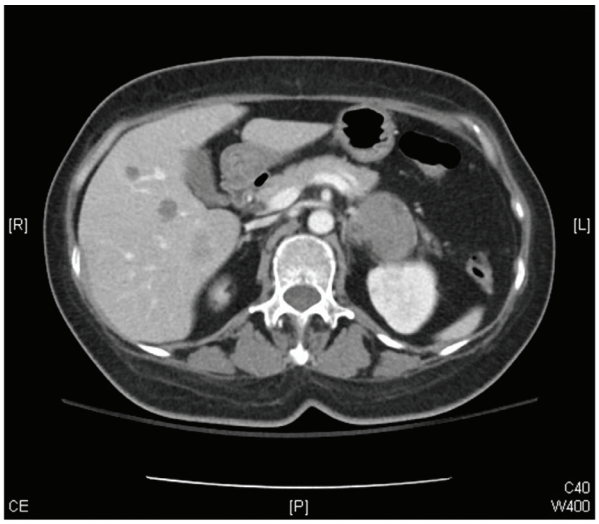

Fig. 3. Abdominal CT revealed metastasis.

However, she suffered from massive tarry stool on 19 March 2020, with hypovolemic shock, followed by apnea on the night of 24 March 2020. We then performed intubation and cardiopulmonary cerebral resuscitation (CPCR) for the patient, and she presented a return of spontaneous circulation after CPCR for 22 minutes. However, she also had dilated pupils after CPCR. We informed the patient's family of the poor prognosis and critical condition of the patient, and the family signed a "do not resuscitate" order. The patient expired on 24 March 2020.

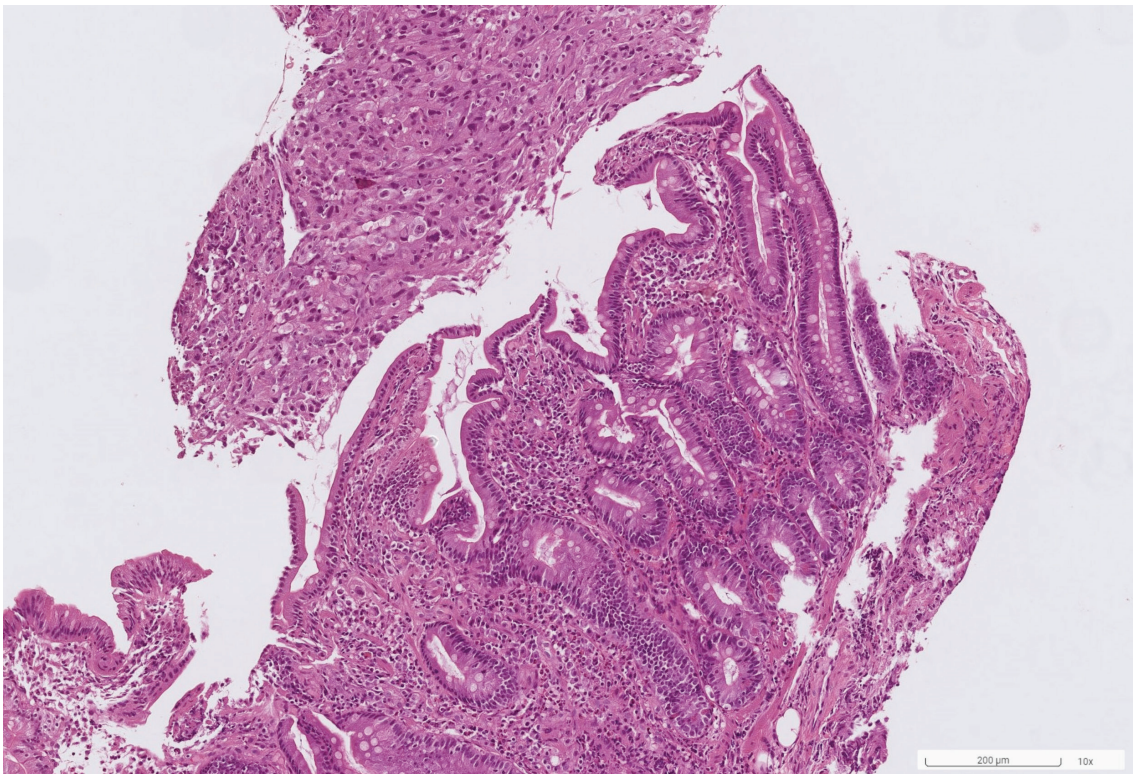

Fig. 4. Tumor tissue with hematoxylin and eosin stain.

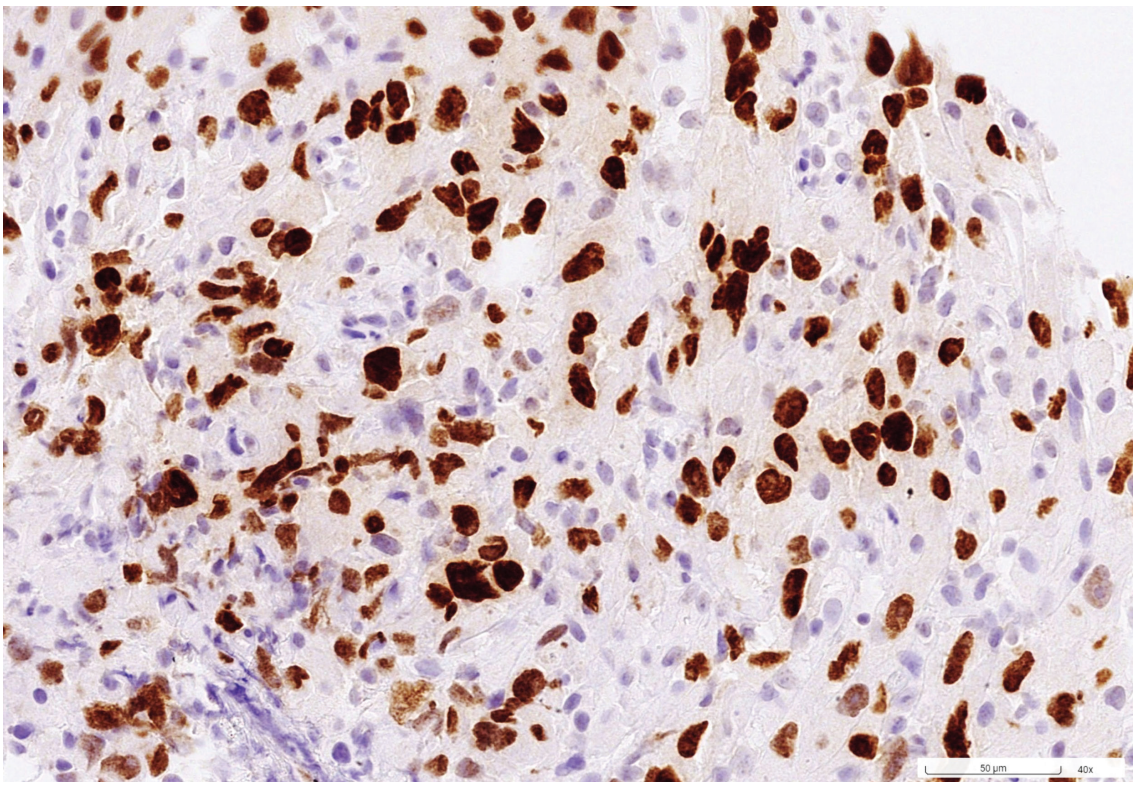

Fig. 5. Tumor tissue with TTF1 staining.

Discussion

Lung cancer with GI system metastasis is rare, with a frequency of 0.2–1.7% in clinical studies [9-14]. However, autopsies of lung cancer patients have revealed a 4.7–14% GI system metastasis occurrence rate [10, 13-15]. Since lung cancer patients with GI metastases are mostly asymptomatic, early diagnosis of GI tract metastasis is difficult [9]. The most common sites of GI tract metastasis from lung cancer were the jejunum and ileum; duodenum metastasis is relatively uncommon [13]. The most common histologies of GI metastasis are squamous cell and large cell, followed by adenocarcinoma [16]. Lung cancer with GI metastases usually have a CK7+/CK20- immunohistochemical staining pattern, whereas primary intestinal carcinomas usually have a CK7-/CK20+ pattern [14].

Lee *et al*. reported the interval between lung cancer diagnosis and gastrointestinal metastasis was 8 months (ranging from 2 to 108 months) in the early stage, and 3.5 months (ranging from 1 to 17 months) in the late stage [17]. The average time from the occurrence of GI metastasis to death was 2.8-4.3 months in previous studies [13, 17]. The most common symptoms of GI tract metastasis are GI bleeding, abdominal pain, nausea, vomiting, weight loss, constipation and cramping [9]. The endoscopic findings of lung cancer with GI tract metastases are nonspecific, and include diffuse intestinal mucosa erosion, nodules with or without mucosa ulceration, or a deep ulcerative lesion mimicking a primary GI tumor [18-21].

Treatment for duodenal metastasis is challenging -- it depends on the site and size of the duodenal involvement, and patient performance status and expected life span. Surgical intervention for GI metastases is mainly for symptoms relief and palliative care [22]. Kim *et al*. reported a patient that survived for more than 5 years after surgical intervention for isolated GI metastasis from the lung [17].

References

1. Riihimaki M, Hemminki A, Fallah M, *et al*. Metastatic sites and survival in lung cancer. Lung Cancer 2014; 86(1): 78-84.
2. Langley RR, Fidler IJ. The seed and soil hypothesis revisited--the role of tumor-stroma interactions in metastasis to different organs. Int J Cancer 2011; 128(11): 2527-35.
3. Valastyan S, Weinberg RA. Tumor metastasis: molecular insights and evolving paradigms. Cell 2011; 147(2): 275-92.
4. Fidler IJ. The pathogenesis of cancer metastasis: the 'seed and soil' hypothesis revisited. Nat Rev Cancer 2003; 3(6): 453-8.
5. Wu SG, Yu CJ, Tsai MF, *et al*. Survival of lung adenocarcinoma patients with malignant pleural effusion. Eur Respir J 2013; 41(6): 1409-18.
6. Socinski MA, Morris DE, Masters GA, *et al*. Chemotherapeutic management of stage IV non-small cell lung cancer. Chest 2003; 123(1 Suppl): 226S-43S.
7. Chen YM, Lai CH, Chang HC, *et al*. The impact of clinical parameters on progression-free survival of non-small cell lung cancer patients harboring EGFR-mutations receiving first-line EGFR-tyrosine kinase inhibitors. Lung Cancer 2016; 93: 47-54.
8. Charloux A, Quoix E, Wolkove N, *et al*. The increasing incidence of lung adenocarcinoma: reality or artefact? A review of the epidemiology of lung adenocarcinoma. Int J Epidemiol 1997; 26(1): 14-23.
9. Sanli Y, Adalet I, Turkmen C, *et al*. Small bowel metastases from primary carcinoma of the lung: presenting with gastrointestinal hemorrhage. Ann Nucl Med 2005; 19(2): 161-3.
10. Antler AS, Ough Y, Pitchumoni CS, *et al*. Gastrointestinal metastases from malignant tumors of the lung. Cancer 1982; 49(1): 170-2.
11. Berger A, Cellier C, Daniel C, *et al*. Small bowel

metastases from primary carcinoma of the lung: clinical findings and outcome. Am J Gastroenterol 1999; 94(7): 1884-7.

12. McNeill PM, Wagman LD, Neifeld JP. Small bowel metastases from primary carcinoma of the lung. Cancer 1987; 59(8): 1486-9.
13. Yang CJ, Hwang JJ, Kang WY, *et al*. Gastro-intestinal metastasis of primary lung carcinoma: clinical presentations and outcome. Lung Cancer 2006; 54(3): 319-23.
14. Rossi G, Marchioni A, Romagnani E, *et al*. Primary lung cancer presenting with gastrointestinal tract involvement: clinicopathologic and immunohistochemical features in a series of 18 consecutive cases. J Thorac Oncol 2007; 2(2): 115-20.
15. Yoshimoto A, Kasahara K, Kawashima A. Gastrointestinal metastases from primary lung cancer. Eur J Cancer 2006; 42(18): 3157-60.
16. Hillenbrand A, Strater J, Henne-Bruns D. Frequency, symptoms and outcome of intestinal metastases of bronchopulmonary cancer. Case report and review of the literature. Int Semin Surg Oncol 2005; 2: 13.
17. Lee PC, Lo C, Lin MT, *et al*. Role of surgical intervention in managing gastrointestinal metastases from lung cancer. World J Gastroenterol 2011; 17(38): 4314-20.
18. Kim HS, Jang WI, Hong HS, *et al*. Metastatic involvement of the stomach secondary to lung carcinoma. J Korean Med Sci 1993; 8(1): 24-9.
19. Hsu CC, Chen JJ, Changchien CS. Endoscopic features of metastatic tumors in the upper gastrointestinal tract. Endoscopy 1996; 28(2): 249-53.
20. Tamura T, Ohara G, Kagohashi K, *et al*. Duodenal and pancreas metastasis from lung cancer. Tuberk Toraks 2017; 65(2): 165-8.
21. Campoli PM, Ejima FH, Cardoso DM, *et al*. Metastatic cancer to the stomach. Gastric Cancer 2006; 9(1): 19-25.
22. Kim MS, Kook EH, Ahn SH, *et al*. Gastrointestinal metastasis of lung cancer with special emphasis on a long-term survivor after operation. J Cancer Res Clin Oncol 2009; 135(2): 297-301.

Pulmonary Endometriosis Diagnosed Using Bronchial Washing Cytology – A Case Report and Literature Review

Felisbela Gomes[1], Ping-Huai Wang[1], Sow-Hsong Kuo[2,3], Shih-Lung Cheng[1,4]

Catamenial hemoptysis is a rare disorder. We reported the case of a 40-year-old woman who had been quite well before experiencing symptoms. She suffered from recurrent hemoptysis in menstruation. The fiberoptic bronchoscopy yielded no endobronchial lesions. The diagnosis of catamenial hemoptysis was confirmed by cytologic examination of a bronchial washing specimen with endometrial cells. She was successfully treated with long-acting gonadotropin-releasing hormone. Based on this case, bronchoscopic examination and further bronchial washing cytology are suggested to be used in the diagnosis of catamenial hemoptysis during the period of menstruation, in spite of the high probability of normal findings by bronchoscopy. ***(Thorac Med 2025; 40: 189-193***)

Key words: Catamenial hemoptysis, thoracic endometriosis syndrome, fiberoptic bronchoscopy, bronchial washing cytology

Introduction

Thoracic endometriosis syndrome (TES) is characterized by the presence of endometriosis within the lung parenchyma, diaphragm and pleura. The syndrome includes a range of clinical and radiological manifestations dependent on the site of the lesions, including catamenial pneumothorax, catamenial hemoptysis, and pulmonary nodules [1].

Catamenial hemoptysis is rare and is difficult to diagnose. The disorder typically presents with periodic hemoptysis occurring at the time of menstruation [1]. Some authors suggest that bronchoscopy is not indicated, especially with the typical temporal relationship and cyclical changes in chest images. In fact, bronchoscopy plays an important role in the workup of all patients with hemoptysis, as well as catamenial hemoptysis.

Case Presentation

This 40-year-old woman was in good health, and had a history of 2 previous artificial abortions. She presented with right upper chest

[1]Division of Thoracic Medicine, Department of Internal Medicine, and [2]Department of Clinical Pathology, Far Eastern Memorial Hospital, New Taipei City, Taiwan, [3]Department of Internal Medicine, National Taiwan University Hospital, Taipei, Taiwan, [4]Department of Chemical Engineering and Materials Science, Yuan-Ze University, Taoyuan, Taiwan.
Address reprint requests to: Dr. Shih-Lung Cheng, Department of Internal Medicine, Far Eastern Memorial Hospital, Taipei, Taiwan.

discomfort on February 22, 2006, and on February 24, 2006, she experienced expectoration of a dark red substance with a blood clot (about 200 mL). She had no fever, weight loss, night sweats or general malaise, and no previous experience with hemoptysis. Non-productive cough and poor appetite were noted during the 2 days. She visited the emergency department (ED) of our hospital in the early morning of February 25, 2006.

At the ED, her hemodynamics were stable without apparent respiratory distress, and her body temperature was 35.9°C. Her physical findings were unremarkable. No coagulopathy was noted. Her white blood cell count was 7230/mm3. Biochemistry studies including renal function and liver function also yielded normal findings. The initial chest radiograph (Fig. 1) showed right upper lobe (RUL) infiltrates.

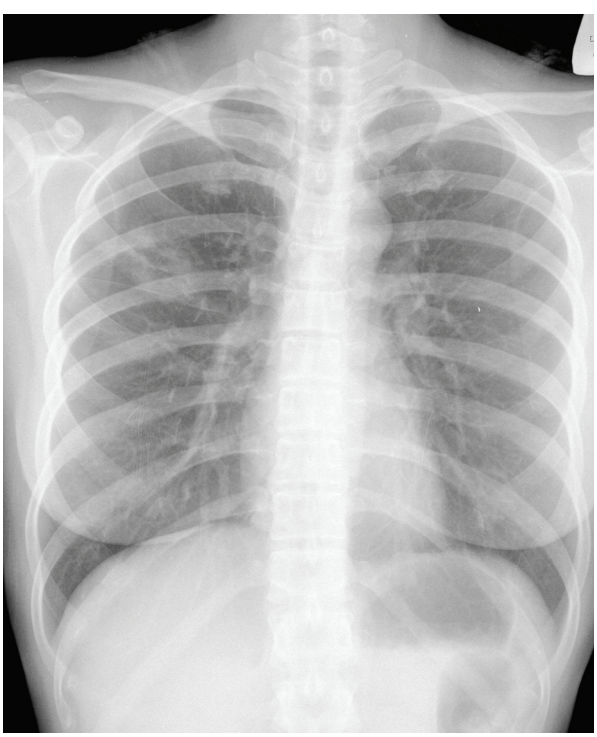

Fig. 1. Initial chest radiograph at the emergency department showed RUL infiltrates.

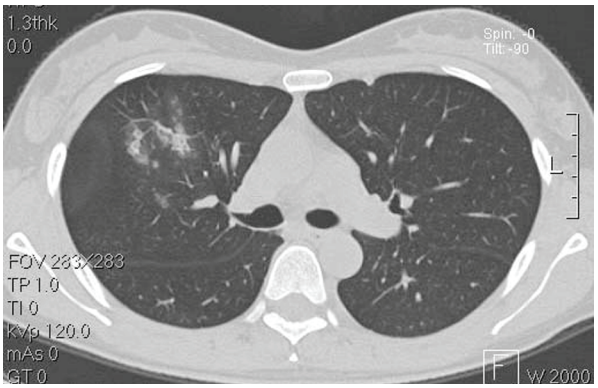

Fig. 2. Chest computed tomography on the second day after the first episode of hemoptysis, revealing ill-defined opacity in the right anterior segment of the RUL.

Computed tomography (CT) of the chest (Fig. 2) revealed an ill-defined opacity at the anterior segment (B3) of the RUL. Fiberoptic bronchoscopy, done on the fourth day after the onset of hemoptysis, showed normal findings. The microbiologic and cytological studies of bronchial washing over the right B3 were inconclusive. After these studies, she was discharged. However, the follow-up image on March 6, 2006, showed that the RUL lesion had disappeared. Then, hemoptysis recurred on March 20, 2006. She underwent fiberoptic bronchoscopy on the second day of hemoptysis, which still showed normal findings. The cytology of the bronchial washing (Fig. 3) from the right B3 yielded a few aggregates of small cuboid cells with some degeneration, compatible with endometrial cells.

A long-acting gonadotropin-releasing hormone (GnRH) agonist was prescribed monthly for 6 months (April to September 2006). Hemoptysis ceased after the third month of GnRH agonist treatment. Hot flushing, hirsutism, and body weight gain of about 4 kilograms were noted after the treatment. No recurrence of hemoptysis was noted 1 year after hormone therapy had been stopped.

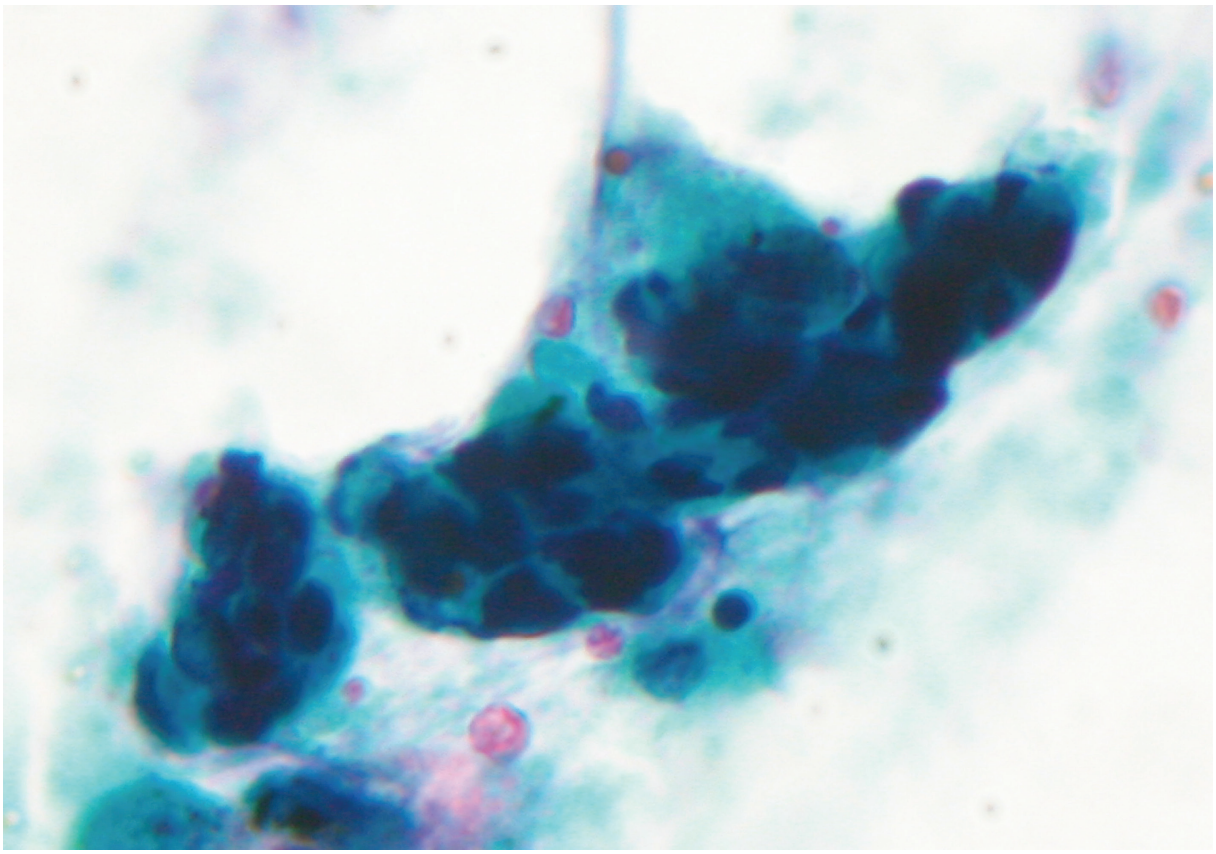

Fig. 3. Cytological study of the bronchial washing on the second day of the second episode of hemoptysis. It yielded a few aggregates of small cuboid cells with some degeneration, compatible with endometrial cells. (Papanicolao staining, 1000x).

Discussion

Endometriosis affects 10% of reproductive-age women, but the true prevalence of endometriosis is uncertain. Prevalence ranges from 2-11% among asymptomatic women, 5-50% among infertile women, and 5-21% among women who are hospitalized for pelvic pain [1]. Nezhat, *et al*, reported that endometriosis in the lung parenchyma or on the diaphragm and pleural surfaces, that presents with catamenial pneumothorax, catamenial hemothorax, catamenial hemoptysis, or pulmonary nodules, is recognized as TES [2]. Bobbio, *et al*. [3] expanded the definition of TES to include endometriosis-related diaphragmatic hernia, catamenial chest pain, and endometriosis-related pleural effusion. Among the 4 TES entities, catamenial hemoptysis is even rarer than catamenial pneumothorax/hemothorax.

Catamenial hemoptysis is a rare manifestation of thoracic endometriosis. The characteristic manifestation of catamenial hemoptysis is cyclic hemoptysis occurring during menses. It often occurs within the first to second day of menses [4]. A temporal relationship between the symptoms and menstruation may not be easily recognized by patients and clinicians. Failure to notice this would result in a delayed diagnosis. Chest radiographs may reveal normal findings, pulmonary infiltrates or opacities [5-6]. CT may reveal pulmonary opacities, a ground glass pat-

tern, or some sequel of recurrent bleeding, such as bullous formation and bronchiectatic changes. MRI may also be a useful tool for diagnosis; T1W imaging may show high signal intensity and DWI is sensitive for small hematomas in pleurodiaphragmatic endometriosis [5].

Since endometriosis often involves the distal airway or lung parenchyma, bronchoscopic studies may not reveal abnormalities, even if they are performed within 24 hours of the onset of hemoptysis [7]. However, there would be positive findings by fiberoptic bronchoscopy in TES involving the proximal airway, varying from single to scattered purplish-red submucosal patches to whitish cystic lesions [7-9].

The differential diagnosis of hemoptysis in women of reproductive age includes pulmonary infarction, bronchial carcinoid, arteriovenous malformation and anomalous vessels, tuberculosis, and bronchogenic carcinoma. The main criterion for the diagnosis of catamenial hemoptysis is the finding of periodic hemoptysis that is synchronous with menstruation, supported by cyclic changes of pulmonary findings revealed in imaging studies, including plain films and CT [4]. In 1 study, the mean diagnostic interval was 7.25 months (ranging from 0 to 15 months) [10].

In the past, some investigators suggested that there is no need for further fiberoptic bronchoscopy in the presence of typical symptoms, because of the low yield rate of bronchoscopic studies [8]. In a case series of 19 patients with catamenial hemoptysis evaluated by Kim C.-J, *et al*, no lesions were noted in the trachea or bronchi of 16 patients that received bronchoscopic examination during episodes of hemoptysis [11].

However, bronchoscopy plays an important role in the differential diagnosis of hemoptysis. Obviating the role of fiberoptic bronchoscopy may be inadequate for a comprehensive workup of hemoptysis. For example, Wood, *et al*. reported a case of arteriovenous malformation that manifested with cyclic hemoptysis in menses [12]. Huang H, *et al*. reported another case of catamenial hemoptysis. The chest CT image taken during the menstrual cycle revealed pneumonia in the left-superior lobe of the lung. Bronchoscopy performed on the fourth day of the menstrual cycle disclosed active bleeding in the distal bronchus of the superior segment of the left lingular lobe [9]. Hence, performing bronchoscopy during menses increases the likelihood of identifying endobronchial endometrial tissue. Bronchoscopy helps in making the diagnosis and localizing the possible lesion, and should always be routinely performed in patients with remarkable hemoptysis.

On the other hand, bronchoscopy performed before the surgical resection helps to identify the bleeding pulmonary segment [13]. Wang HC, *et al*. conducted a retrospective study, in which cytologic evaluation of the brushing material from the patients showed clusters of small cuboid cells consistent with an endometrial origin. These cytologic features, along with the cyclic changes of the bronchoscopic findings, were sufficient to warrant the diagnosis of tracheobronchial endometriosis.

The mean diagnostic interval in this study was 3.25 months. The diagnostic time interval was shortened (compared with ???) [7]. Many patients have undergone obstetrical or gynecologic manipulations and were noted to have coexisting pelvic endometriosis [14].

Our reported patient had no evidence of pelvic endometriosis. However, she had undergone an artificial abortion twice. It was proposed that the obstetrical procedures disrupted the endo-

metrial blood vessels and lymphatic drainage, which might have allowed lymphovascular entry of the endometrial tissue.

Treatment for catamenial hemoptysis includes both medical and surgical procedures. Anti-gonadotropic agents decrease endogenous estrogen production, and as a result, promote atrophy of the endometrial tissue. Anti-gonadotropic agents, including cyclic or continuous oral contraceptives, dienogest, danazol, cyproterone acetate, and GnRH agonists like leuprolide, are recommended. Compared to surgical treatment, hormonal treatment has a higher recurrence rate [4]. There are accumulating successful experiences with surgical treatment by open surgery and video-assisted thoracoscopic surgery [15-16]. Furthermore, Puma, *et al*. reported a case of tracheobronchial endometriosis successfully treated by Nd-YAG laser [17].

Conclusion

The diagnosis of catamenial hemoptysis mainly depends on clinical alertness and on recognizing the temporal relationship between hemoptysis and the menstrual cycle. A comprehensive workup and attempting to confirm it histopathogically are mandatory. Surgical management may be considered if hormone therapy fails or has intolerable side effects.

References

1. Zondervan KT, Becker CM, Missmer SA, *et al*. Endometriosis. N Engl J Med 2020; 382: 1244-56.
2. Nezhat C, Lindheim SR, Backhus L, *et al*. Thoracic endometriosis syndrome: a review of diagnosis and management. JSLS 2019; 23(3): e2019.00029.
3. Bobbio A, Canny E, Mansuet Lupo A, *et al*. Thoracic endometriosis syndrome other than pneumothorax: clinical and pathological findings. Ann Thorac Surg 2017; 104: 1865-1871.
4. Velagapudi RK, Egan, JP III. Thoracic endometriosis: a clinical review and update of current and evolving diagnostic and therapeutic techniques. Current Pulmonol Reports 2021; 10: 22-29.
5. Sanada T, Park J, Hagiwara M, *et al*. CT and MRI findings of bronchopulmonary endometriosis: a case presentation. Acta Radiol Open 2018; 7(10).
6. Alifano M, Trisolini R, Cancellieri A, *et al*. Thoracic endometriosis: current knowledge. Ann Thorac Surg 2006; 81: 761-9.
7. Wang HC, Kuo PH, Kuo SH, *et al*. Catamenial hemoptysis from tracheobronchial endometriosis. Reappraisal of diagnostic value of bronchoscopy and bronchial brush cytology. Chest 2000; 118: 1205-8.
8. Guidry GG, George RB. Diagnostic studies in catamenial hemoptysis. Chest 1996; 51:1060-1.
9. Huang H, Li C, Zarogoulidis P, *et al*. Endometriosis of the lung: report of a case and literature review. Eur J Med Res 2013; 18: 13.
10. Ryu JS, Song ES, Lee KH, *et al*. Natural history and therapeutic implications of patients with catamenial hemoptysis. Respir Med 2007; 101: 1032-6.
11. Kim C-J, Nam H-S, Lee C-Y, *et al*. Catamenial hemoptysis: a nationwide analysis in Korea. Respiration 2010; 79: 296-301.
12. Wood DJ, Krishma K, Stock P, *et al*. Catamenial haemoptysis: a rare cause. Thorax 1993; 48: 1048-9.
13. Marques VD, de Mattos LA, Pimenta AM, *et al*. Resection of pulmonary endometriosis by VATS using bronchoscopy as a preoperative strategy. Ann Thorac Surg 2020; 110: e391-3.
14. Rousset-Jablonski C, Alifano M, Plu-Bureau G, *et al*. Catamenial pneumothorax and endometriosis-related pneumothorax: clinical features and risk factors, Hum Reprod 2011; 26(9): 2322-9.
15. Inoue T, Kurokawa Y, Kaiwa Y, *et al*. Video-assisted thoracoscopic surgery for catamenial hemoptysis. Chest 2001; 120: 655-8.
16. Choi SY, Kim CK, Park CB. Successful treatment of catamenial hemoptysis by video-assisted thoracoscopic surgery. Thorac Cardiovasc Surg 2013; 61(01): 094-096.
17. Puma F, Carloni A, Casucci G, *et al*. Successful endoscopic Nd-YAG laser treatment of endobronchial endometriosis. Chest 2003; 124: 1168-70.